ATTACHMENT A: NARRATIVE REPORT
[40 CFR 146.82(a)]
CTV II

Table of Contents

Document Version History

Version	Submission Date	File Name	Description of Change
1	5/3/2022	Att A - CTV II Project Narrative	Original submission as part of CTV II storage project
2	8/4/2022	Att A - CTV II Project Narrative V2	Updated submission to address EPA Administrative review request for additional information dated 6/9/2022. Updated document, attachments and appendices to cover requests on additional permits required, Tribes to be consulted, Well Construction, Site characterization & Operational info
3	12/14/2022	Att A – CTV II Project Narrative V3	Updated submission to address EPA Administrative review request for additional information dated 9/21/2022, and for project expansion from two to five injectors
4	2/2/2023	Att A – CTV II Project Narrative V3.1	Updated document to address EPA request.
5	2/28/2024	Att A - CTV II Project Narrative V5	Updated document to address EPA Comments.
6	11/26/2024	Att A - CTV II Project Narrative V6	Response to August 29, 2024 EPA Comments

Facility Information

Facility name: CTV II

Facility contact: William Chessum, Technical Manager
(562) 999-8380, William.chessum@crc.com

Well location: Union Island Gas Field, San Joaquin County, CA
37.868/–121.420

1. Project Background and Contact Information

Carbon TerraVault Holdings LLC (CTV), a wholly owned subsidiary of California Resources Corporation (CRC), proposes to construct and operate five carbon dioxide (CO_2) geologic sequestration wells at CTV II, near the Union Island Gas Field, located in San Joaquin County, California. This application was prepared in accordance with the U.S. Environmental Protection Agency's (EPA's) Class VI, in Title 40 of the Code of Federal Regulations (40 CFR 146.81) under the Safe Drinking Water Act (SDWA). CTV is not requesting an injection depth waiver or aquifer exemption expansion.

CTV will obtain the required authorizations from applicable local and state agencies, including the associated environmental review process under the California Environmental Quality Act. **Appendix 1** outlines potential local, state and federal permits and authorizations. The project wells and facilities will not be located on Indian Lands. Federal act considerations and additional consultation, which include the Endangered Species Act, the National Historic Preservation Act, and consultations with Tribes in the area of review, are presented in **Appendix 2: Applicable Federal Acts and Consultation**.

CTV forecasts the potential CO_2 stored in the Winters Formation at 0.97 million tonnes annually for 23.5 years. The anthropogenic CO_2 will be sourced from direct air capture and/or other CO_2 sources in the CTV II area.

The CTV II storage site is located in the Sacramento Valley, 20 miles southeast of the Rio Vista Field near Stockton, California within the southern Sacramento Basin. The project will consist of five injectors, surface facilities, and monitoring wells. This supporting documentation applies to the five injection wells.

CTV will actively communicate project details and submitted regulatory documents to County and State agencies:

- Geologic Energy Management Division (CalGEM)
  Acting District Deputy
  Chris Jones (661)-322-4031
- CA Assembly District 13
  Assemblyman Carlos Villapudua
  31 East Channel Street – Suite 306
  Stockton, CA 95202
  (209) 948-7479
- San Joaquin County
  District 3 Supervisor –Tom Patti
  (209) 468-3113
  tpatti@sjgov.org
- San Joaquin County Community Development
  Director – David Kwong
  1810 East Hazelton Avenue
  Stockton, CA 95205
  (209) 468-3121
- San Joaquin Council of Governments
  Executive Director – Diane Nguyen
  555 East Weber Avenue
  Stockton, CA 95202
  (209) 235-0600
- Region 9 Environmental Protection Agency
  75 Hawthorne Street
  San Francisco, CA 94105
  (415) 947-8000

2. Site Characterization

2.1 Regional Geology, Hydrogeology, and Local Structural Geology [40 CFR 146.82(a)(3)(vi)]

2.1.1 Field History

The CTV II storage site overlaps the Union Island Gas Field, which was discovered in 1972 by Union Oil Company of California. Located in a region of prolific gas production approximately 20 miles southeast of major gas field Rio Vista, the Union Island Field was one of the largest dry gas fields in California (**Figure A-1**). Commercial production from its gas reservoir, the Winters Formation, began in 1976 and continued until the quick decline in early 1988 (Leong, 1994). This formation is now being repurposed for CO_2 storage.

2.1.2 Geology Overview

The Union Island Gas Field lies within the Sacramento Basin in northern California (**Figure A-2**). The Sacramento Basin is the northern, asymmetric sub-basin of the larger Great Valley Forearc. This portion of the basin, which contains a steep western flank and a broad, shallow eastern flank, spans approximately 240 miles in length and is 60 miles wide (Magoon, 1995).

Basin Structure

The Great Valley was developed during mid to late Mesozoic time. The advent of this development occurred under convergent-margin conditions via eastward, Farallon Plate subduction of oceanic crust beneath the western edge of North America (Beyer, 1988). The convergent, continental margin that characterized central California during the Late Jurassic through Oligocene time was later replaced by a transform-margin tectonic system. This occurred as a result of the northward migration of the Mendocino Triple Junction (from Baja California to its present location off the coast of Oregon), located along California's coast (**Figure A-3**). Following this migrational event was the progressive cessation of both subduction and arc volcanism as the progradation of a transform fault system moved in as the primary tectonic environment (Graham, 1984). The major present-day fault, the San Andreas, intersects most of the Franciscan subduction complex, which consists of the exterior region of the extinct convergent-margin system (Graham, 1984).

Basin Stratigraphy

The structural trough that developed subsequent to these tectonic events, the Great Valley, became a depocenter for eroded sediment, and therefore currently contains a thick infilled sequence of sedimentary rocks. These sedimentary formations range in age from Jurassic to Holocene. The first deposits occurred as an ancient seaway and, through time, were built up by erosion of the surrounding structures. The basin is constrained on the west by the Coast Range Thrust, on the north by the Klamath Mountains, on the east by the Cascade Range and Sierra Nevada, and on the south by the Stockton Arch Fault (**Figure A-2**). The western Coastal Range boundary was created by uplifted rocks of the Franciscan Assemblage (**Figure A-4**). The Sierra Nevada, which make up the eastern boundary, are a result of a chain of ancient volcanos.

Basin development is broken out into evolutionary stages at the end of each time period of the arc-trench system, from Jurassic to Neogene, in **Figure A-5**. As previously stated, sediment infill began as an ancient seaway, and was later sourced from erosion of the surrounding structures. Due to the southward tilt of the basin, sedimentation thickens toward the southern end near the Stockton Arch fault, which bounds the southeastern portion of the area of review (AoR), creating sequestration quality sandstones. Sedimentary infill consists of Cretaceous-Paleogene fluvial, deltaic, shelf, and slope sediments.

In the southern Sacramento Basin, the Winters Formation is a thick-bedded sandstone that creates the principal gas reservoir facies in the project area. This field is a structural-stratigraphic trap set up by both structural closure against the Stockton Arch fault and Winters Formation stratigraphic transition to the northeast. The Stockton Arch fault is a northeast-trending thrust fault that dips to the southeast and produces from its footwall on the west end of the fault.

2.1.3 Geological Sequence

Figure A-6 is a schematic representing the local stratigraphy of the project area, highlighting the west side of the Stockton Arch fault and proposed Injection Zone. The injection wells will inject CO_2 into the Cretaceous aged Winters Formation, located in the Stockton Arch footwall. The footwall injection depth is approximately 9,500 feet true vertical depth (TVD). The Injection Zone has a known reservoir capacity demonstrated by historical gas production. Cumulative production is 292 billion cubic feet (bcf) of gas (71 bcf north only) and 3.4 million stock tank barrels (MMSTB) of water (1.4 MMSTB north only), lowering reservoir pressure from 5,040 pounds per square inch (psi) to 1,200 psi (DOGGR, 1998; Leong and Tenzer, 1994).

Following its deposition, the Winters Formation was buried under the Sawtooth Shale, which carries throughout most of its distribution. Above the Sawtooth Shale are several alternating sand-shale sequences: the Tracy Formation, Starkey Shale, H&T Shale, Mokelumne River Formation, Capay Shale, Domengine Sandstone, and Nortonville Shale. The Sawtooth Shale Formation, combined with the overlying Tracy and Starkey Formations, acts as the Upper Confining Zone for the Winters Reservoir due to its low permeability, thickness, and regional continuity that spans beyond the AoR (**Figure A-7**). The Upper Confining Zone refers to the Starkey-Sawtooth Shale throughout this application.

2.2 Maps and Cross Sections of the AoR [40 CFR 146.82(a)(2), 146.82(a)(3)(i)]

As required by 40 CFR 146.82(a)(2), **Figure A-8** is a summary map of the oil and gas wells, water wells, State- or EPA-approved subsurface cleanup sites, and surface features in the project area and the project AoR. AoR delineation is presented in **Attachment B: AoR and Corrective Action Plan (Attachment B)**. **Tables A-1**, **A-2**, **and A-3** list the oil and gas wells, California Department of Water Resources (DWR) Well Completion Report (WCR) water wells, and California State Water Resources Control Board Groundwater Ambient Monitoring Assessment Program (GAMA) water wells shown in **Figure A-7**, respectively. **Figure A-9** is a summary map of oil and gas wells in the AoR.

2.2.1 Data

To date, 37 wells have been drilled to various depths within the Union Island Field (**Figure A-10**). Although there is not an extensive database of wells in this field, seismic coverage, core, and reservoir performance data such as production and pressure give an adequate description of the reservoir.

Well data are used in conjunction with three-dimensional (3D) and two-dimensional (2D) seismic data to define the structure and stratigraphy of the Injection Zone and Confining Zone (**Figure A-11**). The 3D seismic surveys used to characterize faults in the area were part of a 2013 processing effort to merge over 1,100 square miles of data into a single, seamless set of volumes with improved image quality. Each survey was processed individually and then merged using industry leading techniques provided by a major industry service provider. The volume used to interpret the area for CTV II contained a number of pre-stack and post-stack enhancements, along with 5D trace regularization to fill in data gaps and provide the best image possible for structural and fault interpretation. Acquisition parameters for the survey that encompasses CTV II are industry standard for seismic acquisition. The seismic traces are binned into a 110-foot by 110-foot grid.

Figure A-12 shows outlines of the seismic data used and the area of the structural framework that was built from these seismic surveys. The 3D data in this area were merged using industry-standard pre-stack time migration in 2013, allowing for a seamless interpretation across them. The 2D data used for this model were tied to this 3D merge in both phase and time to create a standardized datum for mapping purposes. The following layers were mapped across the 2D and 3D data:

- A shallow marker to aid in controlling the structure of the velocity field
- The approximate base of the Valley Springs Formation, which is unconformable with the Eocene strata below
- Domengine
- Mokelumne River
- H&T Shale
- Winters
- Lathrop (Hanging Wall of Stockton Arch Fault)
- Forbes

The top of the Cretaceous Forbes Formation was used as the base of this structural model due to the depth and imaging of Basement not being sufficient to create a reliable and accurate surface. Interpretation of these layers began with a series of well ties at well locations shown in **Figure A-12**. These well ties create an accurate relationship between well data, which are in depth, and seismic data, which are in time. The layers listed above were then mapped in time and gridded on a 550-foot by 550-foot cell basis. Alongside this mapping was the interpretation

of any faulting in the area, which is discussed further in the Faults and Fracture section of this document.

The gridded time maps and a subset of the highest quality well ties and associated velocity data are then used to create a 3D velocity model. This model is guided between well control by the time horizons, and is iterated to create an accurate and smooth function. The velocity model is used to convert both the gridded time horizons and interpreted faults into the depth domain. The result is a series of depth horizons of the layers listed above, which are then used in the next step of this process.

The depth horizons are the basis of a framework that uses conformance relationships to create a series of depth grids that are controlled by formation well tops picked on well logs. The horizons are used as structural control between these well tops to incorporate the detailed mapping of the seismic data. These grids incorporate the thickness of zones from well control and the formation strike, dip, and any fault offset from the seismic interpretation. **Figure A-13** shows the locations of the wells used to pick well tops for the structural model to create the finalized depth grids. A subset of this structural model is then taken to create the computational model, with grids only used in the footwall of the Stockton Arch Fault, as the fault is a sealing boundary in the computational model. The framework is set up to create the following depth grids for input in to the geologic and plume growth (computational) models:

- Nortonville Shale
- Domengine
- Domengine Top Sand
- Capay Shale
- Mokelumne River
- H&T Shale
- Winters
- Delta Shale
- Delta Shale Base
- Top Lathrop (Hanging Wall)
- Sacramento Shale (Hanging Wall)

2.2.2 Stratigraphy

Major stratigraphic intervals within the field, from oldest to youngest, include the Delta Shale (L. Cretaceous), Winters Formation (L. Cretaceous), Sawtooth Shale (L. Cretaceous), Tracy Formation (L. Cretaceous), Starkey Shale (L. Cretaceous), H&T Shale (L. Cretaceous), Mokelumne River Formation (L. Cretaceous-E. Paleocene), Capay Shale (E. Eocene), Domengine Sandstone (L. Eocene), and Nortonville Shale (L. Eocene) (**Figure A-14**).

Of these formations, the regional upper seal rock that partitions the reservoir consists of the Starkey-Sawtooth Shale. These combined formations create an average thickness of approximately 2,240 feet throughout the AoR. Also shown in **Figure A-14** is a basin-wide unconformity separating overlying Paleocene and younger beds from Cretaceous rocks. This unconformity resides above the Mokelumne River Formation at the base of the Capay Shale, between the injection reservoir and the underground source of drinking water (USDW). During Paleogene time, marine and deltaic deposits continued in the basin until the activity of the Stockton Arch began to separate the Sacramento Basin from the San Joaquin basin in late Paleogene time (Downey, 2010).

Lathrop Sands

The Upper Cretaceous Lathrop sands are interpreted to be shallow marine sandstones that grade from fine-grained, silty sand lenses at the top of Lathrop to massive medium-grained sandstones in the middle and lower Lathrop. Lathrop sands were deposited during a renewed progradational basin filling sequence overlying the Sacramento Shale. These deltaic sands sourced from the Diablo Ranges show a generalized northeast-southwest trend and are best developed in the Southern San Joaquin County, where they can be over 2500 feet thick (CGS, 2006).

As you move south of Vernalis, the sands become coarser, more angular, and less sorted, indicating proximity to the sediment source. Moving eastward, the sands become less sandy and eventually transition into shale. The Lathrop sands interfinger with the Joaquin Ridge sands in the south. These sandstones have produced hydrocarbons in fields like Lathrop and French Camp (Callaway, 1964). The Lathrop sands are underlain by the Sacramento Shale, Forbes Shale, and the Dobbins Shale.

Delta Shale

The Delta Shale Formation consists of approximately 157 feet of shale barrier. This shale has an average permeability of 0.04 millidarcies (mD) and porosity of 14.7 percent (as defined in Section 2.4.2). Due to the sparse well penetrations and subsequent lack of log data, this formation has been primarily mapped using seismic data as stated above. The section below this, above the Lathrop sands is described as the Lower Delta Shale in this application; this shale interval has a relatively higher percentage of interbedded sands compared to the clay-rich section above it.

Winters Reservoir (Injection Zone)

Within the project area, the Winters Reservoir is a generally upward-fining/thinning sequence that lies perpendicular to the depositional slope and thickens toward the basin. This formation was deposited as coalesced channels that formed at the base of the slope, on the upper channelized portion of a sandy suprafan.

This Upper Cretaceous-aged formation is a deep-water sandstone with thinly interbedded sandstone and shale that overlie the Delta Shale. These deposits were part of a large deep-sea fan system that were sourced from granitic areas in the Sierra Nevada and fed into the system via submarine canyons and feeder channels (Williamson, 1981). This creates a blocky, sand-rich reservoir that extends to as much as 1,500 feet thick in the center of the basin. Along the basin axis, this sandy suprafan stacks up due to the high rate of sand supply relative to the size of the

basin, as well as the depositional nature of the fans at basin margins (Williamson, 1981). Moving toward the upslope portion of the fan system is the Union Island Gas Field, where the Winters Formation is closer to 250 feet thick. Core data are supportive of a channelized portion of the suprafan lobe (Williamson, 1981). The Winters isochore map (**Figure A-15a**) shows the channel system trending southwest, and the 2 degree dip to the west can be seen on the structure map (**Figure A-15b**). The Winters Formation has a gross thickness of approximately 256 feet within the model boundary, with sand porosity and permeability averages of 18.9 percent and 13 mD, respectively, as defined in Section 2.4.2.

Outside of the AoR, southwest of the project area, the Winters Formation thickens and fans out, covering a much larger area. Northeast of the AoR, at the base of the slope, the Winters Formation transitions into a predominantly shaly interval (**Figure A-16)**. This stratigraphic trap along the eastern edge of the Winters Formation, where the lobate bodies pinch out upslope, contain the best reservoir quality in the system, and are also in upslope position, optimal for hydrocarbon migration or, in this case, CO_2 storage. The AoR and injectors for this project are shown in **Figure A-17**.

Different gas-water contacts observed at the time of the field's discovery indicate that a flow barrier exists within the Injection Zone, between the northern and southern halves of the field. **Figure A-18** is a reproduction from Hill (1979) displaying the facies change that represents the flow barrier.

Starkey-Sawtooth Confining Zone

Sawtooth Formation

The Sawtooth Shale overlies the Winters Formation, which provides a regional seal ranging from 100 to 500 feet thick. Within the AoR, the average gross thickness of the Sawtooth is 100 feet. At the Union Island Gas Field, the Sawtooth Shale is continuous over the field and has a permeability of less than 0.15 mD and 18.5 percent porosity (as defined in Section 2.4.2). This shale has successfully contained gas operations within the Winters Formation for over 50 years, and has contained original gas deposits for millions of years.

Tracy Formation

The Tracy Formation overlies the Sawtooth Shale and thickens southward into the San Joaquin Basin. This formation was deposited as Upper Cretaceous deep-water sandstone as an east-west trending south-facing depositional slope. Sand quality improves on the east side of the Stockton Arch Fault, outside of the AoR. Inside the AoR, on the west side of the fault, this formation is very shale-rich, with minor interlaminations of low-quality sands.

Starkey Formation

Above the Winters Formation lies another interchannel shale, the Starkey Formation, which adds to the Sawtooth Shale, creating one large confining zone encasing the reservoir.

H&T Shale

The H&T Shale acts as a conformable contact to the Mokelumne River Formation. This shale pinches out and creates an abrupt thickening when it combines with the overlying Capay Shale moving west. The truncation of the H&T Shale results in a thicker Capay Shale that rests

unconformable on the Starkey Sandstone. Moving southwest, the H&T Shale thickens and contains a facies change with the upper marine shale of the Starkey section progressively adding, creating a thicker shale.

Mokelumne Monitoring Zone

Mokelumne River Formation

The Mokelumne River Formation sandstones are excellent reservoir quality sands, whose trap types include fault truncations, stratigraphic traps, and unconformity traps sealed by intervening shales, as well as overlying Menganos submarine canyon mudstone infill (Downey, 2006). This formation truncates to the north by the post-Cretaceous angular unconformity until it pinches out in southern Yolo and Sutter Counties (Downey, 2006). These large sands can be locally eroded or totally gone due to the downcutting by the Menganos submarine canyons, which are located outside of the AoR to the west. This saline reservoir will be monitored, and could effectively detect and monitor any possible CO_2 leakage prior to reaching the Markley Formation.

Capay Shale

The Capay Shale provides upper confinement to the Mokelumne River Formation as it spans across the basin as a major regional flooding surface. This Eocene-aged formation was deposited as a transgressive surface blanketing the shelf with shales. East of the Midland fault zone, the Martinez Shale has been stripped by erosion, and the Mokelumne River Formation sandstones are unconformably overlain by the Capay Shale. Due to its low permeability, this formation acts as a seal to the Mokelumne River Formation monitoring zone, and would act as a barrier to any CO_2 reaching the USDW if any migration were to occur.

Domengine Formation

The Domengine Formation is approximately 800 to 1,200 feet thick on the north flank of Mt. Diablo (Nilsen 1975). Prograding across the Capay Shelf in early middle Eocene, this formation is characterized by interbedded sandstones, shales, and coals. This sand ranges from medium- to coarse-grained silty mudstone and fine sandstone, and onlaps the Capay Shale. It is separated from the Capay Shale by a regional unconformity that progressively truncates older units until the Domengine rests on Cretaceous rocks moving west. The Domengine Formation consists of upper and lower members. The lower member is made up of fluvial and estuarine sandstones. Regionally, the lower member is separated from the upper member by an extensive surface of transgression and change in depositional style. This formation acts as a dissipation zone to CO_2 between the injection site and the USDW.

Nortonville Shale

Above the Domengine Formation is the Nortonville Shale, which is separated by a widespread surface of transgression. The Nortonville Shale is a mudstone member of the Kreyenhagen Formation. It is approximately 500 feet on the north flank of Mt. Diablo, and is considered the upper portion of the Domengine Sandstone (Nilsen, 1975). Overlying the Domengine Sandstone, this shale acts as a seal throughout most of the southern Sacramento and northern San Joaquin Basins.

Marine Strata "Markley/Valley Springs"

The upper Paleogene and Neogene sequence begins with the Valley Springs Formation, which represents fluvial deposits that blanket the entire southern Sacramento Basin. The unconformity at the base of the Valley Springs marks a widespread Oligocene regression and separates the more deformed Mesozoic and lower Paleogene strata below from the less deformed uppermost Paleogene and Neogene strata above. The USDW that resides at the base of the Markley Formation is discussed in Section 2.7.

2.2.3 Map of the Area of Review

As required by 40 CFR 146.82(a)(2), **Figure A-19** shows surface bodies of water, surface features, transportation infrastructure, political boundaries, and cities. Major water bodies in the area are Clifton Court Forebay, Victoria Canals, Grant Line Canal, and the Salmon Slough. The AoR is in San Joaquin County. This figure does not show the surface trace of known and suspected faults because there are no known surface faults in the AoR. There are also no known mines or quarries in the AoR.

Figure A-20 indicates the locations of State- or EPA-approved subsurface cleanup sites. This cleanup site information was obtained from the State Water Resources Control Board's GeoTracker database, which contains records for sites that impact, or have the potential to impact, groundwater quality. Water wells within and adjacent the AoR are discussed in Section 2.7.7.

The GeoTracker website indicates that there is a closed cleanup site within the AoR. The site is at a former Union Oil Company Galli Pad Area located within the Union Island Oil Field. The site is listed in GeoTracker as Global ID SLT5S3033339. The case file includes a Mercury Contamination Soil Remediation Closure Report by Unocal Energy Resources Division (Unocal) and a Unocal transmittal letter to Central Valley Water Board staff from Unocal dated March 22, 1996. The Unocal report states that Unocal is operating natural gas production wells in the Union Island Gas Field, and that there is mercury-contaminated soil in the top 6 inches of two 3-foot by 3-foot areas where the blow-off valves discharge to the ground surface. Unocal stated that it will excavate the contaminated soil and transport it off-site for disposal. The GeoTracker case file also includes a letter dated January 18, 2012 from the Central Valley Regional Water Quality Control Board (Central Valley Water Board). The Central Valley Water Board staff determined that (1) based on the very limited area of impact, there was no indication of groundwater contamination, (2) staff do not consider the site a cleanup site, and (3) staff will not be activating this case and consider it closed.

2.3 Faults and Fractures [40 CFR 146.82(a)(3)(ii)]

2.3.1 Overview

The Stockton Arch subdivides the Great Valley Forearc into the Sacramento and San Joaquin Basins, bounding the Sacramento Basin in the south. Post-Eocene/Pre-Miocene uplift of the Stockton Arch created a series of high-angle reverse faults known as the Stockton Arch Fault Zone (SFZ). This fault bounds the southeast portion of the AoR, trending southwest to northeast

and spanning from Tracy to Linden. The Union Island Gas Field produces from the footwall of this fault-related trap.

The 3D seismic data described in Section 2.2 were used together with well control to define the fault planes within the geologic model boundary. This geologic model is a subset of the larger structural framework that was built using the seismic and well data. Repeat geologic sections seen in the wells are used to guide the fault pick, along with a clear offset and fault plane seen in the modern reprocessing of the 3D seismic data. **Figure A-21** shows the fault at the Winters Formation level, along with the location of an example structural cross section shown in **Figure A-22**. There is a secondary fault in the hanging wall (east side) of the Stockton Arch fault, which may be antithetic to the main fault. Due to the sealing nature of the Stockton Arch Fault and the planned injection in the footwall (west side) of the fault, this secondary fault is not discussed further in this report.

As seen in the cross section provided in **Figure A-22**, the Stockton Arch Fault is cut off at the Base Valley Springs unconformity. There is some folding in the strata above this, which may be related to the structural overprint of the fault beneath the unconformity. The fault appears to have been active through the Eocene section beneath the unconformity due to the missing Domengine section on the east side of it. Further discussion of fault activity is provided in the Seismic History section.

2.3.2 Fault Sealing

The Stockton Arch Fault has trapped natural gas for millions of years and will continue to provide a seal to trap injected CO_2. Project area formation pressure, fault juxtaposition, Injection Zone gas-water contacts, and shale gouge ratio (SGR) have all been analyzed to provide evidence for continued fault sealing.

Union Island Gas Field Winters Formation Pressure

Original reservoir pressure when the field was discovered in 1972 was 5,040 psi:

- SONOL_SECURITIES_1-A was drilled in February 1972 with perforation intervals between 9,697 and 9,707 feet, 9,714 and 9,735 feet, 9,780 and 9,784 feet, and 9,790 and 9,793 feet. A shut-in pressure test was performed and returned a reservoir pressure of 5,040 psi (data sourced from CalGEM).
- DOGGR (1998) shows that Union Island Gas Field initial reservoir pressure is 5,040 psi.
- A paper presented at the Society of Petroleum Engineers Western Regional Meeting in March 1994 shows that initial reservoir pressure for the Winters Formation in the Union Island gas reservoir is 5,040 psi (Leong and Tenzer, 1994).

Production of natural gas and water through time has drawn the discovery pressure down to a current pressure of 1,200 psi. The current pressure is based on the March 2022 pressure and temperature gradient measured in Pool B-2 (**Figure A-23**). Field production was shut down in June 2023, with only minor gas production occurring since the Pool B-2 measurement.

To understand the project area formation pressure, mudlogs from wells drilled on both sides of the fault were reviewed. Wells drilled during production, in the late 2000s, have mudlogs that indicate a normal hydrostatic or lower pressure in the confining zone and other zones above the Winters Formation. Of the wells reviewed, each was drilled with mudweights overbalanced to hydrostatic pressure, and none of them showed any losses above the Winters Formation despite depletion in the Winters Formation.

An example mudlog comes from the Sonol Securities 11 (0407720724) well drilled in 2008, located in Section 10, Township 1S, Range 5E within the Union Island Gas Field. This well was drilled through the Winters Formation in the hanging wall of the Stockton Arch fault in the depth interval of 7,993 to 8,214 feet MD. The mudweight above and below that interval was 10.1 pounds per gallon (ppg), or 0.53 pounds per square inch per foot (psi/ft) equivalent. The well did not encounter any drilling issues, losses, or drop in mudweight in this zone, indicating zonal isolation from the depleted Winters Formation in the footwall of the Stockton Arch fault. Additionally, electric logs indicate that the Winters Formation is not hydrocarbon-bearing in this zone. The well was then further drilled until the Winters sands were hit in the footwall of the fault. Once the presence of footwall Winters sand was confirmed, the well casing point was called and the final casing depth was set at 9,396 feet to isolate the depleted Winters Formation in the footwall from all formations above in the well.

Additional evidence supporting that the Stockton Arch fault is sealing is shown in **Figure A-24**. This figure shows the similarity in the discovery pressure gradient across the Stockton Arch fault at Union Island and Lathrop Gas Fields. The Union Island Gas Field was discovered in 1972. As shown in Figure B-14 (**Attachment B**), the producing Winters Formation at the Union Island Gas Field is juxtaposed against the Lathrop Formation along the Stockton Arch Fault. Because the Lathrop Gas Field was discovered in 1961 and it had already produced 60 percent of its cumulative production by the time the Union Island Gas Field was discovered, a lower discovery pressure gradient would have been expected if the two reservoirs were in communication.

The pressure isolation in the Winters Formation across the fault during active production supports that the Stockton Arch Fault is capable of sealing at pressures up to its original discovery pressure of 5,040 psi. As discussed in Section 2.4 of **Attachment B**, CTV proposes to inject CO_2 into the depleted Winters Formation until the reservoir pressure reaches 90 percent of the discovery pressure (4,500 psi). Restricting the pressure below original reservoir pressure is important for the stability of the fault. Fault stability is discussed further in Section 2.6.

Allan Diagram and Gas-Water Contacts

To further show the sealing nature of the Stockton Arch fault, an Allan diagram and SGR analysis was completed. The Stockton Arch fault Allan diagram is shown in **Figure A-25**. The footwall and hanging wall stratigraphy plotted in the Allan diagram were populated from the depth grids of the structural model, as discussed in Section 2.2.1. As seen in **Figure A-25**, the Winters Injection Zone on the footwall side of the fault is mainly juxtaposed against the Lathrop Sands on the hanging wall, with only a portion juxtaposed against the Lower Delta Shale in the southern portion of the AoR. The Winters Injection Zone gas-water contact is also displayed in **Figure A-25**. **Figure A-26** shows more detailed cross sections of the gas-water contacts and structural spill points for the northern and southern portions of the AoR. Gas-water contact cross

section A-A' corresponds with Allan Diagram cross section ID 8, and gas-water contact cross section B-B' corresponds with Allan Diagram cross section ID 4. While these figures share the same point on the fault, they both display the fault from different angles. **Figure A-25** shows a singular cross section of the fault along the fault plane, while **Figure A-26** shows two cross sections perpendicular to the fault. Similar to the Allan diagram, cross section A-A' shows the Winters Injection Zone juxtaposed against the Lathrop Sands on the hanging wall side of the fault in the northern portion of the AoR, and cross section B-B' shows the Winters Formation juxtaposed against both the Lower Delta Shale and the Lathrop Sands on the hanging wall side of the fault in the southern portion of the AoR. The structural spill point for both sections is above the original gas-water contact in both northern and the southern parts of the field.

If the Stockton Arch Fault was not sealing, the Injection Zone gas-water contact would extend across the fault into the Lathrop Sands. However, wells drilled on the hanging wall side of the Stockton Arch fault reveal a water-bearing Lathrop Formation. Well Moran-1, as shown in **Figure A-27**, is a good example, which suggests that the hydrocarbon accumulation at Union Island Gas Field is not continuous across the fault, supporting that the fault acts as a barrier to fluid flow. The cross section shown in **Figure A-27** also shows lack of hydrocarbon accumulation in the Winters Formation near the fault and updip where the sands transition into a shaley section. **Figure A-28** shows a localized structural section showing a more precise location of the Stockton Arch Fault between wells Sonol_Securities_8 and Moran_1 shown in the **Figure A-27** well correlation panel.

Shale Gouge Ratio

SGR is a fault seal algorithm used to estimate the sealing potential of a fault-zone (Yielding et al, 2010). The SGR calculation takes stratigraphic thickness, throw, and clay volume into consideration using the following equation:

$$SGR = \frac{\sum(Vcl \times \Delta z)}{throw} \times 100\% \qquad \text{(Eq-1)}$$

where Vcl is the clay volume content, Δz is the stratigraphic layer thickness, and $throw$ is the offset of the layer of interest. SGR values can vary along a fault as stratigraphic changes occur (Freeman et al., 1998). For the Stockton Arch Fault, the SGR was calculated at 10 different cross section locations along the length of the fault, each approximately 0.5 mile from the other. Each cross section ID has two SGR values: the first for the top of the Injection Zone and the second for the bottom of the Injection Zone. This give a total of 20 SGR values for the length of the Stockton Arch Fault in the CTV II Project area. The SGR was calculated at each point by using the Δz and Vcl of each layer that moved past the top and bottom of the Winters Injection Zone. $throw$ was calculated using the offset of both the top and bottom of the hanging wall Winters Formation from the top and bottom of the footwall Winters Injection Zone. The stratigraphic thickness and throw values were calculated using the Allan diagram described above. The Vcl values were calculated from well logs from 11 different project area wells located on both sides of the fault. Well locations are displayed in **Figure A-29**. **Table A-4** displays the Vcl values calculated for each well and the averaged stratigraphic value used in the

SGR calculation. **Figure A-30** shows the Allan diagram with SGR results and example calculations, using Eq-1, for cross section ID 4. Cross section ID 4 exhibits an SGR value of 35 percent at the top of the Winter Injection Zone and 43 percent at the bottom of the Winters Injection Zone. SGR values range from 35 to 42 percent and 37 to 43 percent along the top of Winters Sands and bottom of Winters sands at the Stockton Arch Fault, respectively. Overall, the Stockton Arch Fault has an average SGR value of 39 percent, with an average of 38 percent for the top of the Winters Injection Zone and 41 percent for the bottom of the Winters Injection Zone. SGR values >20 percent imply that there is a high chance of fault-zone seal (Yielding et al, 2010); therefore, the SGR values calculated for the Stockton Arch Fault in the project vicinity support that the fault is sealing.

Pressure Confirmation

To confirm pressure isolation within the Winters Formation prior to injection, pre-operational testing will include taking pressure measurements from the shallower zones (Mokelumne Formation) on the footwall side of the Stockton Arch Fault, as well as in the Lathrop Sands on the hanging wall side of the fault. The exact intervals to be tested will be based on reservoir properties during pre-operational testing.

2.4 Injection and Confining Zone Details [40 CFR 146.82(a)(3)(iii)]

2.4.1 Mineralogy

No quantitative mineralogy information exists within the AoR boundary. Mineralogy data will be acquired across all the zones of interest as part of pre-operational testing. Several wells outside the AoR have mineralogy over the respective formations of interest, and those data are presented below.

Winters Formation

Core descriptions for three wells within the AoR mention that the Winters Formation sandstone consists of "quartz, feldspar (plagioclase and K-spar), mica, ferromags, and lithics." Calcite-cemented intervals of sandstone are also present within the core, generally as thin "bones" or "sandstone 'shell,'" and are confirmed by log data. The exact mineralogic content of these bones is unknown. X-ray diffraction (XRD) data from GP_Dohrmann_1_RD1 in the Winters Formation confirm this general mineralogy (see **Figure A-31**). Reservoir sand from two samples in this well averages 67 percent quartz, 14 percent plagioclase and potassium feldspar, and 12 percent total clay (**Table A-5**). The primary clay minerals are kaolinite and smectite. Calcite and dolomite make up less than 3 percent of the samples.

Upper Confining Zone (Starkey-Sawtooth Shale)

No representative mineralogy data are available for the Upper Confining Zone. Mineralogy data are available for the H&T Shale, a similar Cretaceous-age shale directly above the Upper Confining Zone, from the Speckman_Decarli_1 well (see **Figure A-31**) in the form of XRD and Fourier transform infrared (FTIR) data. A total of 9 samples for this zone show an average of 46 percent total clay, with mixed layer illite/smectite the dominant species, with kaolinite and

chlorite still prevalent. They also contain 23 percent quartz, 29 percent plagioclase and potassium feldspar, 2 percent pyrite, and 1 percent calcite and dolomite (**Table A-5**).

Delta Shale

X-ray diffraction data are available for the Delta Shale in the GP_Dohrmann_1_RD1, but most of the samples were taken within sandy intervals. Two data points (10,077.5 and 10,090.5 feet MD) can be classified as shale based on their total clay weight percent. These samples average 46 percent total clay, with smectite and kaolinite as the major clay species. They also contain 40 percent quartz, 10 percent plagioclase and potassium feldspar, and 1 percent calcite and dolomite.

2.4.2 Porosity and Permeability

Winters Formation

Wireline log data were acquired with measurements that include but are not limited to spontaneous potential (SP), natural gamma ray, borehole caliper, compressional sonic, resistivity, neutron porosity, and bulk density. Formation porosity is determined one of two ways: from bulk density using 2.65 gram per cubic centimeter (g/cc) matrix density as calibrated from core grain density and core porosity data, or from compressional sonic using 55.5 microsecond per foot (μsec/ft) matrix slowness and the Raymer-Hunt equation.

Volume of clay is determined by spontaneous potential, and is calibrated to core data. Log-derived permeability is determined by applying a core-based transform that uses capillary pressure porosity and permeability along with clay values from XRD or FTIR analysis. Core data from two wells with 13 data points were used to develop a permeability transform. An example of the transform from core data is illustrated in **Figure A-32**.

In the example well Sonol_Securities_6 for the Winters Formation, the porosity ranges from 1 to 26 percent with a mean of 17 percent (**Figure A-33**). The permeability ranges from 0.0004 to 290 mD with a log mean of 5.6 mD (**Figure A-34**).

A log plot for Sonol_Securities_6 is included in **Figure A-35**. Core porosity and permeability are shown in comparison to log calculated porosity and permeability.

The average porosity for the Winters Formation is 18.9 percent, based on 19 wells with porosity logs and 8,518 individual logging data points. See **Figure A-36** for locations of wells used for porosity and permeability averaging.

The geometric average permeability for the Winters Formation is 13 mD, based on 19 wells with porosity logs and 7,993 individual logging data points. A total of 89 core data points from 2 wells, Sonol_Securities_4 and Sonol_Securities_6 (see **Figure A-36** for well locations) are from the Winters Formation. Porosity and permeability from these core data are in agreement with the log averages (see **Table A-6**).

Upper Confining Zone (Starkey-Sawtooth Shale)

The average porosity of the upper confining zone is 23.0 percent, based on 16 wells with porosity logs and 50,563 individual logging data points.

The geometric average permeability of the upper confining zone is 0.59 mD, based on 16 wells with porosity logs and 49,662 individual logging data points.

Delta Shale

The average porosity of the Delta Shale is 14.7 percent, based on 13 wells with porosity logs and 2,983 individual logging data points.

The geometric average permeability of the Delta Shale is 0.04 mD, based on 13 wells with porosity logs and 2,906 individual logging data points. A total of 25 core data points from the GP_Dohrmann_1_RD1 well (see **Figure A-31** for well location) are from this zone. Porosity and permeability from these core data are in agreement with the log averages (see **Table A-7**).

2.4.3 Injection and Confining Zone Capillary Pressure

Capillary pressure is the difference across the interface of two immiscible fluids. Capillary entry pressure is the minimum pressure required for an injected phase to overcome capillary and interfacial forces and enter the pore space containing the wetting phase.

No capillary pressure data were available for the Upper Confining Zone. These data will be acquired as part of pre-operational testing.

For the Injection Zone, capillary pressure data obtained from well Sonol Securities 5 in the Union Island Gas Field were used. **Figure A-37** shows the capillary pressure curve for the Injection Zone that was used for the computational modeling. Further details and location of the well are discussed in **Attachment B**.

2.4.4 Depth and Thickness

Depths and thickness of the Winters Formation reservoir and Starkey-Sawtooth Confining Zone (**Table A-8**) are determined by structural and isopach maps (**Figure A-38**) based on well data (wireline logs). Starkey-Sawtooth Shale and Winters Formation structural variability is due to the slight anticlinal structure. Starkey-Sawtooth Shale thickness variability is due to deposition of the Winters Formation. In the AoR, the shale minimum thickness corresponds to a high in Winters Formation sand thickness.

2.4.5 Structure Maps

Structure maps are provided to indicate a depth to reservoir adequate for supercritical-state injection.

2.4.6 Isopach Maps

SP logs from surrounding gas wells were used to identify sandstones. Negative millivolt deflections on these logs, relative to a baseline response in the enclosing shales, define the

sandstones. These logs were baseline shifted to 0 millivolts (mV). Due to the log vintage variability, there is an effect on quality that creates a degree of subjectivity within the gross sand; however, this will not have a material impact on the maps.

Variability in the thickness and depth of either the Starkey-Sawtooth Shale or the Winters Formation sandstone will not impact confinement. CTV will use thickness and depth shown when determining operating parameters and assessing project geomechanics.

2.5 Geomechanical and Petrophysical Information [40 CFR 146.82(a)(3)(iv)]

2.5.1 Caprock Ductility

Ductility and the unconfined compressive strength (UCS) of shale are two properties used to describe geomechanical behavior. Ductility refers to how much a rock can be distorted before it fractures, while the UCS is a reference to the resistance of a rock to distortion or fracture. Ductility generally decreases as compressive strength increases.

Ductility and rock strength calculations were performed based on the methodology and equations from Ingram and Urai (1999) and Ingram et al. (1997). Brittleness is determined by comparing the log-derived UCS to an empirically derived UCS for a normally consolidated rock (UCSNC):

$$\log UCS = -6.36 + 2.45 \log\left(0.86V_p - 1172\right) \quad \text{(Eq-2)}$$

$$\sigma' = OB_{pres} - P_p \quad \text{(Eq-3)}$$

$$UCS_{NC} = 0.5\sigma' \quad \text{(Eq-4)}$$

$$BRI = \frac{UCS}{UCS_{NC}} \quad \text{(Eq-5)}$$

Units for the UCS equation are *UCS* in MPa and V_p (compressional velocity) in m/s. OB_{pres} is overburden pressure, P_p is pore pressure, σ' is effective overburden stress, and *BRI* is brittleness index.

If the value of BRI is less than 2, empirical observation shows that the risk of embrittlement is lessened, and the confining zone is sufficiently ductile to accommodate large amounts of strain without undergoing brittle failure. However, if BRI is greater than 2, the "risk of development of an open fracture network cutting the whole seal depends on more factors than local seal strength and therefore the BRI criterion is likely to be conservative, so that a seal classified as brittle may still retain hydrocarbons" (Ingram and Urai, 1999).

Upper Confining Zone (Starkey-Sawtooth Shale)

Within the AoR, four wells had compressional sonic and bulk density data over the Upper Confining Zone to calculate ductility, comprising 9,633 individual logging data points (see pink squares in **Figure A-31**). A total of 16 wells had compressional sonic data over the Upper Confining Zone to calculate UCS, comprising 59,014 individual logging data points (see black circles in **Figure A-31**). The average ductility of the confining zone based on the mean value is 2.0. Additionally, 65 percent of the shale within the confining layer has a ductility less than 2. The average rock strength of the confining zone, as determined by the log-derived UCS equation above, is 4,593 psi.

An example calculation for the well Sonol_Securities_6 is shown below (**Figure A-39**). UCS_CCS_VP is the UCS based on the compressional velocity, UCS_NC is the UCS for a normally consolidated rock, and BRI is the calculated brittleness using this method. Brittleness less than 2 (representing ductile rock) is shaded red.

Within the upper confining zone, the brittleness calculation drops to a value less than 2. As a result of the Upper Confining Zone ductility, there are no fractures that will act as conduits for fluid migration from the Winters Formation. This conclusion is supported by the following:

- Prior to discovery, the Upper Confining Zone provided a seal to the underlying gas reservoir of the Winters Formation for millions of years.

2.5.2 Stress Field

The stress of a rock can be expressed as three principal stresses. Formation fracturing will occur when the pore pressure exceeds the least of the stresses. In this circumstance, fractures will propagate in the direction perpendicular to the least principal stress (**Figure A-40**).

Stress orientations in the Sacramento basin have been studied using both earthquake focal mechanisms and borehole breakouts (Snee and Zoback, 2020; Mount and Suppe, 1992). The azimuth of maximum principal horizontal stress (SHmax) was estimated at N40ºE ± 10º by Mount and Suppe (1992). Data from the World Stress Map 2016 release (Heidbach et al., 2016) show an average SHmax azimuth of N37.4ºE once several far field earthquakes with radically different SHmax orientations are removed (**Figure A-41**), which is consistent with Mount and Suppe (1992). The earthquakes in the area indicate a strike-slip/reverse faulting regime.

In the project AoR, there is no site-specific Winters Formation fracture pressure or fracture gradient. A Winters Formation step rate test will be conducted as per the preoperational testing plan. However, several wells have formation integrity tests (FITs) for shallower formations such as the H&T Shale and Mokelumne River Formation. A FIT performed in the H&T Shale in Sonol_Securities_8 recorded a minimum fracture gradient of 0.809 psi/ft. Four other wells within the field recorded minimum fracture gradients of 0.75 to 0.76 psi/ft based on FITs in the H&T Shale and Mokelumne River Formation (Yamada_Line_Well_1, Pool_B_2, Galli_1, and Galli_2). FIT data for three other wells across the Sacramento basin at depths between 8,800 and 10,800 feet TVD averaged 0.84 psi/ft (Transamerica_2-3, Serpa_5, and Wilcox_21). See **Figure A-42** for locations of all wells and **Table A-9** for the fracture gradient data points. For computational modeling, a frac gradient of 0.7 psi/ft was used, which should be below the actual frac gradient, assuming that the Winters Formation frac gradient would be similar to shallower zones.

In the project AoR, there are no site-specific fracture pressure or fracture gradient data for the Upper Confining Zone. A step rate test will be conducted in the Upper Confining Zone per the pre-operational testing plan. In the interim, CTV assumes that the upper confining zone will have a similar fracture gradient to the Winters Formation.

The overburden stress gradient in the reservoir and confining zone is 0.94 psi/ft. The overburden gradient was calculated by integrating density logs using methodology laid out in Fjaer et al (2008):

$$\sigma_v = \int_0^D \rho(z) g \, dz \quad \text{(Eq-6)}$$

where ρ is the density of the sediments, g is the acceleration due to gravity, D is the depth of interest, z is the vertical depth interval, and σ_v is the vertical stress. This calculation was completed using the "Overburden Gradient Calculation" module in the software Interactive Petrophysics 5.1.0. **Figure A-43** displays the overburden gradient calculation inputs and outputs from the software. See **Table A-10** for a list of the wells used for overburden stress gradient calculations.

No data currently exist for the pore pressure of the Confining Zone. This will be determined as part of the pre-operational testing plan.

2.5.3 Fault Reactivation

The stability of the Stockton Arch fault was analyzed using Mohr coulomb criteria at present-day conditions. The input parameters for the Mohr Circle are shown in **Table A-11**, and can be referenced in Sections 2.3.1 and 2.5.2. The maximum horizontal stress gradient was determined using data from Lund-Snee and Zoback (2020). The Stockton Arch fault was broken into two segments along the AoR boundary. Segment 1 has an average strike of 20 degrees and a dip of 50 degrees, and Segment 2 has an average strike of 40 degrees and a dip of 50 degrees. The maximum horizontal stress direction is 37.4 degrees as stated in Section 2.5.2. Based on Mohr circle analysis, the Winters Formation is currently far from failure, and will continue to be stable even after CO_2 injection has ceased (**Figure A-44**). The Stockton Arch fault plane is also aligned almost parallel to SHmax, which, in conjunction with its shallower dip, means that very large pore pressure increases would be required to cause reactivation in the present stress field. Analysis by Mohr circle shows that the pore pressure increase necessary to reactivate the two segments of the Stockton Arch fault is over 4,500 psi above present-day conditions (**Figure A-45**). This equates to a reservoir pressure of over 5,700 psi, far above both the reservoir pressure at field discovery (5,040 psi) and the final pressure after CO_2 injection has ceased (4,500 psi).

2.5.4 Reservoir Compaction

Compressibility was calculated for the Winters Formation using Newman's equation for consolidated sandstones (Newman, 1973). Using the average porosity of the Winters Formation of 18.9 percent, this yields a pore volume compressibility of 2.95 x 10^{-6} psi. From field discovery conditions to the present day, reservoir pressure has dropped from 5,040 psi to 1,200 psi, resulting in an effective stress increase on the rock of 3,840 psi. This results in a decrease in porosity from 18.9 to 18.69 percent, or a change of only 1 percent in porosity from the initial conditions.

2.6 Seismic History [40 CFR 146.82(a)(3)(v)]

Due to its lack of surface expression, the Stockton Arch fault has only been identified via subsurface data. As discussed in the prior Faults and Fractures section, 3D seismic and well data were used to create a depth surface for the fault. The trace of this fault generally agrees with that shown by the Fault Activity Map created by the California Geologic Survey and the U.S.

Geological Survey (USGS) (**Figure A-46**). The top of the fault is cut off by the base of the Valley Springs Formation, which unconformably overlays Eocene strata beneath it. The age of the Valley Springs Formation dates back to Early Miocene times, approximately 20 to 23 million years ago. While there is some folding of units above this unconformity, it is likely related to remnant structure associated with the fault. The seismic interpretation indicates that there is no appreciable offset on the Stockton Arch fault above this unconformity. The seismic interpretation of the base of the Valley Springs Formation and fault being cut off agree with the California Department of Conservation of Oil, Gas & Geothermal Resources Oil & Gas Technical Reports Volume III. (https://www.conservation.ca.gov/calgem/pubs_stats/Pages/technical_reports.aspx?msclkid=08d3028aa96811ec886f3c2f6cc3a20a).

The seismic interpretation provides an estimation of the time when the Stockton Arch fault was last actively growing. USGS (2024) provides an earthquake catalog tool that can be used to search for recent seismicity that could be associated with faults in the area for movement. A search was made for earthquakes in the greater vicinity of the project area from 1850 to modern day with events of a magnitude greater than 3. **Figure A-47** shows the results of this search and **Table A-12** summarizes some of the data taken from it.

The events in **Figure A-47** that could be associated with the Stockton Arch fault are Events 1, 10, and 5. Event 1 is a deep event (14.6 kilometers [km]) in 2010 that is likely related to basement movement, much deeper than the proposed Injection Zone or any of the sedimentary section in the basin. Event 10 is a shallower event (6.0 km) that occurred in 1944, before the Union Island Gas Field was discovered in 1972. Event 5 does sit along the trace of the Stockton Arch fault, but is farther away from Union Island Gas Field, and is therefore unrelated to Union Island Gas Field production or injection. The average depth of events from the USGS search results is 8.5 km, substantially deeper than the proper Winters Formation and the entire sedimentary section within the AoR.

While there is historical seismicity associated within the greater area, there is no clear link to the proposed injection site. There does not appear to be a causal relationship between natural gas and fluid production or injection and any seismic event in cataloged history around the depths of the Winters Formation. Seismic history shows no clustering of events around pre-existing Class II injection wells or increased levels of seismicity due to injection (**Figure A-47 and Table A-13**). Well "A. Lucas 1" is in proximity to a seismic event that occurred in 2010. However, this well was abandoned in 1988, having been drilled to 11,503 feet total depth in 1975. The event also had a recorded depth of 14.6 km, much deeper than the Class II well and the base of the sedimentary section in this locale (estimated to be 14,000 to 17,000 feet, or 4.3 to 5.2 km across the Stockton Arch fault).

By limiting the modeled reservoir pressure associated with the proposed injection to less than the original reservoir pressure, along with a 90 percent threshold, there is an effort to minimize any additional pressure on the fault beyond historical pressures. Additionally, due to the nature of the Stockton Arch fault and Union Island Gas Field being in the footwall of a thrust fault, the proposed Winters Injection Zone is offset against older strata with the same Confining Zones above. There would have to be significant reactivation of the fault as a normal fault to create offset that posed a risk for containment leaking across the fault. This would have to be in the order of thousands of feet. Pre-operational testing will include taking pressure measurements

from these shallower zones to confirm that the Winters Formation is an isolated reservoir with no vertical communication.

Lund-Snee and Zoback (2020) published updated maps for crustal stress estimates across North America. **Figure A-48** shows a modified image from that work highlighting CTV II. This work is in agreement with previous estimates of maximum horizontal stress in the region of approximately N40°E in a strike-slip to reverse stress regime (Mount and Suppe, 1992), and is consistent with World Stress map data for the area (Heidbach et al., 2016). During pre-operational testing and future injection, the fault will be monitored in both the hanging wall and footwall for pressure changes and any associated seismicity. **Attachment C** of this application discusses the seismicity monitoring plan for this injection site.

2.6.1 Seismic Hazard Mitigation

The Union Island Gas Field is in an area of historical seismicity, but no events have impacted its reservoirs or oil and gas infrastructure. There are several confining zones, beginning with the Starkey-Sawtooth Shale, that separate the Winters injection interval from USDWs.

The following is a summary of CTVs seismic hazard mitigation for CTV II:

The project has a geologic system capable of receiving and containing the volumes of CO_2 proposed to be injected.

- Extensive historical operations in the Winters Formation at Union Island Gas Field and other oil and gas fields that produce from the equivalent zone is valuable experience to understand operating conditions such as injection volumes and reservoir containment. The strategy to limit the injected CO_2 to beneath the initial reservoir pressure with a 90 percent threshold will mitigate the potential for induced seismic events and endangerment of the USDW.
- There are no faults or fractures identified in the AoR that will impact the confinement of CO_2 injectate. The Stockton Arch fault has proven to seal hydrocarbons at pressures above those at which CTV will operate.

Will be operated and monitored in a manner that will limit risk of endangerment to USDWs, including risks associated with induced seismic events.

- The strategy to limit the injected CO_2 to at or beneath the initial reservoir pressure will mitigate the potential for induced seismic events and endangerment of the USDW.
- Injection pressure will be lower than the fracture gradient of the sequestration reservoir with a safety factor (90 percent of the fracture gradient).
- Injection and monitoring well pressure monitoring will ensure that pressures are beneath the fracture pressure of the sequestration reservoir and Confining Zone. Injection pressure will be lower than the fracture gradients of the sequestration reservoir and Confining Zone with a safety factor (90 percent of the fracture gradients).

- A seismic monitoring program will be designed to detect events lower than seismic events that can be felt. This will ensure that operations can be modified with early warning events, before a felt seismic event.

Will be operated and monitored in a way that in the unlikely event of an induced event, risks will be quickly addressed and mitigated.

- Via monitoring and surveillance practices (pressure and seismic monitoring program), CTV personnel will be notified of events that are considered an early warning sign. Early warning signs will be addressed to ensure that more significant events do not occur.
- CTV will establish a central control center to ensure that personnel have access to the continuous data being acquired during operations.

Minimizing potential for induced seismicity and separating any events from natural to induced.

- Pressure will be monitored in each injector and sequestration monitoring well to ensure that pressure does not exceed the fracture pressure of the reservoir or Confining Zone.
- Seismic monitoring program will be installed pre-injection for a period to monitor for any baseline seismicity that is not being resolved by current monitoring programs.
- Average depth of prior seismic hazard in the region based on reviewed historical seismicity has been approximately 8.5 km, significantly deeper than the proposed Injection Zone.
- There is no evidence of causal seismicity associated with fluid production in the field.

2.7 Hydrologic and Hydrogeologic Information [40 CFR 146.82(a)(3)(vi), 146.82(a)(5)]

The California Department of Water Resources has defined 515 groundwater basins and subbasins with the state. The AOR is within the Tracy Subbasin (Subbasin No. 5-22.15), which lies in the northwestern portion of the San Joaquin Valley Groundwater Basin. **Figure A-49** shows the Tracy Subbasin and the surrounding areas. The Subbasin encompasses an area of about 238,429 acres (370 square miles) in San Joaquin and Alameda Counties (DWR, 2006).

2.7.1 Hydrologic Information

Major surface water bodies within the Tracy Subbasin consist of the San Joaquin, Old, and Middle Rivers. **Figure A-49** shows the locations of these surface water bodies. The San Joaquin River makes up almost the entire eastern boundary of the Subbasin. It feeds water into the SWP Clifton Court Forebay, which is located just west of the Subbasin.

Two major pump stations pump water out of the Old River from the Clifton Court Forebay into two large canals: the California Aqueduct and the Delta-Mendota Canal. These large canals traverse the southwestern portion of the Subbasin, and transport water from the Delta to other agricultural and urban water suppliers in the San Joaquin Valley and southern California. In addition to the major natural waterways, there is a large network of irrigation canals, which convey surface water to agricultural properties.

2.7.2 Base of Fresh Water and Base of USDWs

The owner or operator of a proposed Class VI injection well must define the general vertical and lateral limits of all USDWs and their positions relative to the Injection Zone and confining zones. The intent of this information is to demonstrate the relationship between the proposed injection formation and any USDWs, and it will support an understanding of the water resources near the proposed injection wells. A USDW is defined as an aquifer or its portion that supplies any public water system, or that contains a sufficient quantity of ground water to supply a public water system and currently supplies drinking water for human consumption, or contains less than 10,000 milligrams per liter (mg/L) total dissolved solids (TDS), and that is not an exempted aquifer.

Base of Fresh Water

The base of fresh water (BFW) helps define the aquifers that are used for public water supply. Local water agencies in the Tracy Subbasin have participated in various studies to comply with the 2014 Sustainable Groundwater Management Act (SGMA). Luhdorff & Scalmanini (2016) performed a study that focused on the geologic history of freshwater sediments from which groundwater is extracted for beneficial uses as defined and regulated under SGMA.

Few groundwater wells exist in the Tracy Subbasin because surface water is the source for irrigation use within delta islands. Groundwater usage is limited to eastern Contra Costa County and the Tracy area to the south. In most of western San Joaquin County in the Delta the fresh groundwater aquifers are limited to relatively shallow depths of 500 to 700 feet in the Contra Costa County area, and to 1,600 feet in the Tracy area (Luhdorff & Scalmanini, 2016).

Luhdorff & Scalmanini (1999) performed a study of over 500 well logs in eastern Contra Costa County groundwater for five water agencies. The focus of this study was the uppermost 500 feet, where most water wells were completed. Subsequently Luhdorff & Scalmanini (2016) used logs also examined for the nature of geologic units at greater depths to better define the BFW. The top of the geophysical logs tended to be at 800 feet or greater depths. These logs generally show fine-grained geologic units with few sand beds. The depth to BFW was difficult to discern in available geophysical logs because of the lack of sand beds. The elevation of the base of freshwater aquifers determined from logs were plotted on a base map (see **Figure A-50**). Contour lines of 100 feet were drawn, but are variable based on well control.

Base of USDWs

CTV has used geophysical logs to investigate the base of the USDW. The calculation of salinity from 41 wells used by CTV is a four-step process (see **Table A-14** for list of wells and well locations displayed at **Figure A-51**):

1. Convert measured density or sonic to formation porosity

The equation to convert measured density to porosity is:

$$POR = \frac{(Rhom - RHOB)}{(Rhom - Rhof)} \qquad \text{(Eq-7)}$$

where POR = formation porosity

Rhom = formation matrix density (g/cc); 2.65 g/cc used for sandstones
RHOB = calibrated bulk density taken from well log measurements (g/cc)
Rhof = fluid density (g/cc); 1.00 g/cc used for water-filled porosity

The equation to convert measured sonic slowness to porosity is:

$$POR = -1\left(\frac{\Delta tma}{2\Delta tf} - 1\right) - \sqrt{\left(\frac{\Delta tma}{2\Delta tf} - 1\right)^2 + \frac{\Delta tma}{\Delta tlog} - 1} \quad \text{(Eq-8)}$$

where POR = formation porosity
Δtma = formation matrix slowness (μs/ft); 55.5 μs/ft used for sandstones
Δtf = fluid slowness (μs/ft); 189 μs/ft used for water-filled porosity
Δtlog = formation compressional slowness from well log measurements (μs/ft)

2. Calculate apparent water resistivity using the Archie equation:

$$Rwah = \frac{POR^m R_t}{a} \quad \text{(Eq-9)}$$

where Rwah = apparent water resistivity (ohmm)
POR = formation porosity
m = the cementation factor; 2 is the standard value
Rt = deep reading resistivity taken from well log measurements (ohm-m)
a = the Archie constant; 1 is the standard value

3. Correct apparent water resistivity to a standard temperature of 75°F:

$$Rwahc = Rwah\frac{TEMP+6.77}{75+6.77} \quad \text{(Eq-10)}$$

where Rwahc = apparent water resistivity (ohm-m), corrected to surface temperature
TEMP = downhole temperature based on temperature gradient (°F)

4. Covert temperature-corrected apparent water resistivity to salinity (Davis 1988):

$$SAL\_a\_EPA = \frac{5500}{Rwahc} \quad \text{(Eq-11)}$$

where SAL_a_EPA = salinity from corrected Rwahc (ppm)

The BFW and the USDW are shown on the geologic cross section A-A' (**Figure A-14**). **Figure A-52** displays a plan-view map of the base USDW elevation. The BFW and base of the lowermost USDW are at measured depths of approximately 600 feet below ground surface (bgs) and 2,400 feet bgs, respectively.

2.7.3 Formations with USDWs

Formations with USDWs, from youngest to oldest, include alluvium, flood basin and intertidal deposits, alluvial fan deposits, Older Alluvium, Modesto Formation, Los Banos Alluvium, Tulare Formation, and fanglomerates. These formations, except for the Tulare Formation, are shown on **Figure A-49**. The Tulare Formation is not exposed at ground surface. The cumulative thickness of these formations increases from about 330 feet near the Coast Range foothills to

about 2,000 feet just north of Tracy. Information regarding the water-bearing units and groundwater conditions were taken from several sources (Hotchkiss and Balding, 1971; Bertoldi et al., 1991; Davis et al., 1959) and sorted to agree with more recent geologic map compilation (Wagner et al., 1991).

Alluvium

The alluvium (Q) includes sediments deposited in the channels of active streams, as well as overbank deposits and terraces of those streams. They consist of unconsolidated silt, sand, and gravel. Sand and gravel zones in the younger alluvium are highly permeable and yield significant quantities of water to wells. The thickness of the younger alluvium in the Tracy Subbasin is less than 100 feet (DWR, 2006).

Flood Basin and Intertidal Deposits

The flood basin deposits (Dos Palos Alluvium [Qdp]) and intertidal deposits (Qi) are in the Delta portions of the Subbasin. These sediments consist of peaty mud, clay, silt, sand, and organic materials. Stream-channel deposits of coarse sand and gravel are also included in this unit. The flood basin deposits have low permeability, and generally yield low quantities of water to wells due to their fine-grained nature. Flood basin deposits generally contain poor quality groundwater with occasional zones of fresh water. The maximum thickness of the unit is about 1,400 feet (DWR, 2006).

Alluvial Fan Deposits

Along the southern margin of the Subbasin in the Non-Delta uplands areas of the Subbasin, are fan deposits (Qf) from the Coast Ranges. These deposits consist of loosely to moderately compacted sand, silt, and gravel deposited in alluvial fans during the Pliocene and Pleistocene ages. The fan deposits likely interfinger with the flood basin deposits. The thickness of these fans is about 150 feet (DWR, 2006).

Modesto Formation

The Modesto Formation (Qm) is located along the east side of the San Joaquin River, and is slightly older that the alluvial fan deposits. The formation consists of granitic sands over stratified silts and sands. Near the southern margin of the Tracy Subbasin, there are small occurrences of Los Banos Alluvium (Qlb) and Older Alluvium (Qo) that are of similar age to the Modesto Formation (GEI, 2021).

Tulare Formation

The Tulare Formation is Pleistocene in age, and consists of semi-consolidated, poorly sorted, discontinuous deposits of clay, silt, sand, and gravel. The Tulare Formation is not exposed at ground surface in the Tracy Subbasin. The Tulare Formation sand and gravel deposits are moderately permeable, and most of the larger agricultural, municipal, and industrial supply wells extract water from this formation. Wells completed in the Tulare Formation can produce up to 3,000 gallons per minute (gpm). The thickness of the Tulare Formation is about 1,400 feet (GEI, 2021).

Within the Tulare Formation is the Corcoran Clay, one of the largest lakebed deposits in the San Joaquin Valley. The clay is about 60 to 100 feet thick. **Figure A-53** shows the lateral extent and structure of the Corcoran Clay. Near the southern edge of the Subbasin, the Corcoran Clay is apparently absent. The extent of the Corcoran Clay is not fully characterized to the west and north (Page, 1986) due to the lack of deep wells. Geologic sections indicate that the clay likely continues to the west, into the East Contra Costa Subbasin (GEI, 2007).

Undifferentiated Non-Marine Sediments

The upper Paleogene and Neogene sequence begins with the Valley Springs Formation, which represents fluvial deposits that blanket the entire southern Sacramento Basin. The unconformity at the base of the Valley Springs marks a widespread Oligocene regression, and separates the more deformed Mesozoic and lower Paleogene strata below from the less deformed uppermost Paleogene and Neogene strata above. These undifferentiated non-marine sediments contain approximately 3,000 to 10,000 mg/L TDS water and comprise the lowermost USDW in the AoR.

2.7.4 Geologic Cross Sections Illustrating Formations with USDWs

Geologic sections (locations are shown on **Figure A-49**) cross the length of the Subbasin to illustrate the relationship of the geologic units. The geologic sections were originally prepared for the Tracy Subbasin Groundwater Management Plan (GEI, 2007), and were modified for the Tracy Subbasin GSP (GEI 2021) to reflect additional information obtained since 2007. Lithologic information from well logs was normalized and digitized to generally conform with the Unified Soil Classification System (USCS). Lithology and well screens from groundwater monitoring wells constructed since the sections were created were also added to the geologic sections. The soil profiles show the subsurface relationships and location of the formations and coarse-grained sediments that comprise the principal aquifers. The cross sections show the sediment types, the approximate BFW, and the estimated contact between the Tulare Formation sediments and younger formations. The cross sections also illustrate the location and extent of the Corcoran Clay (GEI, 2021).

Geologic cross section B-B' (**Figure A-54**) runs northwest-southeast through the non-Delta and Delta portions of the Tracy Subbasin. The Subbasin generally has low-permeability clays and silts (shown in brown color) near surface and permeable sediments (sands and gravels shown in light blue) scattered throughout the profile. Continuous layers of sand and gravels, other than one at the top of the Corcoran Clay, have not been identified. The lack of continuous layers of sand and gravels is likely due to the nature of the river channels and flood deposits associated with these types of sediments. The Corcoran Clay (or its equivalent) seems to extend to the west and into the East Contra Costa Subbasin. In the southern non-Delta portion of the Subbasin, fine-grained sediments are more prevalent. Based upon groundwater levels and water quality information, the shallow aquifer is likely unconfined and separated from the deeper confined aquifer (GEI, 2021).

Geologic cross section C-C' (**Figure A-55**) runs in a northeast-southwest orientation across the Delta area. This geologic section illustrates the types of sediments, the estimated BFW, and the possible location of the Corcoran Clay (or its equivalent). Where the clay location is uncertain, no wells were present that penetrated deep enough to confirm its presence or absence. The BFW

varies throughout the Subbasin, and is shown on the sections. It is as shallow as -400 feet msl to as deep as -2,000 feet msl (GEI, 2021).

2.7.5 Principal Aquifers

The Tracy Subbasin has two principal aquifers that are separated by the Corcoran Clay. Where the clay is absent, which is the condition within most of the Delta area, only the Upper Aquifer is present. The Upper and Lower Aquifers combine where the Corcoran Clay is absent, near the southwestern portion of the Subbasin adjacent to the foothills. In this area, the aquifers would be unconfined and are the Upper Aquifer. The Upper and Lower Aquifers also merge north of the Old River in the northern part of the Subbasin (GEI, 2021).

TDS data from water supply wells in the vicinity of CTV II were obtained from GAMA (2023), and maximum values at each well location (2013–2023) are shown on **Figure A-56**. TDS values range from 159 to 1,070 mg/L at these wells. In most cases, well depth and perforated interval are not known for the GAMA wells with TDS data; however, where available, well depth ranges from 140 to 732 feet.

Upper Aquifer

The Upper Aquifer is used by domestic, community water systems and for agriculture. The Upper Aquifer also supports native vegetation where groundwater levels are less than 30 feet bgs (GEI, 2021).

The Upper Aquifer is an unconfined to semi-confined aquifer. It is present above the Corcoran Clay and where the clay is absent. The Upper Aquifer exists in the alluvial fan deposits, intertidal deposits, Modesto Formation, flood basin deposits, and the upper portions of the Tulare Formation.

There are multiple coarse-grained sediment layers that make up the unconfined aquifer; however, the water levels are generally similar. The aquifer confinement generally tends to increase with depth, becoming semi-confined. There is also typically a downward gradient in the aquifers (Hotchkiss and Balding, 1971) in the non-Delta areas; the gradient ranges from a few feet bgs to as much as 70 feet bgs. The groundwater levels in the Upper Aquifer are usually 10 to 30 feet higher than in the Lower Aquifer. The groundwater levels in the Delta are typically at sea level, and artesian flowing wells are common in the center of the islands (Hydrofocus, 2015).

The hydraulic characteristics of the unconfined aquifer are highly variable. USGS estimated horizontal hydraulic conductivity values for organic sediments ranging from 0.0098 feet per day (ft/d) to 133.86 ft/d (Hydrofocus, 2015). Wells in the unconfined aquifer produce 6 to 5,300 gpm. The transmissivity of the unconfined aquifers ranges from 600 gallons per day per foot (gpd/ft) to greater than 2,300 gpd/ft. The storativity is about 0.05 (GEI, 2021).

Water quality in the Upper Aquifer is mostly transitional, with no single predominant anion. Most waters are characterized as sulfate bicarbonate and chloride bicarbonate type (Hotchkiss and Balding, 1971). The TDS of these transitional water ranges from 400 to 4,200 mg/L. Nitrate concentrations are generally high in the Upper Aquifer in the non-Delta portions of the

Subbasin. Nitrate concentrations are generally low in the Delta portions of the Subbasin (GEI, 2021).

Lower Aquifer

The Lower Aquifer is typically used by community water systems (City of Tracy) and agriculture. The Lower Aquifer is mainly composed of the lower portions of the Tulare Formation below the Corcoran Clay, and extends to the BFW. The clay is present in the southern third of the Subbasin; the clay's extent to the west and north is uncertain, and has been estimated to have a vertical permeability ranging from 0.01 to 0.007 ft/d (Burow et al., 2004).

The groundwater levels are generally deeper than water levels in the Upper Aquifer (Hotchkiss and Balding, 1971). Groundwater levels in the confined aquifer are about -25 to -75 feet msl. Groundwater levels are normally 60 to 200 feet above the top of the Corcoran Clay.

Wells in the Lower Aquifer produce about 700 to 2,500 gpm. The transmissivity typically ranges from 12,000 to 37,000 gpd/ft, but can be 120,000 gpd/ft. The storage coefficient or storativity has been measured to be 0.0001 (Padre, 2004).

Water quality in the Lower Aquifer in the western portions is chloride type water, but mostly transitional type of sulfate chloride near the valley margins and sulfate bicarbonate and bicarbonate sulfate near the San Joaquin River (Hotchkiss and Balding, 1971). In general, the TDS concentrations range from 400 to 1,600 mg/L. Nitrate concentrations are typically low in the Lower Aquifer. Wells completed below the Corcoran Clay sometimes have elevated levels of sulfate and TDS above the drinking water maximum contaminant levels (MCLs). Chloride concentrations are elevated at only one deep location, east of Tracy (GEI, 2021).

2.7.6 Potentiometric Maps

The Tracy Subbasin GSP (GEI, 2021) used groundwater level measurements in over 226 wells, which have been reported to DWR's CASGEM or Water Data Library systems. To evaluate groundwater levels, the GSP only used wells with known total depths and construction details so that the wells were assigned to a principal aquifer. To supplement data from these wells, additional monitoring wells were located that were being used for other regulatory programs.

Upper Aquifer

Groundwater elevations in the Delta area are typically below sea level because the ground surface in the islands has subsided to below sea level; the drains within the island keep groundwater levels below ground surface to allow for farming. **Figure A-57** shows a schematic profile for groundwater surfaces that are expected at the islands. Although each island has distinct groundwater elevations, there are similar hydraulics on all islands. Groundwater elevations are higher near the island edges (adjacent to waterways), and deepen equivalent with the deepest land surface and drain. Groundwater elevations in the islands are managed by the elevations of the drains and canals. There is very little, if any, pumping of wells for agriculture. Because drains and canals control the groundwater elevations, groundwater contours are not developed/monitored for the Delta islands (GEI, 2021).

In the non-Delta areas west of the San Joaquin River, groundwater contours for the Upper Aquifer indicate that groundwater elevations are highest near the Coast Ranges and decrease toward the Delta. Flow directions indicate that recharge areas are present along the foothills, and that groundwater discharges into the Old River and/or Tom Paine Slough (**Figure A-58**). Groundwater gradients in the non-Delta portions of the Subbasin are the steepest, at approximately 0.008 foot per foot (ft/ft). East of the San Joaquin River, near Lathrop, the river recharges the Upper Aquifer, and flows toward a pumping depression near Stockton. Groundwater contours at the southeastern edge of the Subbasin are perpendicular to the Stanislaus-San Joaquin County line, suggesting that there is no flow in the Upper Aquifer between the subbasins other than the areas of the Delta Mendota Subbasin north of the County line, where water apparently flows into and out of both subbasins.

Lower Aquifer

The Corcoran Clay extends throughout the non-Delta areas and only slightly into the Delta area, at Union Island. Groundwater contours for the Lower Aquifer were developed using data from the CASGEM monitoring wells that are constructed below the Corcoran Clay and supplemented by data from municipal wells (**Figure A-59**). Groundwater monitoring well data were used from the adjacent Delta Mendota Subbasin (GEI, 2021).

Groundwater elevation contours in the Lower Aquifer imply that groundwater is entering the subbasin from the south (Delta Mendota Subbasin) and from the east (Eastern San Joaquin Subbasin). Pumping in the vicinity of the City of Tracy has apparently modified this overall regional flow, resulting in a pumping depression toward the City of Tracy. The groundwater levels are expected to be at sea level near the northern edge of the Corcoran Clay extent (GEI, 2021).

The groundwater gradient in fall 2019 from the Delta Mendota and the Eastern San Joaquin subbasins is estimated to be 0.0009 ft/ft into the Tracy Subbasin. Due to the pumping depression, the gradient increases around the City of Tracy. The gradient near the western edge of the subbasin cannot be determined due to the lack of monitoring wells constructed below the Corcoran Clay (GEI 2021).

2.7.7 Water Supply and Groundwater Monitoring Wells

The GAMA, DWR, CASGEM, and other public databases were searched to identify any water supply and groundwater monitoring wells within a 1-mile radius of the AOR. A total of 87 water wells were identified within 1 mile of the AoR. Data provided from public databases indicate that the wells identified are completed much shallower than the proposed Injection Zone. A map of well locations and table of information are found in **Figure A-60 and Table A-15**, respectively.

Groundwater in the Subbasin is used for municipal, industrial, irrigation, domestic, stock watering, frost protection, and other purposes. The number of water wells is based on well logs filed and contained within public records, and may not reflect the actual number of active wells because many of the wells contained in files may have been destroyed and others may not have been recorded.

There are many more wells in the non-Delta areas, south of the Old River, than in the Delta area of the Subbasin. The depths of wells are generally deeper in the non-Delta portion of the Subbasin than in the Delta portion of the Subbasin. The domestic wells are constructed to shallower depths than the production wells. The municipal wells are generally constructed deeper than either the domestic or production wells (GEI, 2021).

2.8 Geochemistry [40 CFR 146.82(a)(6)]

2.8.1 Formation Geochemistry

Winters Formation

As noted in the mineralogy section (Section 2.4.1).

Upper Confining Zone (Starkey-Sawtooth Shale)

As noted in the mineralogy section (Section 2.4.1).

Delta Shale

As noted in the mineralogy section (Section 2.4.1).

2.8.2 Fluid Geochemistry

The Winters Formation contains both saline water and gaseous hydrocarbon within the AoR. The well Sonol_Securities_4 was sampled for water in 2015. The measurement of TDS for the sample was 15,595 mg/L. The complete water chemistry is shown in **Figure A-61**.

Gas analysis for Sonol_Securities_5 was performed in 2022. The gas is primarily methane and nitrogen, with very minor ethane and carbon dioxide. The full gas chromatography is included in **Figure A-62**.

The locations of Sonol_Securities_4 and Sonol_Securities_5 are shown in **Figure A-63**.

The properties of the formation fluids are summarized in **Table A-16**.

2.8.3 Fluid-Rock Reactions

Winters Formation

Mineralogy and formation fluid interactions have been assessed for the Winters Formation. The following applies to potential reactions associated with the CO_2 injectate: The Winters Formation has a negligible quantity of carbonate minerals, and is instead dominated by quartz and feldspar. These minerals are stable in the presence of CO_2 and carbonic acid, and any dissolution or changes that occur will be on grain surfaces.

The water within the Winters Formation contains minimal calcium and magnesium cations, which would be expected to react with CO_2 to form calcium-bearing minerals in the pore space. Also, the relatively low salinity will reduce the “salting out” effect seen in higher salinity brine under the presence of CO_2.

Upper Confining Zone (Starkey-Sawtooth Shale)

There is no fluid geochemistry analysis for the Upper Confining Zone. The shale will only provide fluid for analysis if stimulated. However, given the low permeability of the rock and the low carbonate content, the Upper Confining Zone is not expected to be impacted by the CO_2 injectate.

Delta Shale

There is no fluid geochemistry analysis for the Delta Shale. The shale will only provide fluid for analysis if stimulated. However, given the low permeability of the rock and the low carbonate content, the Delta Shale is not expected to be impacted by the CO_2 injectate.

Geochemical Modeling

Using fluid geochemistry data for the Injection Zone and the available mineralogy data for the Injection Zone and the Upper Confining Zone, geochemical modeling was conducted using PHREEQC (ph-REdox-Equilibrium), the USGS geochemical modeling software, to evaluate the compatibility of the injectates being considered for the project with formation rocks and fluid.

PHREEQC software was used to evaluate the behavior of minerals and changes in aqueous chemistry and mineralogy over the life of the project, and to identify major potential reactions that may affect injection or containment.

Based on the geochemical modeling, the injection of CO_2 at the CTV II site does not cause significant reactions that will affect injection or containment. Detailed methodology and results can be found in **Appendix 3: CTV II Geochemical Modeling**.

2.9 Other Information (Including Surface Air and/or Soil Gas Data, if Applicable)

No additional information necessary.

2.10 Site Suitability [40 CFR 146.83]

Sufficient well and seismic data demonstrate the lateral continuity of the Starkey-Sawtooth Shale Confining Zone and the Winters Formation Injection Zone. Regional mapping completed by West Coast Regional Carbon Sequestration Partnership (WESTCARB), CGS, and the National Energy and Technology Lab (NETL) support our local stratigraphy, indicating both lateral continuity and regional thickness across the AoR (Downey, 2010). This study covers formations with sequestration and seal potential from southern Sutter County down to the Stockton Arch fault in San Joaquin County, encompassing an area far beyond the AoR presented in **Attachment B**.

The vertically confined and laterally continuous reservoir will compensate for the CO_2 as the plume migrates further to the northwest away from the barrier and the Stockton Arch fault. The Starkey-Sawtooth is a continuous shale, and will guide the lateral dispersion of CO_2 across the AoR (**Figures A-64a and A-64b**). Surrounding oil and gas fields in the area demonstrate adequate seal capacity in the Upper Confining Zone and surrounding faults.

Thickness maps and petrophysics demonstrate confinement based on the Upper Confining Zone's lateral continuity, low permeability, and thickness. Faulting does exist on the east edge of the CO_2 plume; however, thickness maps support an adequate seal across this offset as discussed in Section 2.6. Pressures along bounding faults will be estimated using computational modeling and in-zone monitoring wells to mitigate the possibility of fault reactivation.

Due to the regional continuity and low permeability of the Upper Confining Zone (Starkey-Sawtooth), no Secondary Confining Zone is necessary; however, other shale barriers do exist above the Mokelumne River Formation monitoring sand. These act as additional impermeable zones of confinement separating the Injection Zone from the USDW.

CTV estimates that maximum storage for the proposed project is 23 MMT of CO_2. This was derived from computational modeling as described below.

As discussed in **Attachment B**, a dynamic model was generated with data from the static model (structure, porosity, absolute permeability, net to gross ratio, facies), special core analysis (relative permeability and capillary pressure), pressure, volume, temperature (PVT) analysis (fluid PVT), geochemical analysis (water salinity), and a 2022 pressure temperature survey (reservoir pressure). In addition, model structures and contacts are based on field development history, engineering analysis, and material balance modeling. Injector locations are based on geologic interpretation, petrophysical properties, production history, wellbore integrity, and economic optimization. Injection rates are based on field history, and were analyzed with flexibility to handle offset well failure during the project period. Injectors were also designed with a maximum allowable injection pressure limit. To assure storage site safety during the injection period, reservoir pressure was controlled below the discovery reservoir pressure. The proposed post-injection reservoir pressure of 4,500 psi is 90 percent of the discovery pressure. Dynamic model results predicted a storage volume of 22.7 MMT at 23.5 years.

A study completed by Stanford University estimated CO_2 storage volumes of gas reservoirs near the vicinity of the Union Island gas reservoir (Kim et al., 2022). Estimated storage volumes were calculated for Rio Vista gas reservoir (130.6 MMT CO_2), Grimes gas reservoir (60.6 MMT CO_2), Lathrop gas reservoir (43.5 MMT CO_2), McDonald Island Gas reservoir (22.2 MMT CO_2), and Wild Goose Gas reservoir (22.1 MMT CO_2). The Lathrop gas reservoir located approximately 4 miles east of the Union Island gas reservoir provides a fair comparison based on similar geology. Cumulative gas production from the Lathrop gas reservoir is 365 bcf plus minor water, while cumulative gas production from Union Island gas reservoir is 292 bcf plus minor water. Using the Stanford University methodology CTV expects the Union Island Gas Field to have a similar CO_2 storage capacity to the Lathrop Gas Field. This methodology shows that the dynamic model predicted storage volume of 22.7 MMT is conservative.

3. AoR and Corrective Action

Attachment B, pursuant to 40 CFR 146.82(a)(4), 40 CFR 146.82(a)(13) and 146.84(b), and 40 CFR 146.84(c), describes the process, software, and results to establish the AoR, and the wells that require corrective action.

AoR and Corrective Action GSDT Submissions
GSDT Module: AoR and Corrective Action ***Tab(s):*** All applicable tabs Please use the checkbox(es) to verify the following information was submitted to the GSDT: ☒ Tabulation of all wells within AoR that penetrate confining zone ***[40 CFR 146.82(a)(4)]*** ☒ AoR and Corrective Action Plan ***[40 CFR 146.82(a)(13) and 146.84(b)]*** ☒ Computational modeling details ***[40 CFR 146.84(c)]***

4. Financial Responsibility

CTV's Financial Responsibility demonstration pursuant to 140 CFR 146.82(a)(14) and 40 CFR 146.85 is met with a line of credit for Injection Well Plugging and Post-Injection Site Care and Site Closure and insurance to cover Emergency and Remedial Responses.

Financial Responsibility GSDT Submissions
GSDT Module: Financial Responsibility Demonstration ***Tab(s):*** Cost Estimate tab and all applicable financial instrument tabs Please use the checkbox(es) to verify the following information was submitted to the GSDT: ☒ Demonstration of financial responsibility ***[40 CFR 146.82(a)(14) and 146.85]***

5. Injection and Monitoring Well Construction

CTV requires 15 wells for injection and monitoring associated with CTV II, including 5 injectors, 4 Injection Zone monitoring wells, 2 above zone monitoring wells, 1 eastern fault block monitoring well, and 3 USDW monitoring wells. A total of 5 injection wells, 2 Injection Zone monitoring wells, 1 eastern fault block monitoring well, and 3 USDW monitoring wells will be designed and constructed specifically for CTV II. CTV plans to repurpose 4 existing wells by converting them to monitoring wells (2 Injection Zone monitoring wells, and 2 above zone monitoring wells). During pre-operational testing, the existing wells will undergo diagnostic testing to ensure suitability for conversion and reuse with CTV II. Based on results, CTV will either demonstrate applicability pursuant to 40 CFR 146.81(c) or will propose to construct a new well in the same location. **Figure A-65** shows the wells proposed for the project.

All planned new wells will be constructed with components that are compatible with the injectate and formation fluids encountered such that corrosion rates and cumulative corrosion over the duration of the project are acceptable. The proposed well materials will be confirmed based on actual CO_2 composition such that material strength is sufficient to withstand all loads encountered throughout the life of the well with an acceptable safety factor incorporated into the design. Casing points will be verified by trained geologists using real-time drilling data such as

LWD and mud logs to ensure non-endangerment of USDW. Due to the depth of the base of USDW, a secondary casing string will be used to isolate the USDW. Cementing design, additives, and placement procedures will be sufficient to ensure isolation of the Injection Zone and protection of USDWs using cementing materials that are compatible with injectate, formation fluids, and subsurface pressure and temperature conditions.

The pressure within the Injection Zone has been depleted to approximately 1,200 psi, and the temperature is approximately 218°F. These conditions are not extreme, and CTV has extensive experience successfully constructing, operating, working over, and plugging wells in depleted reservoirs.

Appendix 5: Injection and Monitoring Well Schematics provides casing diagram figures for all injection and monitoring wells with construction specifications and anticipated completion details in graphical and/or tabular format.

5.1 Proposed Stimulation Program [40 CFR 146.82(a)(9)]

There are currently no proposed stimulation programs.

5.2 Well Construction Procedures [40 CFR 146.82(a)(12)]

CTV has created Construction and Plugging documents for each project well throughout the application documentation pursuant to 40 CFR 146.82(a)(8). Each **Attachment G: Well Construction and Plugging Plan** document includes well construction information based on requirements defined within 40 CFR 146.82. The relevant attachments are:

- Attachment G1: Sonol Securities 1-A Construction and Plugging Plan
- Attachment G2: Sonol Securities 3 Construction and Plugging Plan
- Attachment G3: Pool B-2 Construction and Plugging Plan
- Attachment G4: UI_INJ-1 Construction and Plugging Plan
- Attachment G5: UI_INJ-2 Construction and Plugging Plan

6. Pre-Operational Logging and Testing

CTV has indicated a proposed pre-operational logging and testing plan throughout the application documentation pursuant to 40 CFR 146.82(a)(8). Each **Attachment G: Well Construction and Plugging Plan** document (listed in Section 5.2) includes logging and testing plans for each individual project well based on requirements defined within 40 CFR 146.87.

Pre-Operational Logging and Testing GSDT Submissions
GSDT Module: Pre-Operational Testing ***Tab(s):*** Welcome tab Please use the checkbox(es) to verify the following information was submitted to the GSDT: ☒ Proposed pre-operational testing program ***[40 CFR 146.82(a)(8) and 146.87]***

7. Well Operation

7.1 Operational Procedures [40 CFR 146.82(a)(10)]

The Operational Procedures for all injectors associated with the project are detailed in **Appendix 4: Operational Procedures** included with this application.

7.2 Proposed Carbon Dioxide Stream [40 CFR 146.82(a)(7)(iii) and (iv)]

CTV is planning to construct a carbon capture and sequestration "hub" project (i.e., a project that collects CO_2 from multiple sources over time and injects the CO_2 stream(s) via a Class VI UIC permitted injection well[s]). Therefore, CTV is currently considering multiple sources of anthropogenic CO_2 for the project. The potential sources include capture from existing and potential future industrial sources, as well as direct air capture (DAC). CTV would expect the CO_2 stream to be sampled at the transfer point from the source and/or between the final compression stage and the wellhead. Samples will be analyzed according to the analytical methods described in **Appendix 11: QASP** (Table 4) and **Attachment C** (Table C-1).

For the purposes of geochemical modeling, CO_2 plume modeling, AoR determination, and well design, two major types of injectate compositions were considered based on the source:

- Injectate 1: A potential injectate stream composition from direct air capture or a pre-combustion source (such as a blue hydrogen facility that produces hydrogen using steam methane reforming process) or a post-combustion source (such as a natural gas fired power plant or steam generator). The primary impurity in the injectate is nitrogen.
- Injectate 2: A potential injectate stream composition from a biofuel capture source (such as a biodiesel plant that produces biodiesel from a biologic source feedstock) or from an oil and gas refinery. The primary impurity in the injectate is light end hydrocarbons (methane and ethane).

The compositions for these two injectates are shown in **Table A-17**, and are based on engineering design studies and literature.

For geochemical and plume modeling scenarios, these injectate compositions were simplified to a 4-component system, shown in **Table A-18**, and then normalized for use in the modeling. The 4-component simplified compositions cover 99.9 percent by mass of Injectate 1 and 2 and cover particular impurities of concern (H_2S and SO_2). The estimated properties of the injectates at downhole conditions are specified in **Table A-19**.

The anticipated injection temperature at the wellhead is 90 to 130°F.

No corrosion is expected in the absence of free phase water provided that the entrained water is kept in solution with the CO_2. This is ensured by maintaining a <25 lb/mmscf injectate specification limit, and this specification will be a condition of custody transfer at the capture facility. For transport through pipelines, which typically use standard alloy pipeline materials, this specification is critical to the mechanical integrity of the pipeline network, and out of specification product will be immediately rejected. Therefore, all product transported through pipeline to the injection wellhead is expected to be dry-phase CO_2 with no free-phase water present.

Injectate water solubility will vary with depth and time as temperature and pressures change. The water specification is conservative to ensure water solubility across supercritical operating ranges. Corrosion-resistant alloy (CRA) tubing will be used in the injection wells to mitigate any potential corrosion impact should free-phase water from the reservoir become present in the wellbore, such as during shut-in events when formation liquids, if present, could backflow into the wellbore. CTV may further optimize the maximum water content specification prior to injection based on technical analysis.

8. Testing and Monitoring

Attachment C: Testing and Monitoring Plan (**Attachment C**), pursuant to 40 CFR 146.82 (a)(15) and 40 CFR 146.90, describes the strategies for testing and monitoring to ensure protection of the USDW, injection well mechanical integrity, and plume monitoring.

Testing and Monitoring GSDT Submissions
GSDT Module: Project Plan Submissions ***Tab(s):*** Testing and Monitoring tab Please use the checkbox(es) to verify the following information was submitted to the GSDT: ☒ Testing and Monitoring Plan ***[40 CFR 146.82(a)(15) and 146.90]***

9. Injection Well Plugging

Attachment D: Injection Well Plugging Plan (**Attachment D**), pursuant to 40 CFR 146.92, describes the process, materials and methodology for injection well plugging.

Injection Well Plugging GSDT Submissions
GSDT Module: Project Plan Submissions ***Tab(s):*** Injection Well Plugging tab Please use the checkbox(es) to verify the following information was submitted to the GSDT: ☒ Injection Well Plugging Plan ***[40 CFR 146.82(a)(16) and 146.92(b)]***

10. Post-Injection Site Care (PISC) and Site Closure

CTV has developed **Attachment E: Post-Injection Site Care and Site Closure Plan** (**Attachment E**) pursuant to 40 CFR 146.93(a) to define post-injection testing and monitoring.

At this time, CTV is not proposing an alternative PISC time frame.

PISC and Site Closure GSDT Submissions
GSDT Module: Project Plan Submissions ***Tab(s):*** PISC and Site Closure tab Please use the checkbox(es) to verify the following information was submitted to the GSDT: ☒ PISC and Site Closure Plan ***[40 CFR 146.82(a)(17) and 146.93(a)]***
GSDT Module: Alternative PISC Timeframe Demonstration ***Tab(s):*** All tabs (only if an alternative PISC timeframe is requested) Please use the checkbox(es) to verify the following information was submitted to the GSDT: ☐ Alternative PISC timeframe demonstration ***[40 CFR 146.82(a)(18) and 146.93(c)]***

11. Emergency and Remedial Response

Attachment F: Emergency and Remedial Response Plan (**Attachment F**), pursuant to 40 CFR 164.94, describes the process and response to emergencies to ensure USDW protection.

Emergency and Remedial Response GSDT Submissions
GSDT Module: Project Plan Submissions ***Tab(s):*** Emergency and Remedial Response tab Please use the checkbox(es) to verify the following information was submitted to the GSDT: ☒ Emergency and Remedial Response Plan ***[40 CFR 146.82(a)(19) and 146.94(a)]***

12. Injection Depth Waiver and Aquifer Exemption Expansion

No depth waiver or aquifer exemption expansion is being requested as part of this application.

Injection Depth Waiver and Aquifer Exemption Expansion GSDT Submissions
GSDT Module: Injection Depth Waivers and Aquifer Exemption Expansions ***Tab(s):*** All applicable tabs Please use the checkbox(es) to verify the following information was submitted to the GSDT: ☐ Injection Depth Waiver supplemental report ***[40 CFR 146.82(d) and 146.95(a)]*** ☐ Aquifer exemption expansion request and data ***[40 CFR 146.4(d) and 144.7(d)]***

References

Bartow. 1985. Maps showing Tertiary stratigraphy and structure of the Northern San Joaquin Valley, California. United States Geological Survey (USGS).

Berkstresser, C.F. Jr. 1973. Base of Fresh Ground-Water -- Approximately 3,000 micromhos -- in the Sacramento Valley and Sacramento-San Joaquin Delta, California. U.S. Geological Survey Water-Resource Inv. 40-73. 1973

Bertoldi, G., Johnston, R., & Evenson, K. 1991. Groundwater in the Central Valley, California - A Summary Report. USGS Professional Paper 1401-A. https://doi.org/10.3133/pp1401A.

Beyer, L.A. Summary of Geology and Petroleum Plays Used to Assess Undiscovered Recoverable Petroleum Resources of Sacramento Basin Province, California. United States Department of the Interior Geological Survey, 1988.

Burow, Karen R., Jennifer L. Shelton, Joseph A. Hevesi, and Gary S. Weissmann. 2004. Hydrologic Characterization of the Modesto Area, San Joaquin Valley, California. Preliminary Draft. U.S. Geological Survey. Water-Resources Investigation Report. Prepared in cooperation with Modesto Irrigation District. Sacramento, California.

California Department of Conservation Division of Soil, Gas and Geothermal Resources (DOGGR). 1998. California Oil and Gas Fields. Volume III – Northern California.

California Department of Water Resources (DWR). 1995. Sacramento Delta San Joaquin Atlas.

California Department of Water Resources (DWR). 2006. California's Groundwater, Bulletin 118. San Joaquin Valley Groundwater Basin Tracy Subbasin. Last updated November 2021.

California Geological Survey (CGS). 2006. An overview of Geologic Carbon Sequestration Potential in California.

Callaway, D. C. 1964. Distribution of Uppermost Cretaceous Sands in the Sacramento-Northern San Joaquin Basin of California. Selected Papers Presented to San Joaquin Geological Society - Volume 2, pp. 5-18.

Davis G.H., J.H. Green, S.H. Olmstead, and D.W. Brown 1959. Davis, G. H., J.H. Green, S.H. Olmstead, and D.W. Brown. 1959. Ground water conditions and storage capacity in the San Joaquin Valley, California. U.S. Geological Survey Water Supply Paper No. 1469, 287 p.

Downey, C., and Clinkenbeard, J. 2010. Preliminary Geologic Assessment of the Carbon Sequestration Potential of the Upper Cretaceous Mokelumne River, Starkey, and Winters Formations – Southern Sacramento Basin, California. California Geological Survey.

Downey, C., and Clinkenbeard, J. 2006. An overview of geologic carbon sequestration potential in California, California Energy Comission, PIER Energy-Related Environmental Research Program.

Fjaer, E., Holt, RM., Raaen, AM., and Horsrud, P, 2008. Petroleum Related Rock Mechanics (2nd ed.). Elsevier Science.

Freeman, B., Yielding, G., Needham, T., and Badley, M (1998): Fault Seal Prediction: The Gouge Ratio Method. Geological Society, Lond, Special Publications. 127. 19-25.

Groundwater Ambient Monitoring and Assessment Program (GAMA), 2023. https://www.waterboards.ca.gov/gama/

GEI Consultants, Inc. (GEI) 2007. Tracy Regional Groundwater Management Plan.

GEI Consultants, Inc. (GEI) 2021. Tracy Subbasin Groundwater Sustainability Plan. November 1, 2021.

Graham, S.A., McCloy, C., Hitzman, M., Ward, R., Turner, R. 1984. Basin Evolution During Chance from Convergent to Transform Continental Margin in Central California. The American Association of Petroleum Geologists Bulletin V.68 No. 3.

Hotchkiss, W. R., and G.O. Balding. 1971. Geology, hydrology, and water quality of the Tracy-Dos Palos area, San Joaquin Valley, California. U.S. Geological Survey. Open-File Report. Hotchkiss and Balding. 1971.

Heidbach, O., M. Rajabi, X. Cui, K. Fuchs, B. Müller, J. Reinecker, K. Reiter, M. Tingay, F. Wenzel, F. Xie, M. O. Ziegler, M.-L. Zoback, and M. D. Zoback (2018): The World Stress Map database release 2016: Crustal stress pattern across scales. Tectonophysics, 744, 484-498, doi:10.1016/j.tecto.2018.07.007

Heidbach, Oliver; Rajabi, Mojtaba; Reiter, Karsten; Ziegler, Moritz; WSM Team (2016): World Stress Map Database Release 2016. GFZ Data Services, doi:10.5880/WSM.2016.001

Hill, 1979. California Well Sample Repository Special Publication No. 2: Display of Cores From The Winters Sand (Upper Cretaceous), Sacramento Valley California. May 7 – 12, 1979.

Hydrofocus, 2015. San Joaquin County and Delta Quality Coalition Groundwater Quality Assessment Report, April 27, 2015.

Ingram G. M., Urai J. L., Naylor M. A. 1997. in Hydrocarbon Seals: Importance for Exploration and Production, Sealing processes and top seal assessment, Norwegian Petroleum Society (NPF) Special Publication, eds Moller-Pedersen P., Koestler A. G. 7, pp 165–175.

Ingram, Gary and Urai, Janos. 1999. Top-seal leakage through faults and fractures: the role of mudrock properties. Geological Society, London, Special Publications. 158. 125-135. 10.1144/GSL.SP.1999.158.01.10.

Johnson, D.S. 1990. Depositional environment of the Upper Cretaceous Mokelumne River Formation, Sacramento Basin. California. American Assoc. of Petroleum Geologists Bulletin 74: 5 1990: 686 p.

Kim T.W., Callas C., Saltzer S.D., Kovscek A.R. 2022. Assessment of oil and gas fields in California as potential CO2 storage sites. International Journal of Greenhouse Gas Control. Volume 114, 103579.

Leong, J.K., and J.R. Tenzer. 1994. Production Optimization of a Mature Gas Field. Paper presented at the SPE Western Regional Meeting, Long Beach, California.

Lund Snee, J-E, and Zoback, M. 2020. Multiscale variations of the crustal stress field throughout North America", Nature Communications 11, 1951.

Magoon, L.B., and Valin, Z.C. 1995. Sacramento Basin Province (009). United States Department of the Interior Geological Survey, National assessment of United States oil and gas resources-results, methodology, and supporting data.

Mount, Van and Suppe, John. 1992. Present-day stress orientations adjacent to active strike-slip faults - California and Sumatra. Journal of Geophysical Research. 971. 11995-12013. 10.1029/92JB00130.

Newman, G.H. 1973. Pore-Volume Compressibility of Consolidated, Friable, and Unconsolidated Reservoir Rocks Under Hydrostatic Loading. *J Pet Technol* 25. 129–134. doi: https://doi.org/10.2118/3835-PA

Nilsen, T. H., and Clarke, Jr. S.H. 1975. Sedimentation and Tectonics in the Early Tertiary Continental Borderland of Central California. Geological Survey Professional Paper 925,.

O'Geen A, Saal M, Dahlke H, Doll D, Elkins R, Fulton A, Fogg G, Harter T, Hopmans J, Ingels C, Niederholzer F, Sandoval Solis S, Verdegaal P, Walkinshaw M. 2015. Soil suitability index identifies potential areas for groundwater banking on agricultural lands.

Padre and Associates, Inc. 2004. personnel communication with Mike Burke regarding aquifer testing at City of Tracy Well 8.

Page, R.W. 1986. Geology of the Fresh Ground-Water Basin of the Central Valley, California, with Texture Maps and Sections. USGS Professional Paper 1401-C.

Sullivan, Ray and Sullivan, Morgan. 2012. Sequence Stratigraphy and Incised Valley Architecture of the Domengine Formation, Black Diamond Mines Regional Preserve and the Southern Sacramento Basin, California, U.S.A. Journal of Sedimentary Research.

Towell, T. 1992. Public Health and Safety- Seismic and Geological Hazards.

U.S. Environmental Protection Agency Underground Injection Control Program. 1988. Survey of Methods to Determine Total Dissolved Solids Concentrations. Prepared by Ken E. Davis Associates under subcontract to Engineering Enterprises, INC. EPA LOE Contract No. 68-03-3416, Work Assignment No. 1-0-13, Keda Project No. 30-956.

U.S. Geological Survey (USGS), 2024. Earthquake Catalog.
URL: https://earthquake.usgs.gov/earthquakes/search/

Wagner, D.L., Bortugno, E.J., and Mc Junkin, R.D. 1991. Geologic Map of the San Francisco – San Jose Quadrangle. California Geological Survey, Regional Geologic Map No. 5A, 1:250,000 scale.

IEAGHG, 2011. Effects of impurities on geological storage of CO2. International Energy Agency Greenhouse Gas programme.

Wetenhall, B., Race, J.M., Downie, M.J. 2014. The Effect of CO2 Purity on the Development of Pipeline Networks for Carbon Capture and Storage Schemes. International Journal of Greenhouse Gas Control 30 (2014) 197–211.

Williamson, C.R., and Hill, D.R. 1981. Submarine-Fan Deposition of the Upper Cretaceous Winters Sandstone, Union Island Gas Field, Sacramento Valley, California.: The Society of Evonomic Paleontologists and Mineralogists (SEPM) Deep-Water Clastic Sediments (CW2).

Yielding, G., Bretan, P., and Freeman, B. (2010): Fault Seal Calibration: A Brief Overview. Geological Society of London Special Publications. 347. 243-255.

Figures

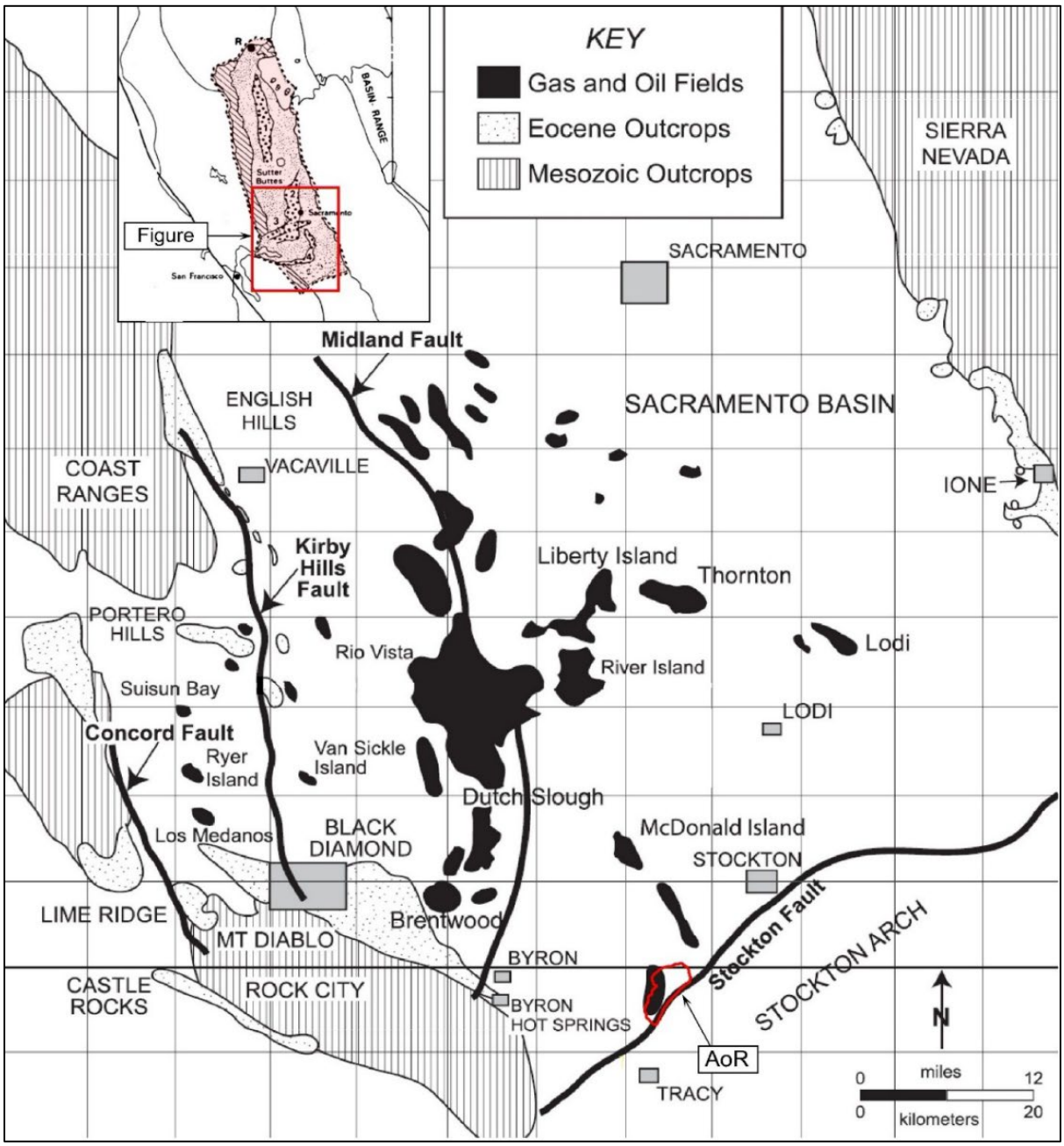

Figure A-1. Location map of the Union Island Gas Field with the proposed injection AoR in relation to the Sacramento Basin.

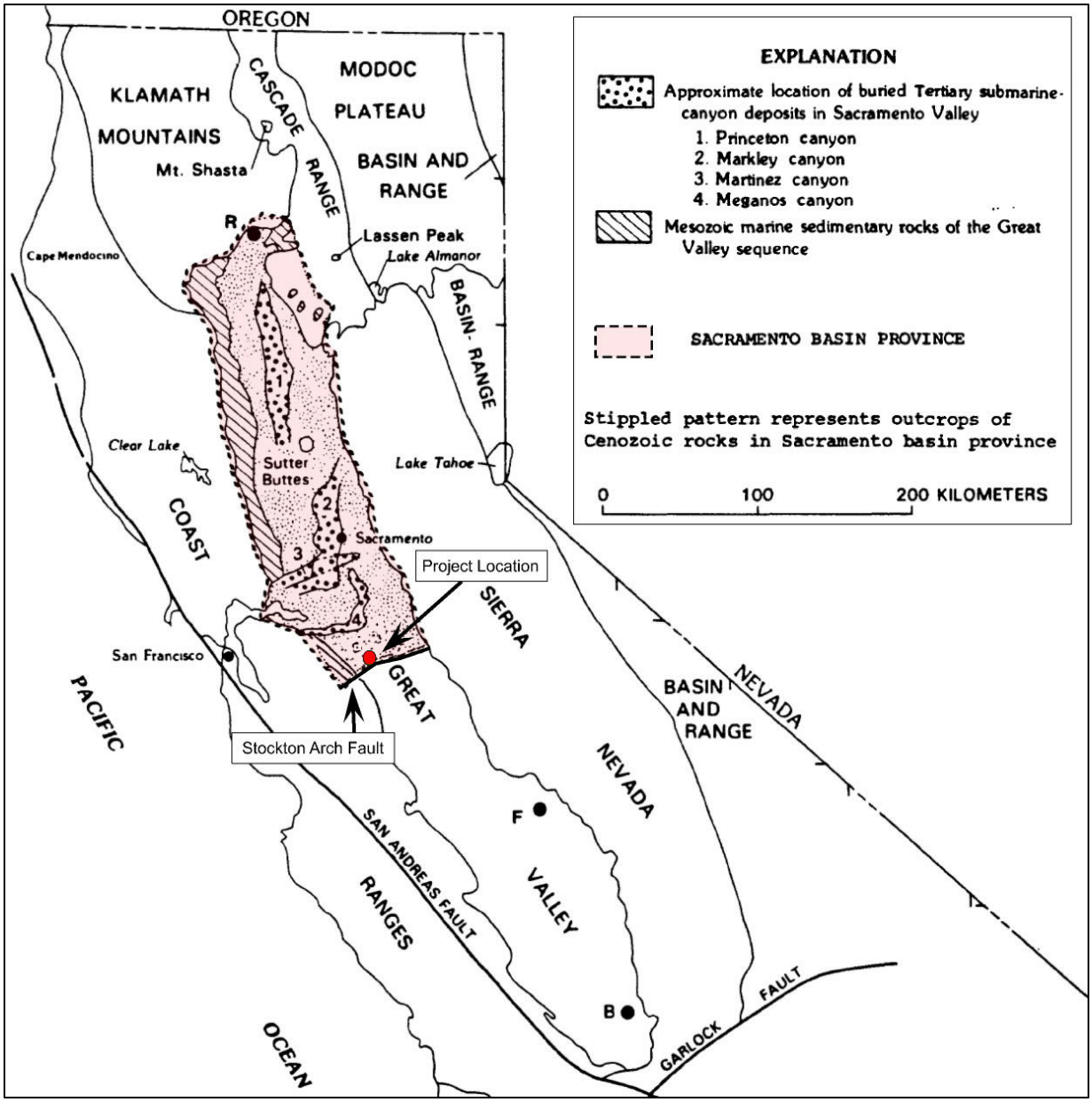

Figure A-2. Location map of California. Modified from (Beyer, 1988) & (Sullivan, 2012). The Sacramento Basin regional study area is outlined by a dashed black line. B – Bakersfield; F – Fresno; R – Redding.

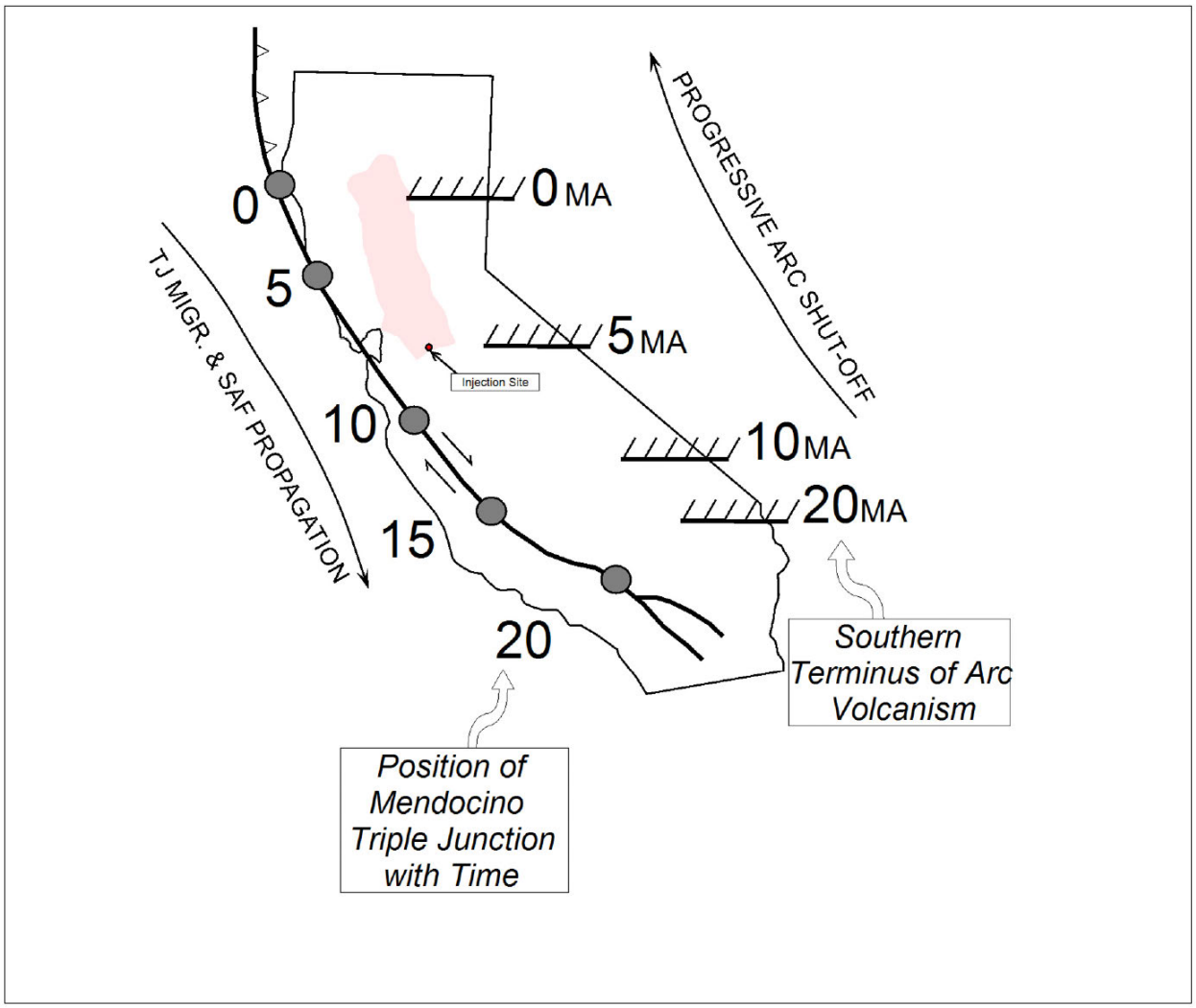

Figure A-3. Migrational position of the Mendocino triple junction (Connection point of the Gorda, North American and Pacific plates) on the west and migrational position of Sierran arc volcanism in the east. Source: Graham, 1984. Figure indicates space-time relations of major continental-margin tectonic events in California during Miocene.

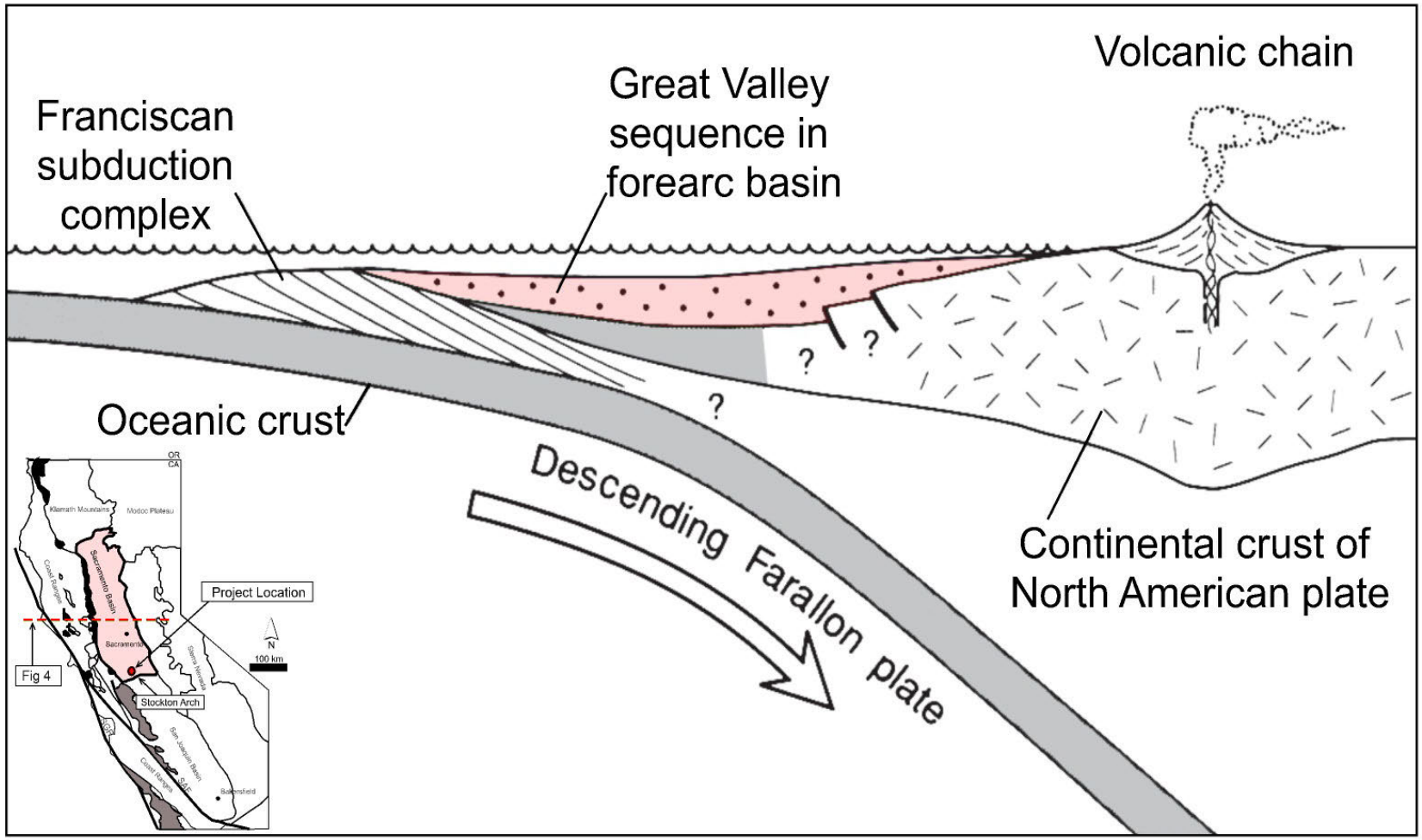

Figure A-4. Schematic west to east cross-section of California, highlighting the Sacramento Basin, as a continental margin during late Mesozoic. The oceanic Farallon plate was forced below the west coast of the North American continental plate.

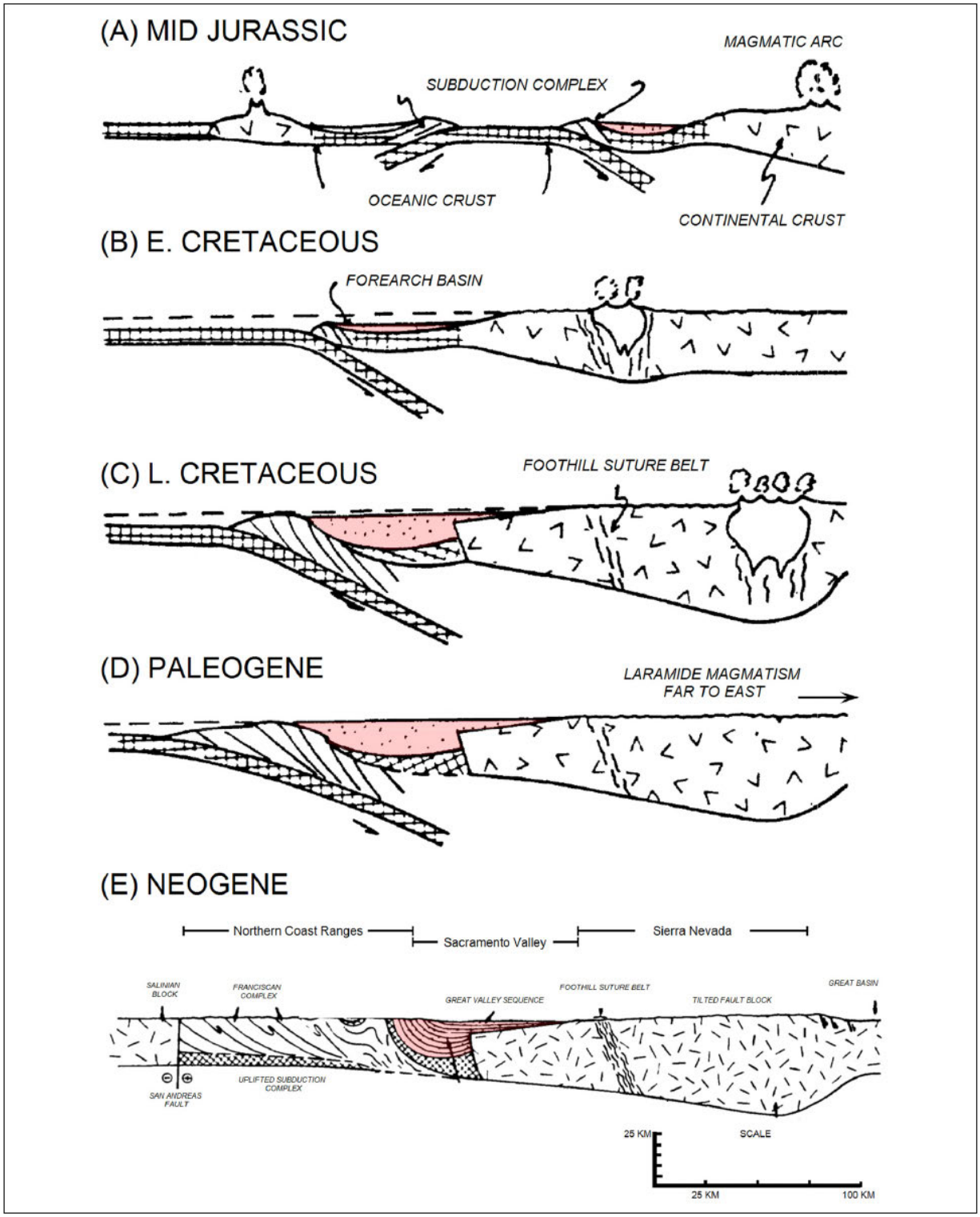

Figure A-5. Evolutionary stages showing the history of the arc-trench system of California from Jurassic (A) to Neogene (E). Modified from Beyer, 1988.

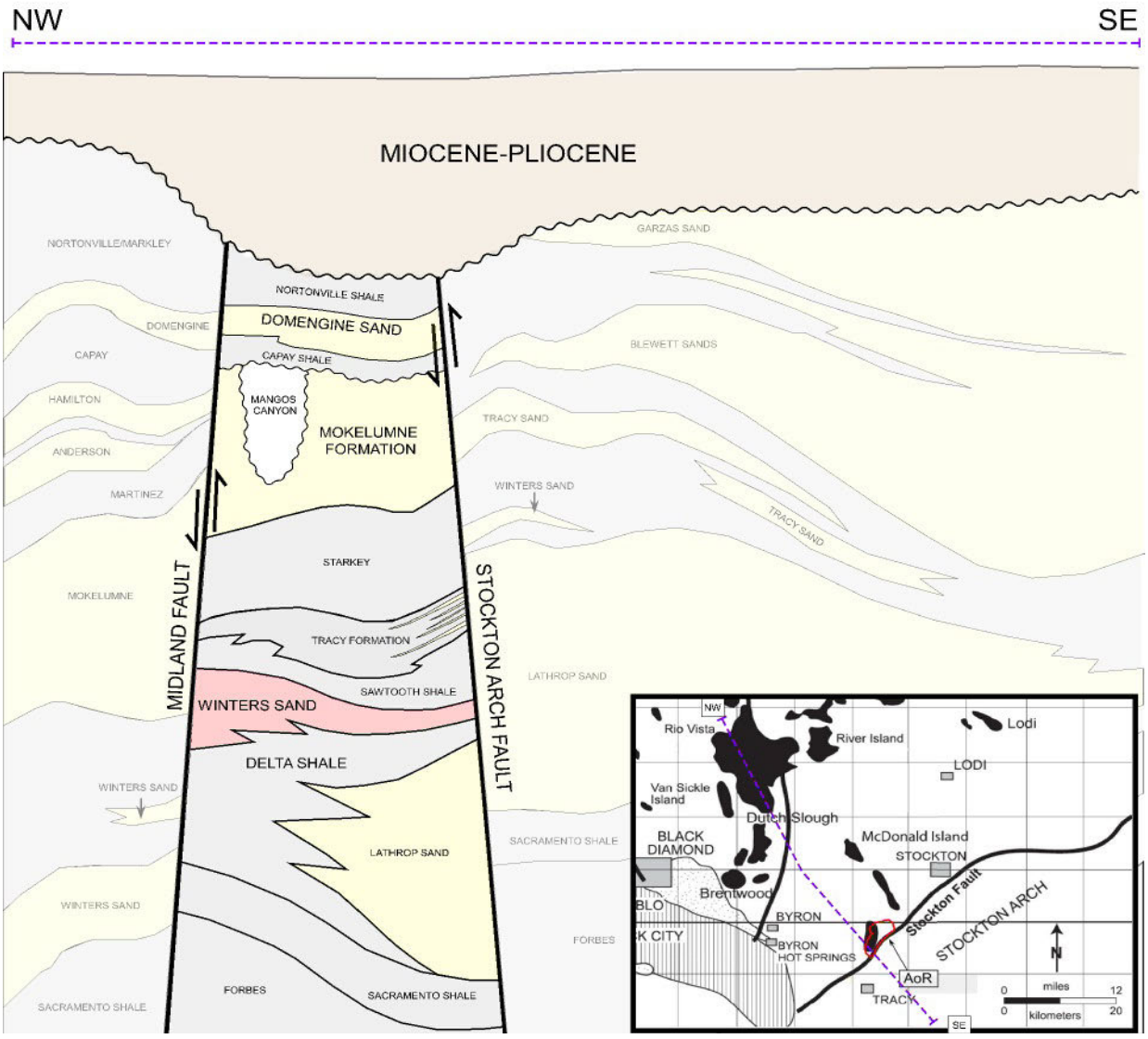

Figure A-6. Schematic northwest to southeast cross section in the Sacramento basin, intersecting the project AoR.

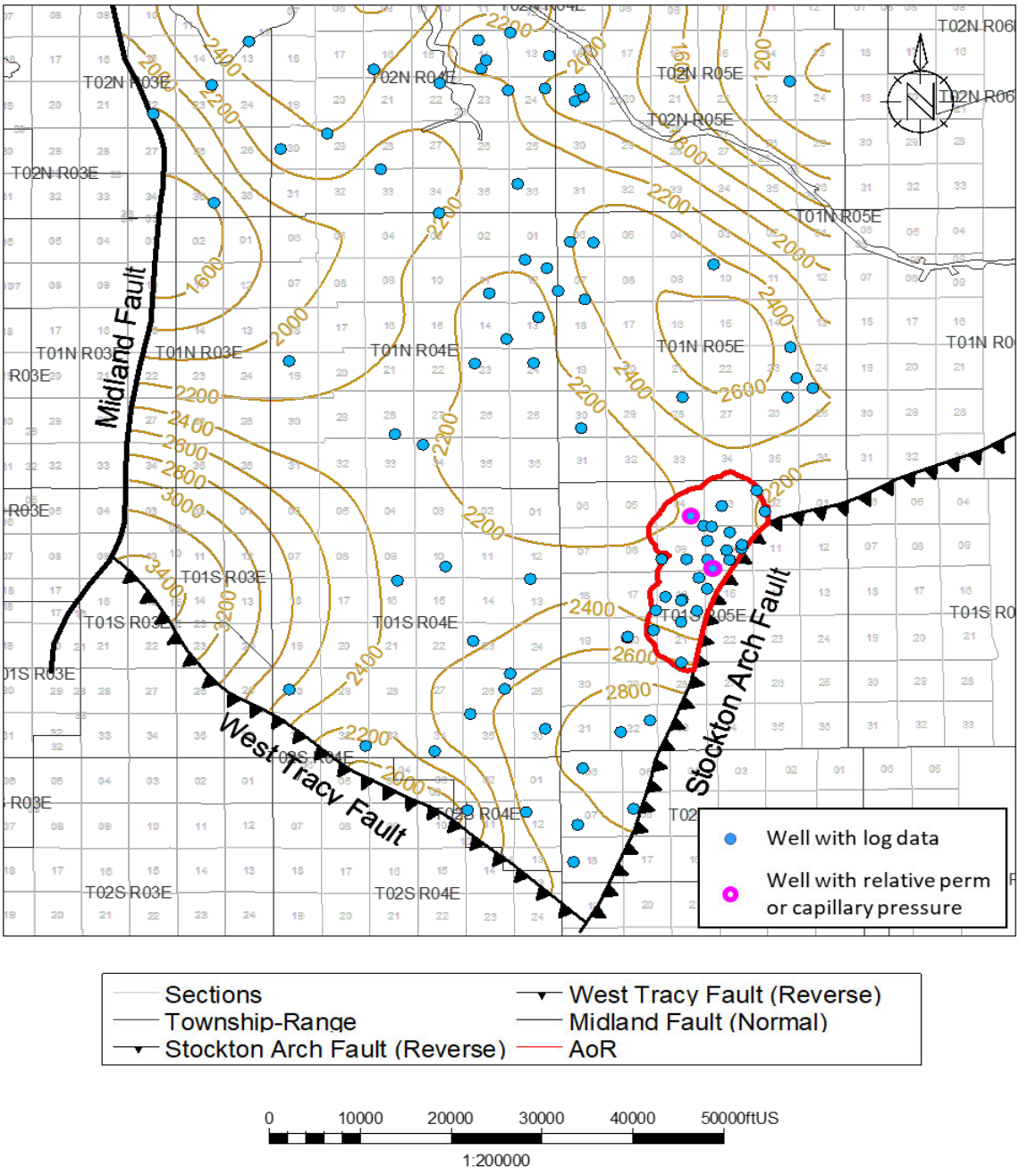

Figure A-7. Starkey-Sawtooth Shale isopach map for the greater storage project area. Wells shown as blue dots on the map penetrate the Starkey-Sawtooth Shale and have open-hole logs. Wells with relative permeability or capillary pressure data are shown as magenta circles.

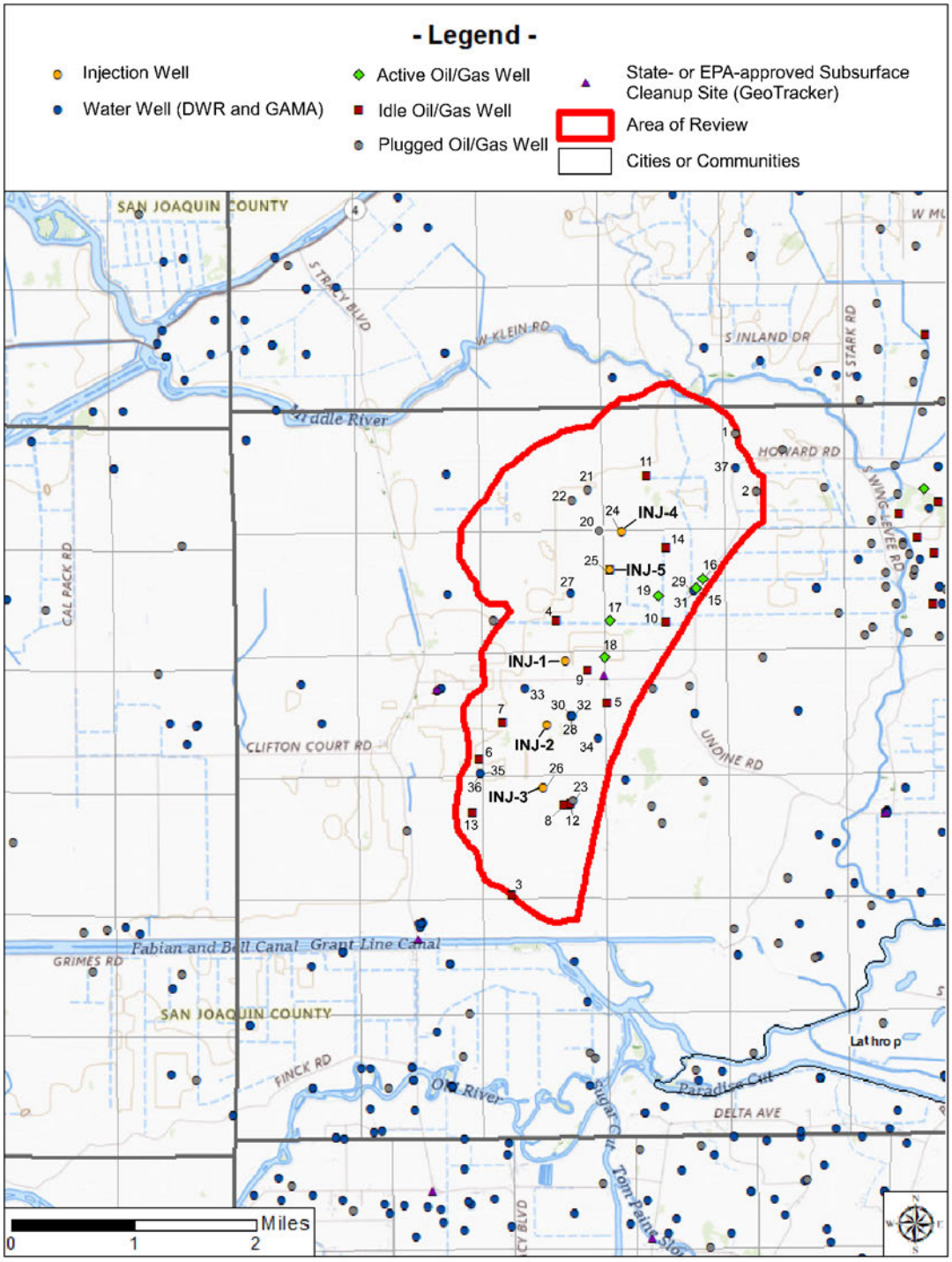

Figure A-8. Summary map of the oil or gas wells, water wells, State- or EPA-approved subsurface cleanup sites, and surface features in the project area. Water wells from California Division of Drinking Water (DWR) and Groundwater Ambient Monitoring and Assessment (GAMA) program. No known mines, quarries, springs or tribal lands are identified near the AoR. Active wells include: Dry Gas. Plugged wells include: Dry Hole and Dry Gas. Idle wells include: Dry Gas and Water Disposal. Wells in the AoR are listed in Tables A-1, A-2, and A-3.

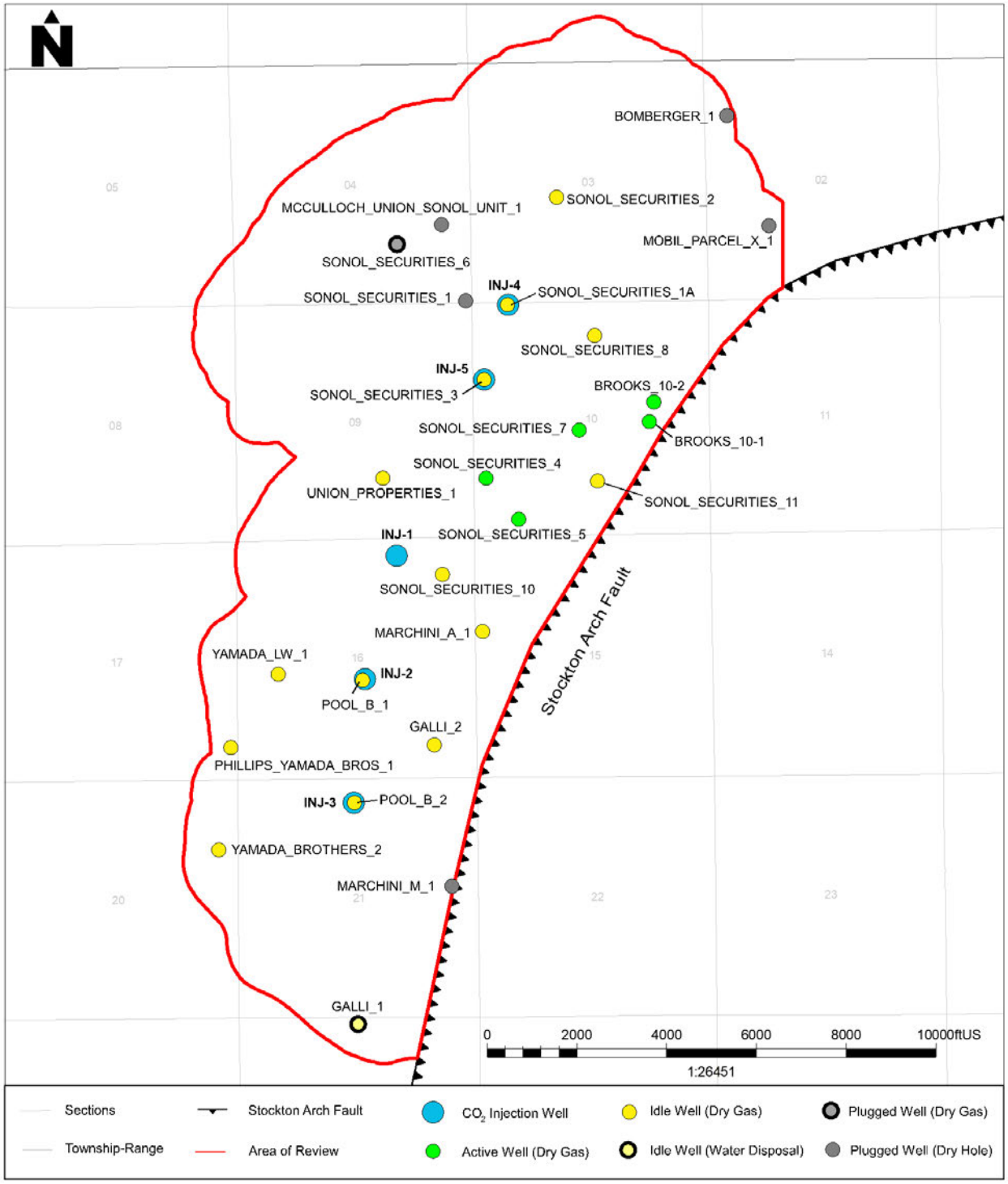

Figure A-9. Summary map of oil or gas wells in the AoR.

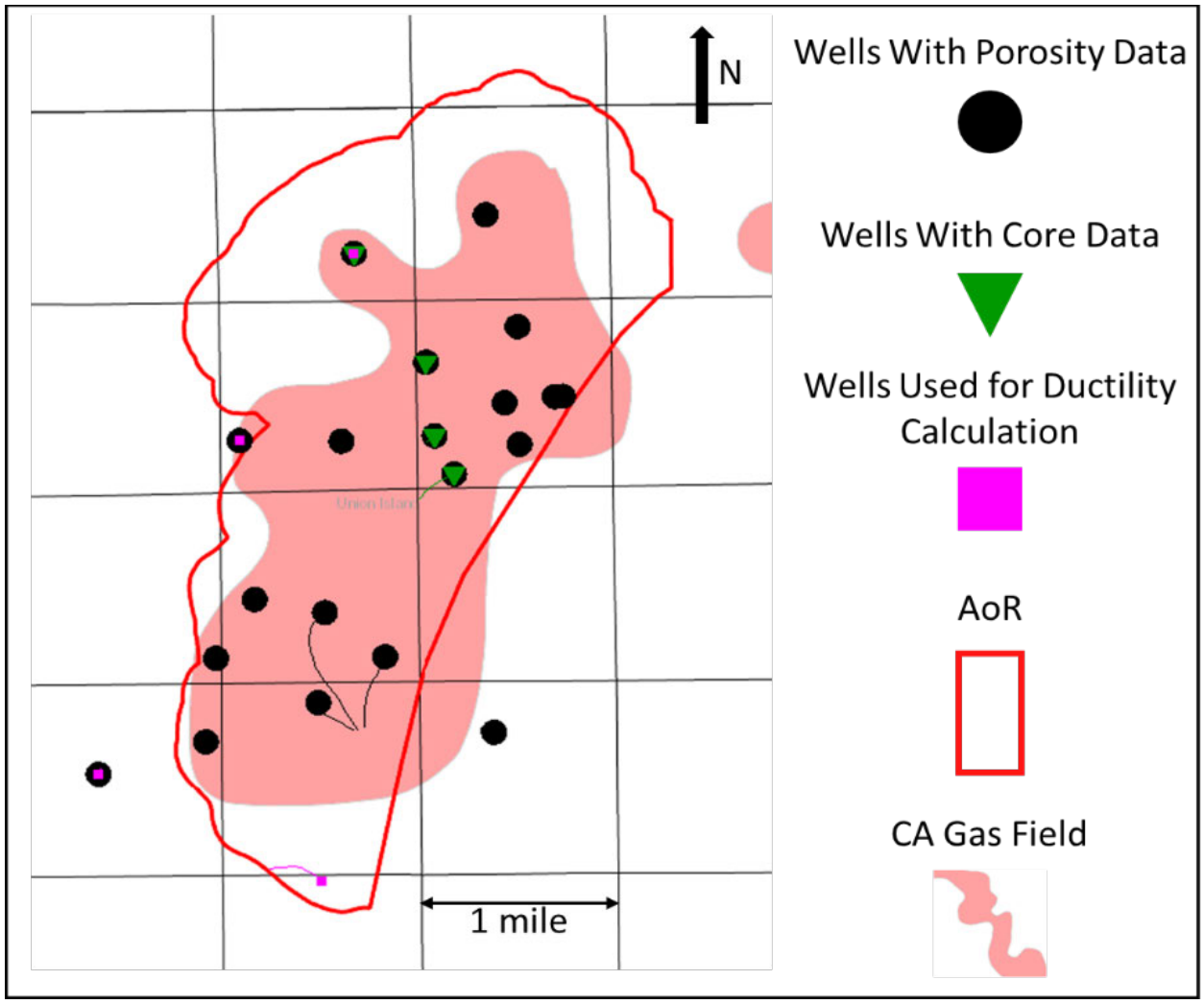

Figure A-10. Wells drilled in the Union Island Gas Field. Wells with porosity data are shown in black, wells with core are shown in green, and wells used for ductility calculation are shown in pink.

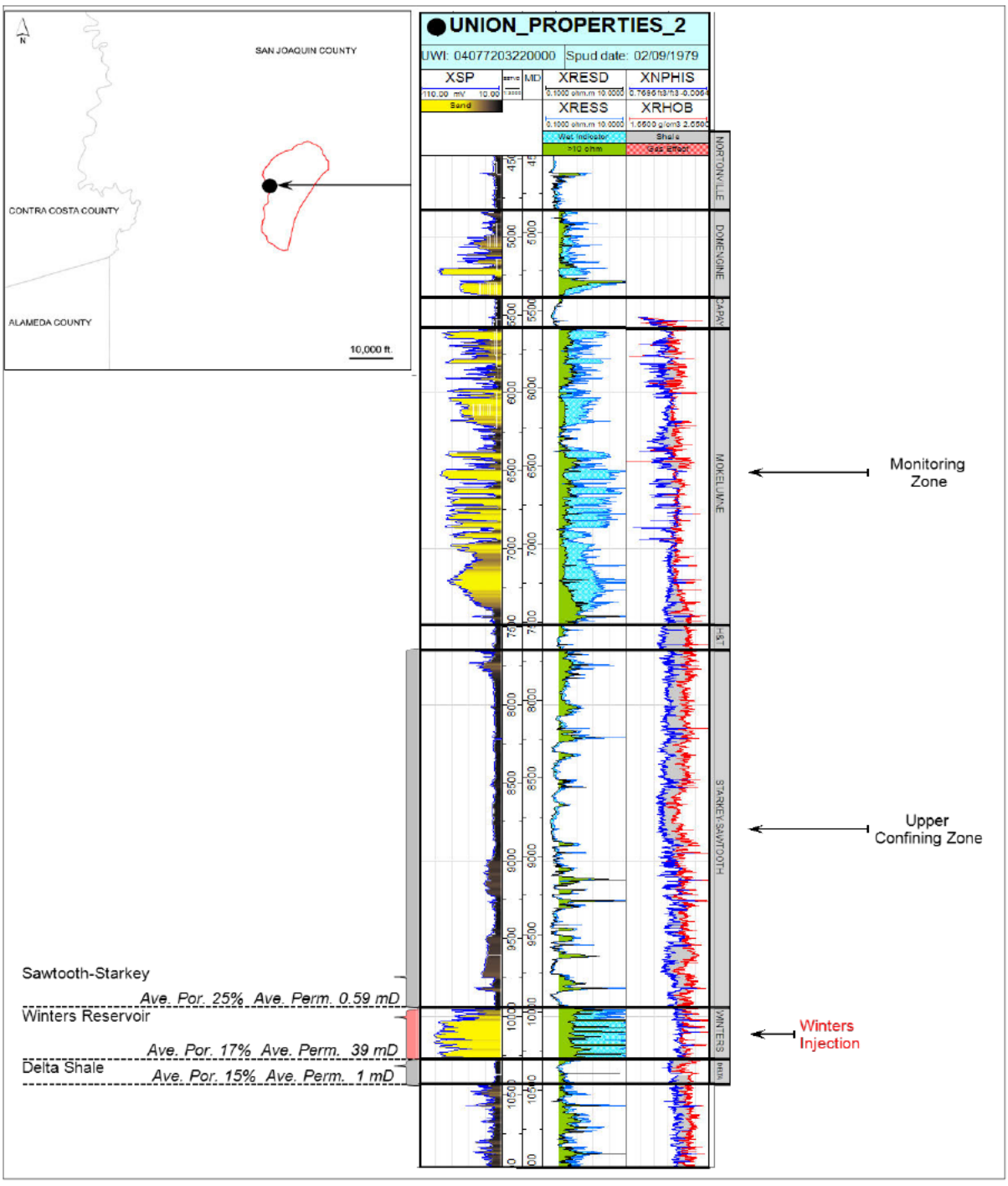

Figure A-11. Type well from the western edge of the AoR boundary showing average rock properties used in the model for confining and injection zones.

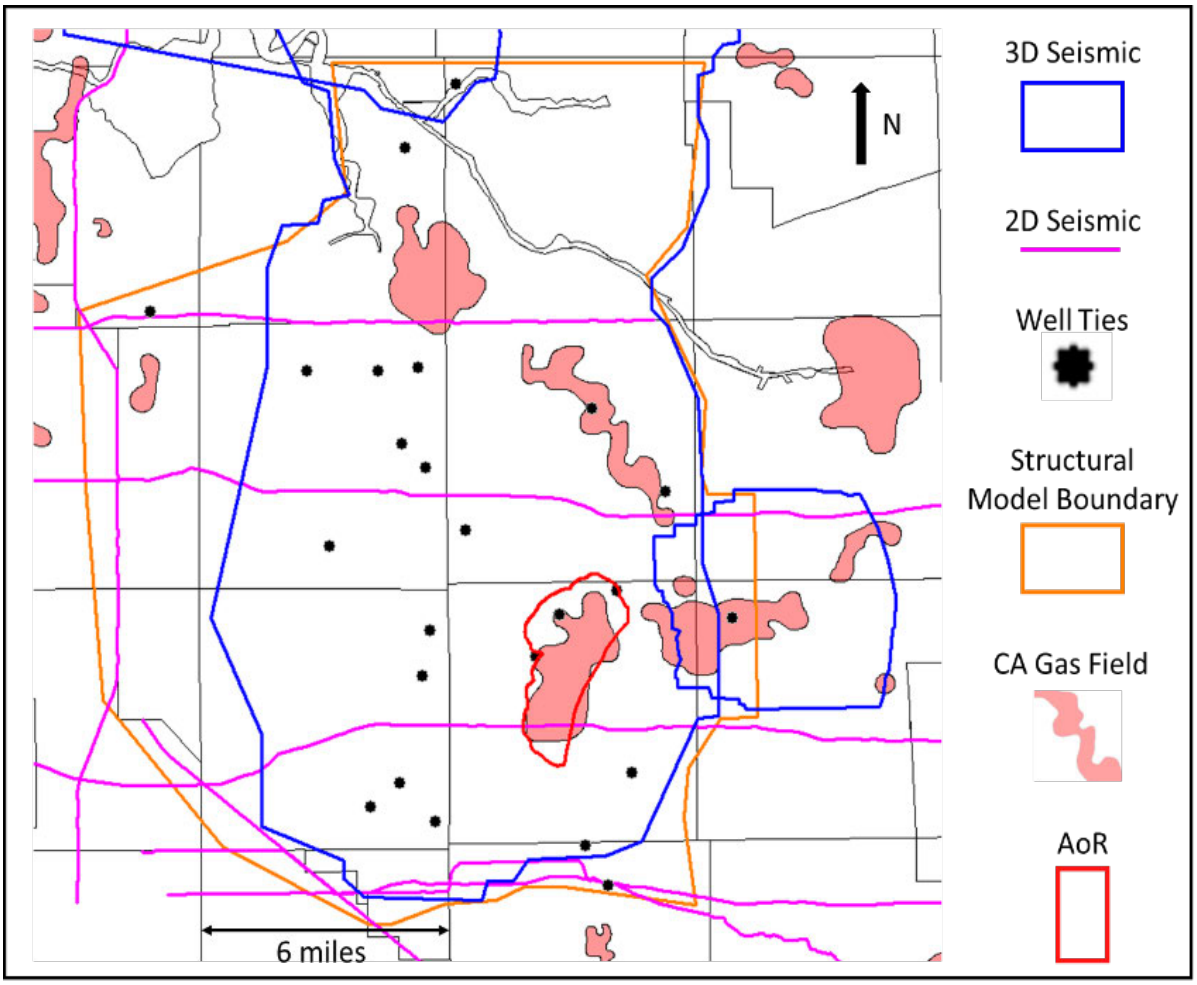

Figure A-12. Summary map and area of seismic data used to build structural model. Both 3D surveys were acquired in 1998 and reprocessed in 2013. The 2D seismic were acquired between 1980 and 1985. California gas fields are shown for reference.

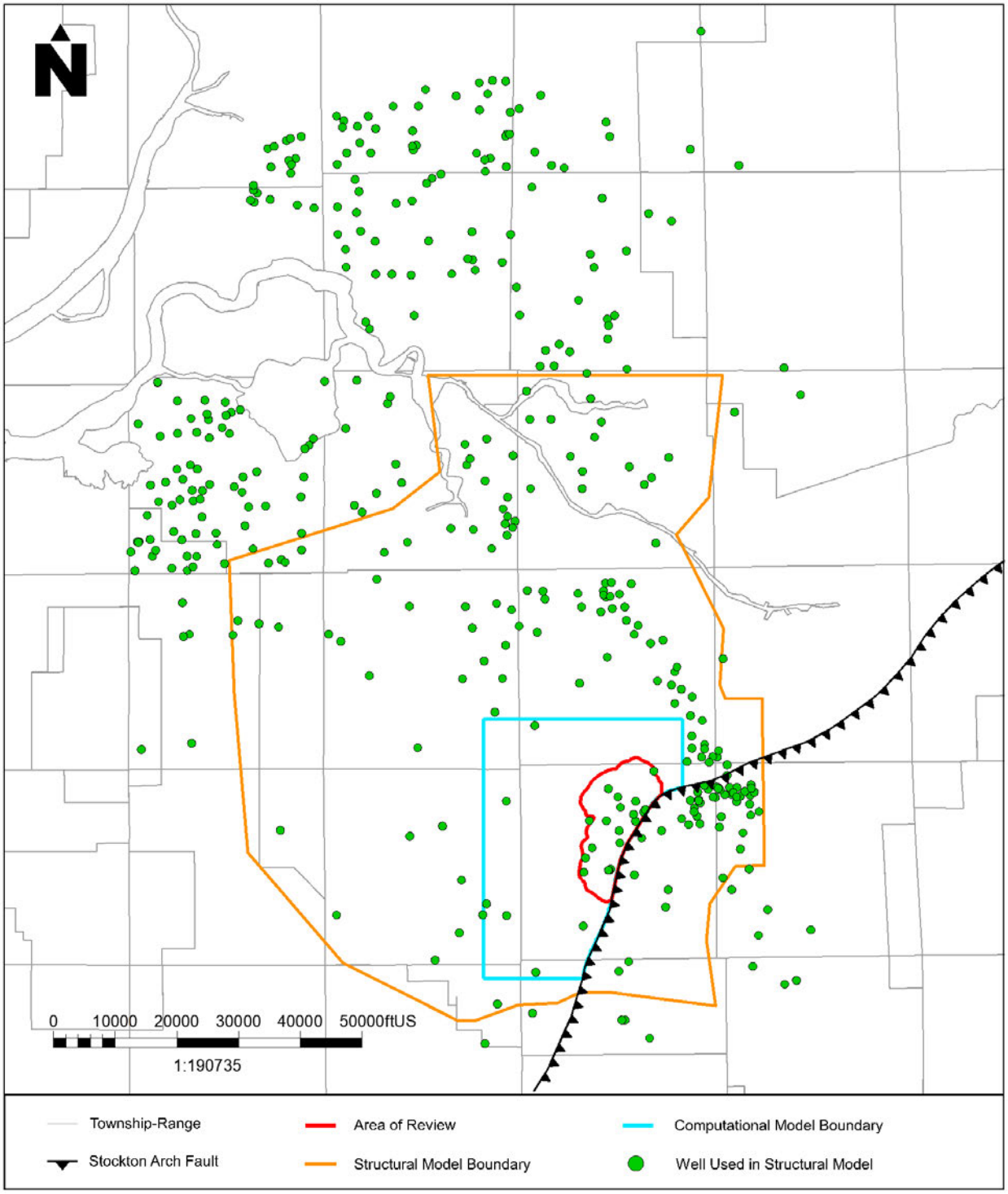

Figure A-13. Map of wells used in the Structural Model.

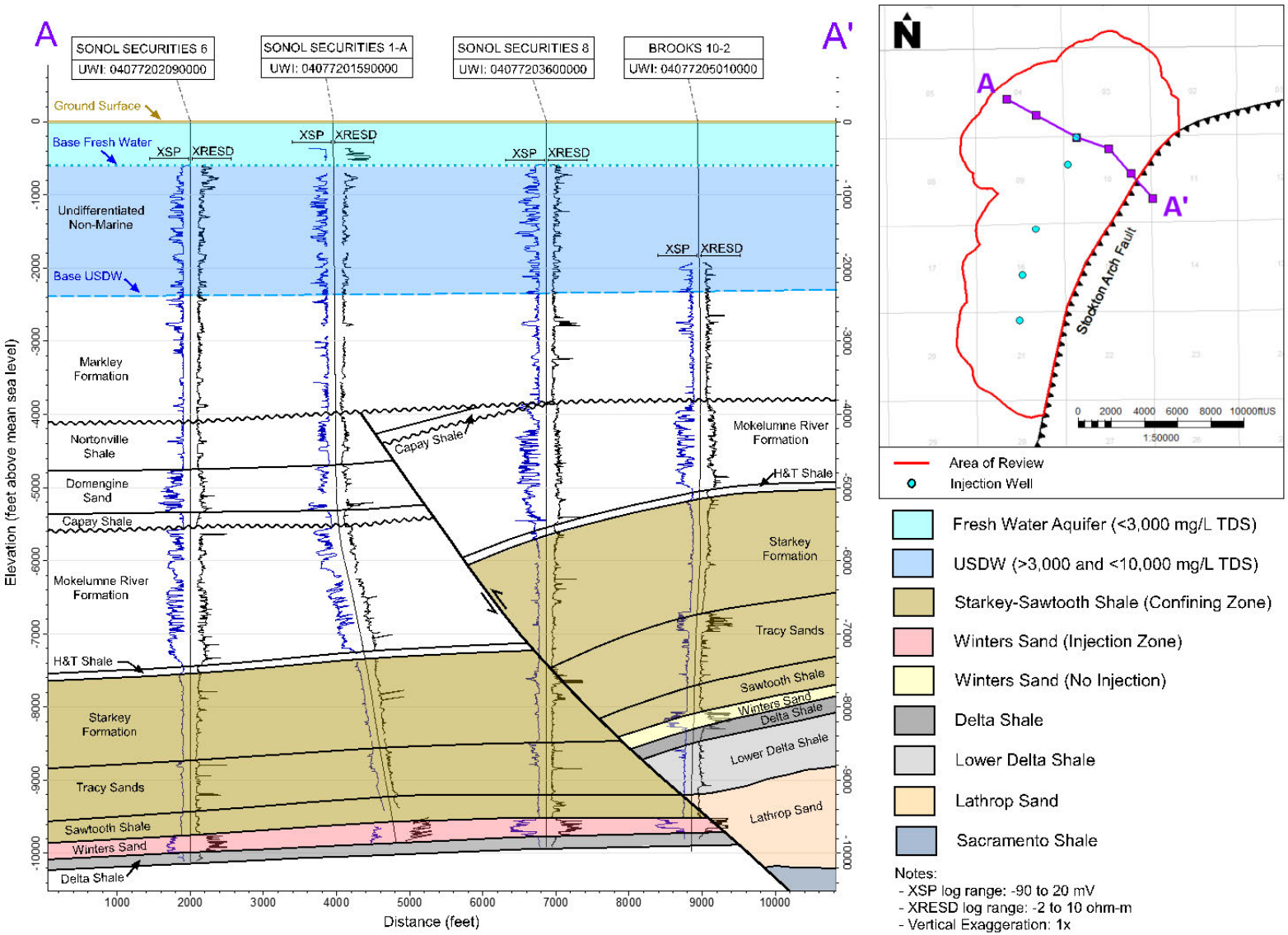

Figure A-14. Dip cross section showing stratigraphy and lateral continuity of major formations across the project area. Section is representative of formations and sand continuity at all five CO_2 injector locations.

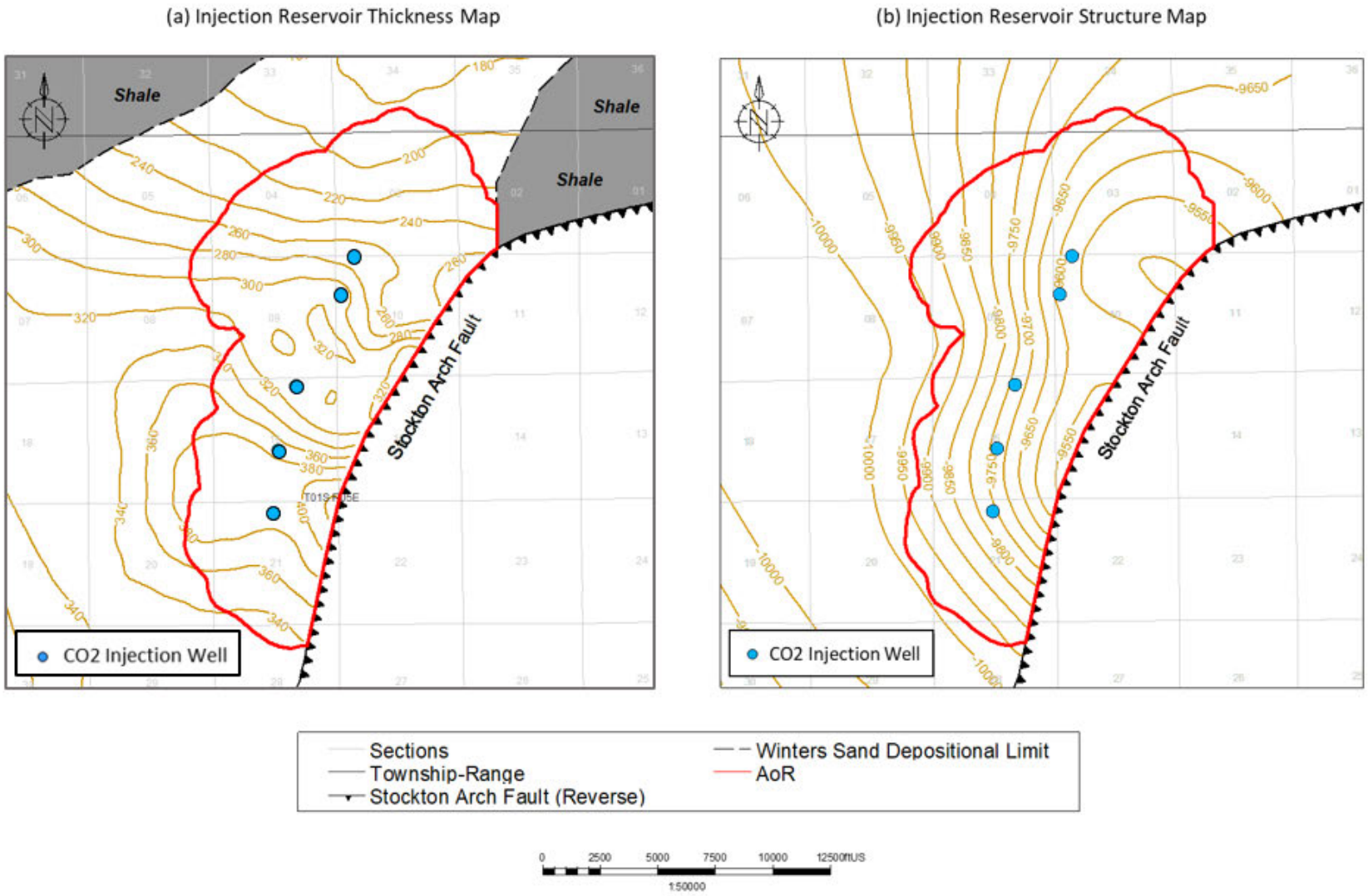

Figure A-15. (a) Injection reservoir thickness map (b) Injection reservoir structure map. AoR in red.

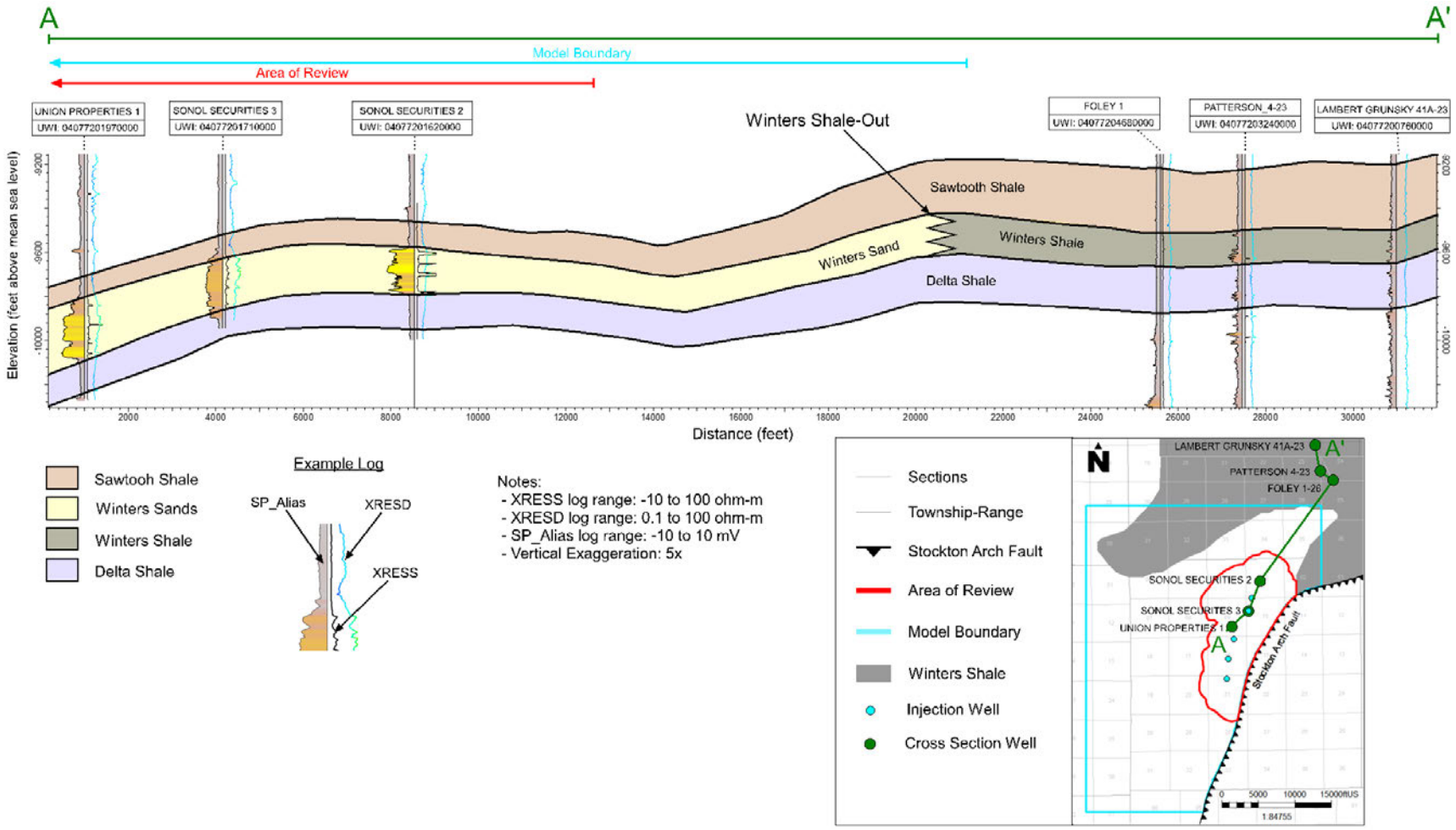

Figure A-16. Winters Shale-out cross section.

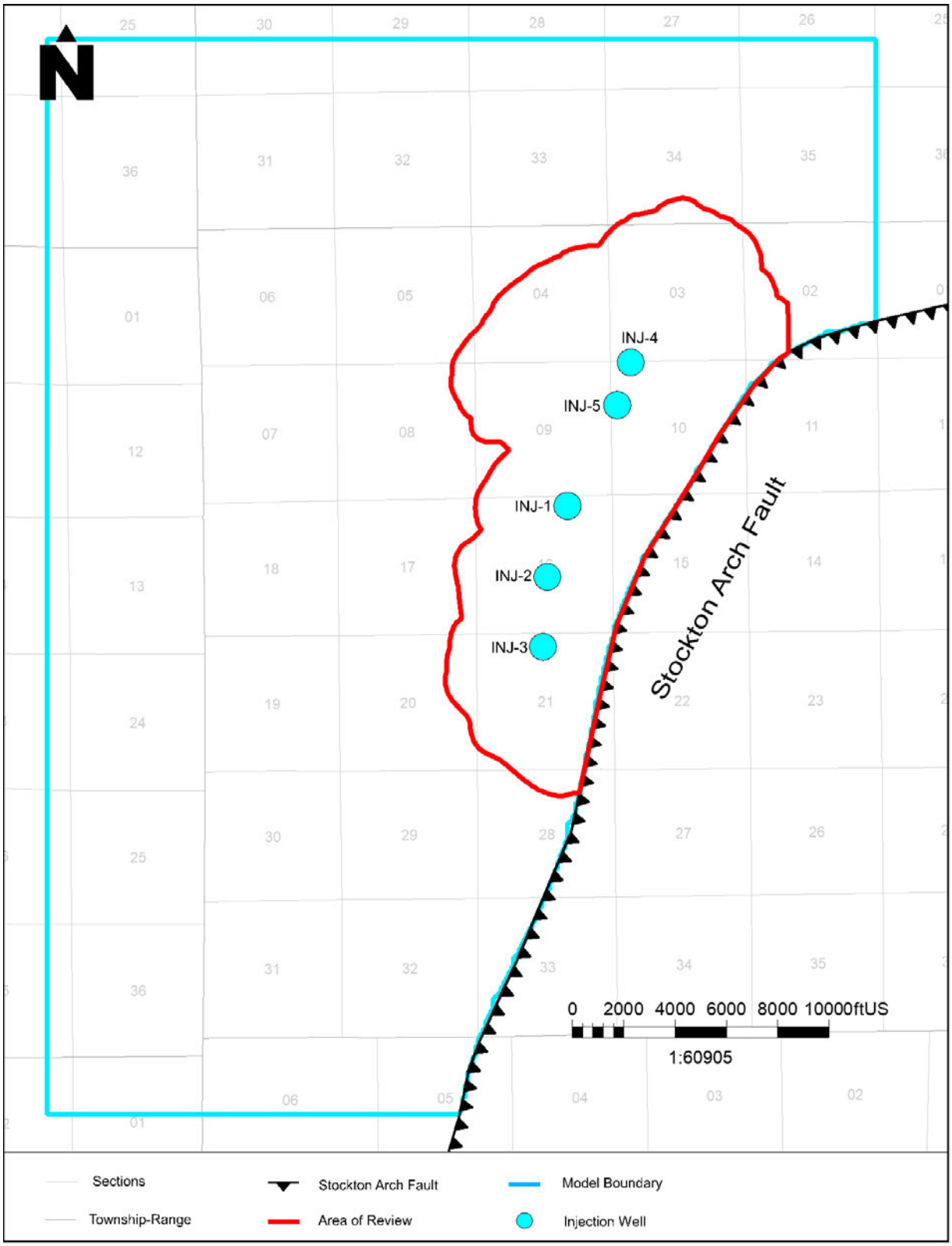

Figure A-17. AoR and injection well location map for the project area. Minimum distance between injection wells is 1,735 feet and maximum distance is 4,390 feet.

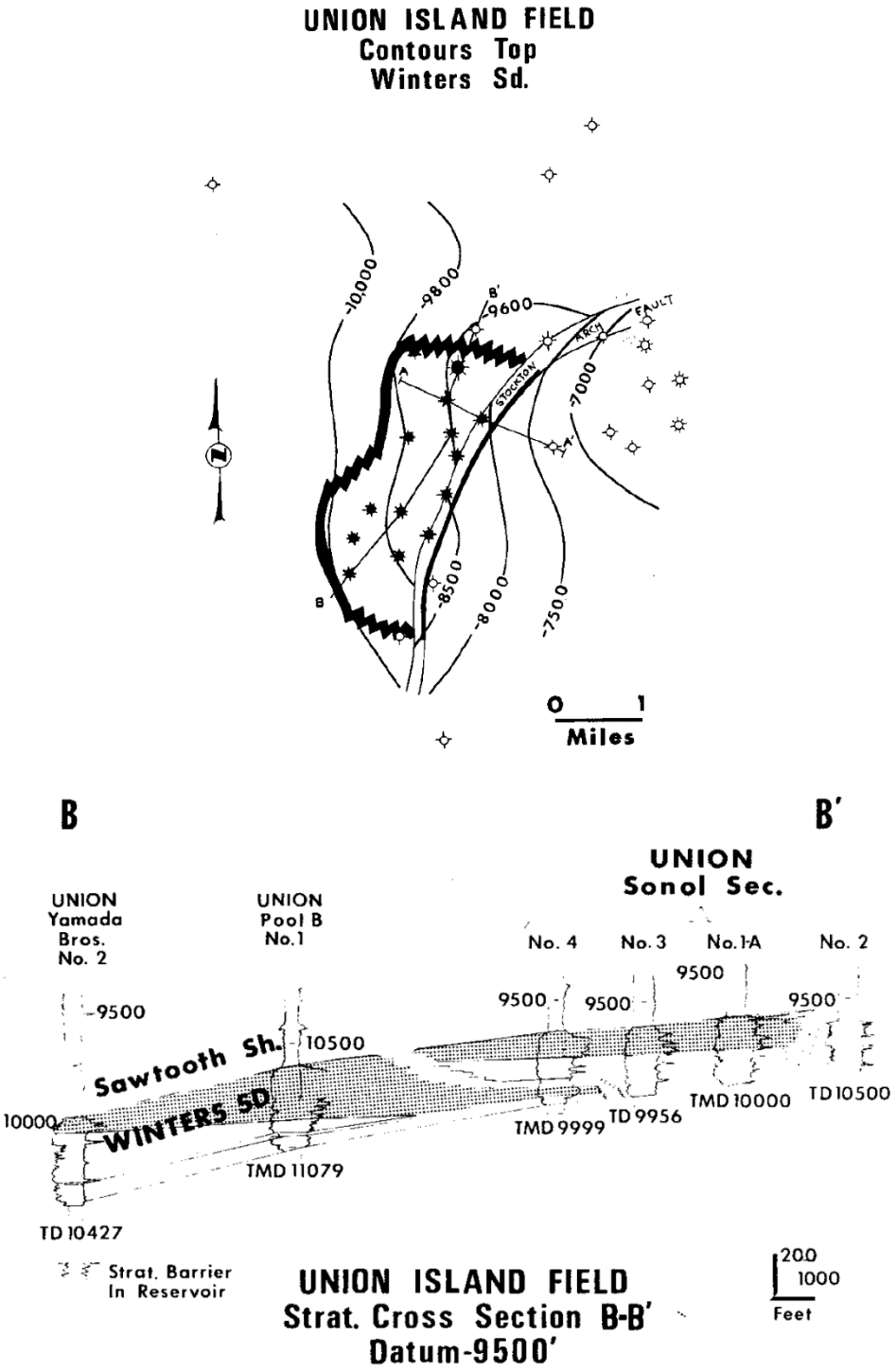

Figure A-18. Cross section B-B' across Union Island Gas Field. Figure shows the flow barrier which separates the Northern and Southern field. Figures taken from Hill (1979), Figure 2 and 8.

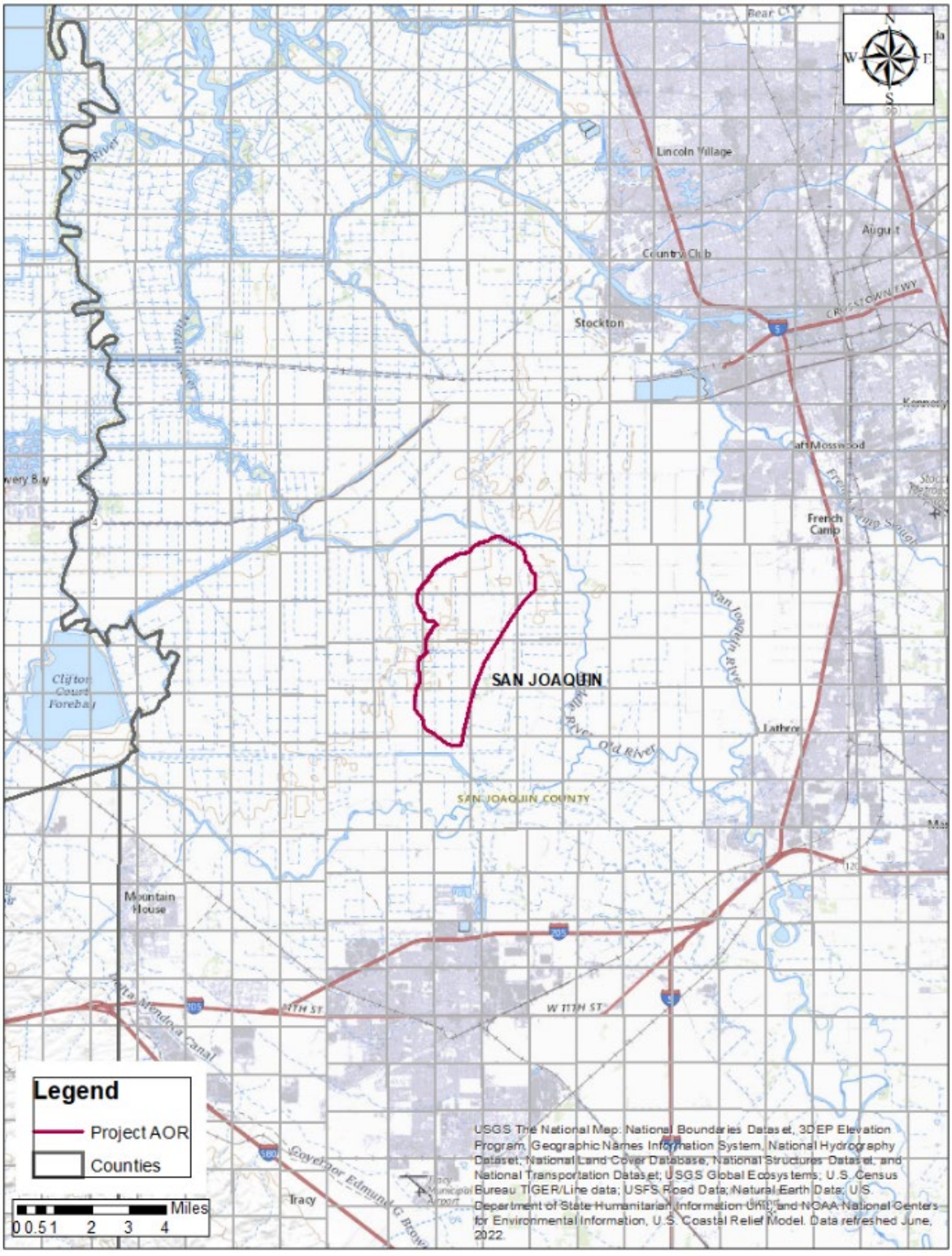

Figure A-19. Surface Features and the AoR.

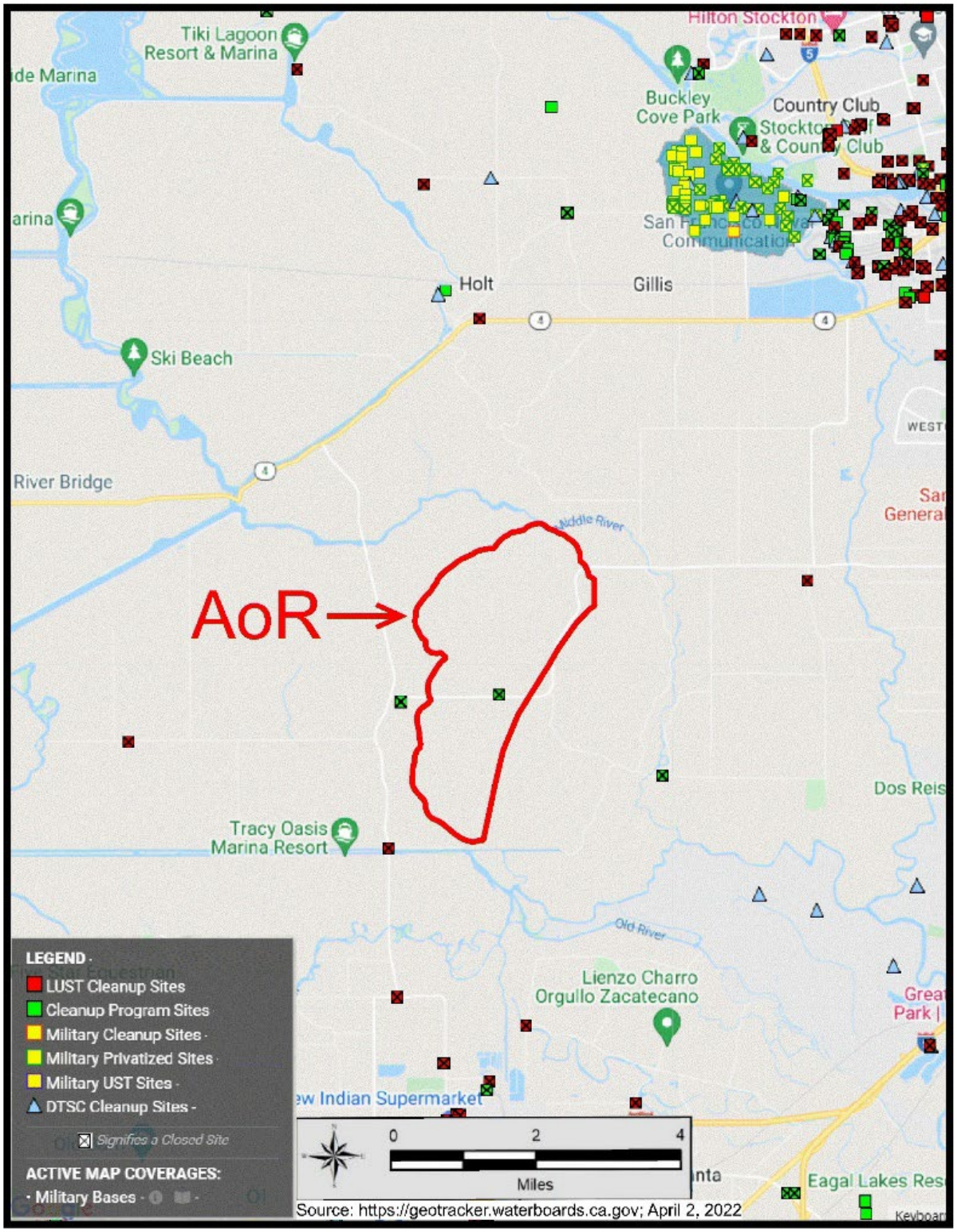

Figure A-20. State or EPA Subsurface Cleanup Sites.

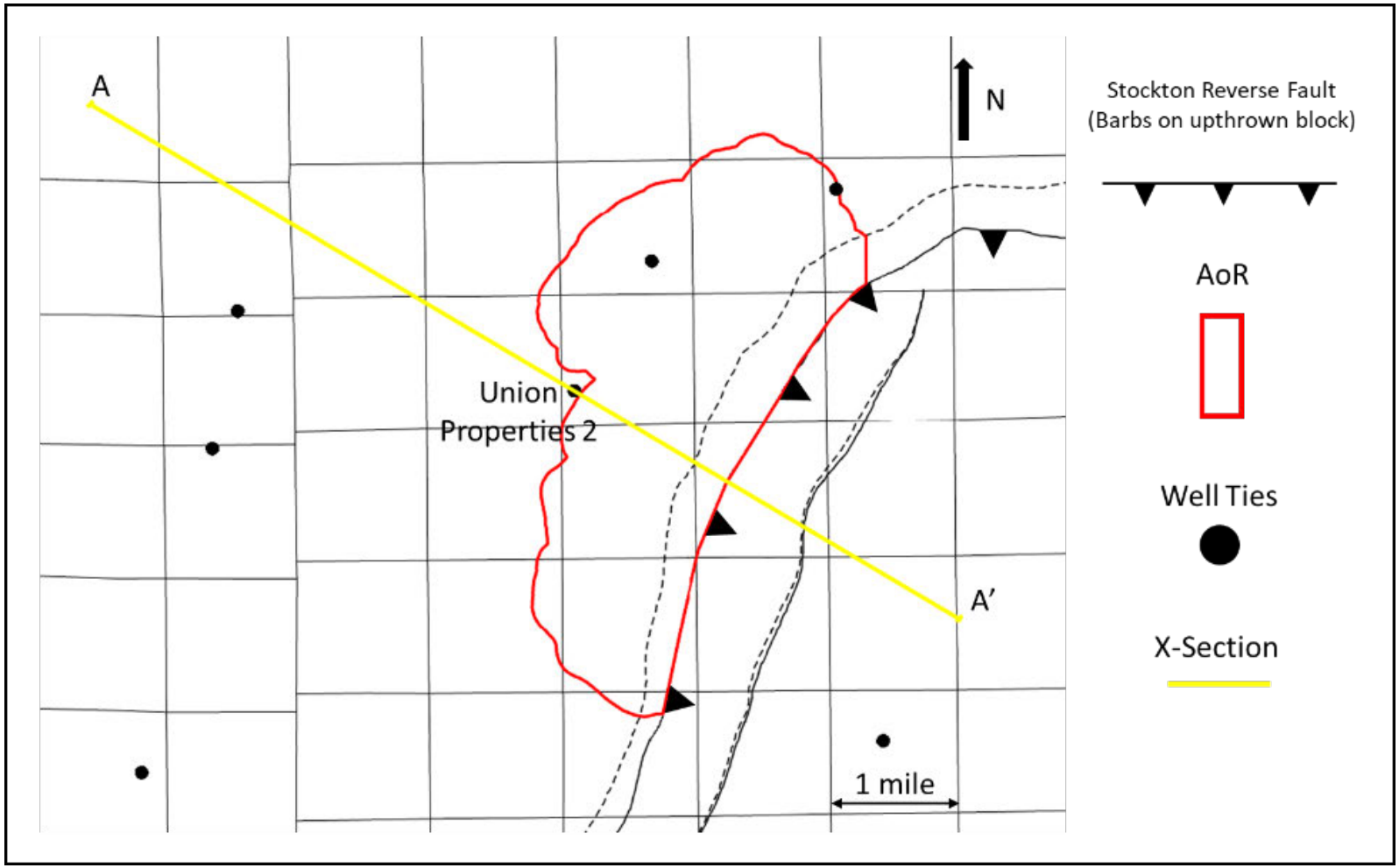

Figure A-21. The two faults within the model are shown at the Winters level. The fault to the east is believed to be antithetic to the main Stockton Arch fault and is dashed into it in cross-section. Yellow line highlights the cross section shown in Figure A-20.

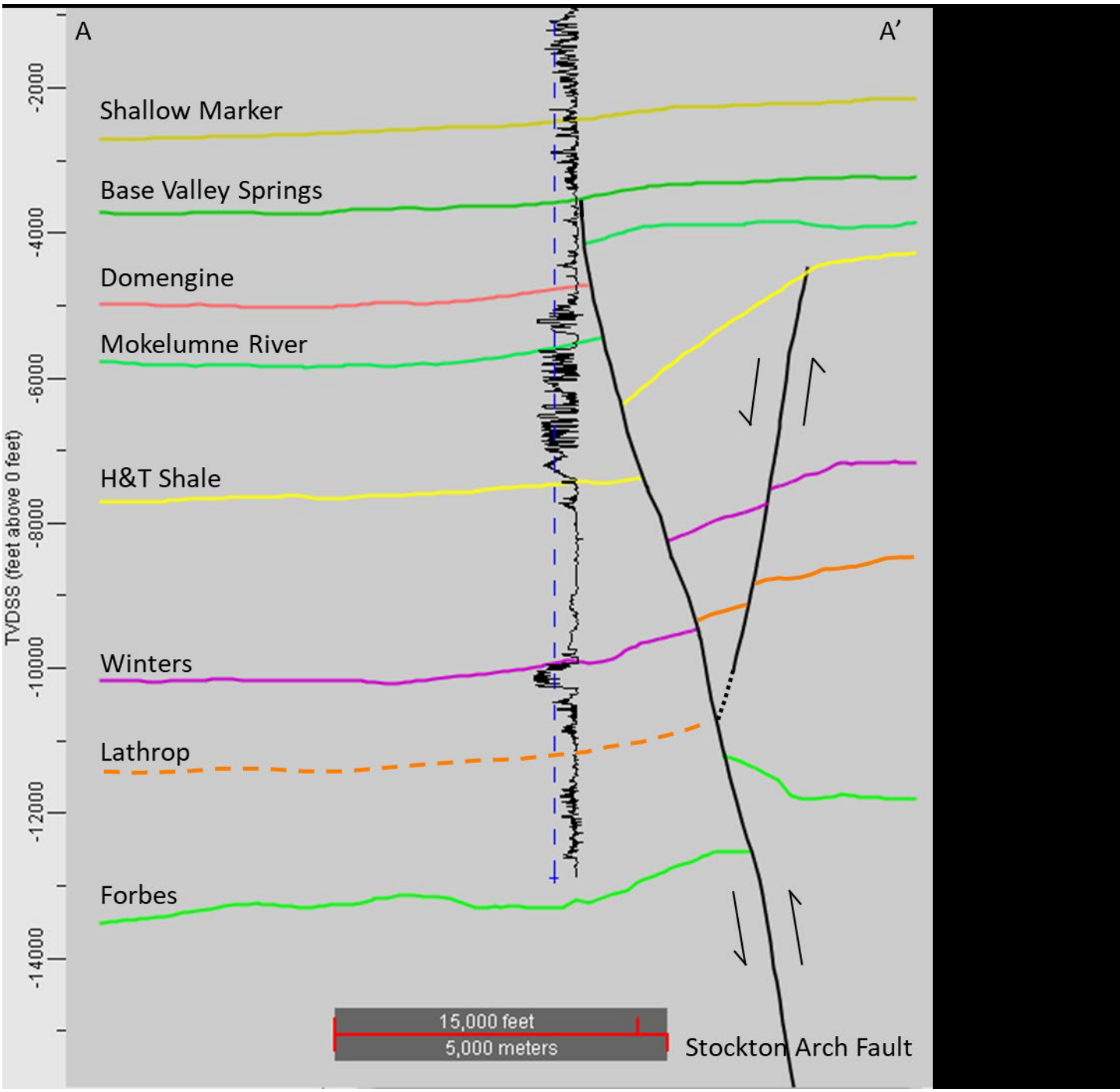

Figure A-22. Structural cross section across the geologic model. Well Union Properties 2 (04077203220000) is shown with SP log (negative values to left) for correlation and geologic packages. Geologic surfaces developed from seismic interpretation. The Stockton Arch Fault is cut-off by the Base Valley Springs. The interpreted antithetic fault to the east is dashed into the Stockton Arch Fault.

Company:	CRC									
Well:	Pool B-2					Date:	3-1-2022			
Field:	Lathrop					Test Type:				
Elev:						Zero Point:				
Top of Perforations:			End of Perforations:			Mid. Perfs:				
		Going In Hole Gradients					Pressure	Temp		Gas-lift
Stop	Time	WLD	MD	TVD	BHP	BHT	Gradient	Gradient		Valves
#	HH:MM:SS	(feet)	(feet)	(feet)	(psi)	(Deg.F)	(psi/ft)	(F/100 ft)		(feet)
1	11:31:00	10040	10053	10053	1171.42	218.05	-	-		
2	11:50:15	9487	9500	9500	1155.54	212.72	0.029	0.964		
3	11:56:00	8987	9000	9000	1145.81	205.93	0.019	1.358		
4	12:01:40	8487	8500	8500	1137.86	199.01	0.016	1.385		
5	12:07:10	7987	8000	8000	1128.56	192.78	0.019	1.245		
6	12:13:20	7487	7500	7500	1119.12	185.39	0.019	1.479		
7	12:18:35	6987	7000	7000	1109.33	177.64	0.020	1.550		
8	12:23:20	6487	6500	6500	1099.07	170.04	0.021	1.519		
9	12:28:40	5987	6000	6000	1088.60	162.41	0.021	1.526		
10	12:34:30	5487	5500	5500	1077.62	155.50	0.022	1.382		
11	12:40:00	4987	5000	5000	1066.76	149.17	0.022	1.266		
12	12:45:50	4487	4500	4500	1055.74	142.08	0.022	1.419		
13	12:51:30	3987	4000	4000	1044.79	134.20	0.022	1.576		
14	12:56:55	3487	3500	3500	1033.85	125.07	0.022	1.826		
15	13:02:10	2987	3000	3000	1022.48	116.21	0.023	1.772		
16	13:07:30	2487	2500	2500	1010.51	107.48	0.024	1.746		
17	13:12:55	1987	2000	2000	998.70	98.17	0.024	1.863		
18	13:18:35	1487	1500	1500	986.70	89.41	0.024	1.751		
19	13:23:40	987	1000	1000.0	974.94	80.2	0.024	1.847		
20	13:28:50	487	500	500.0	963.26	71.4	0.024	1.848		

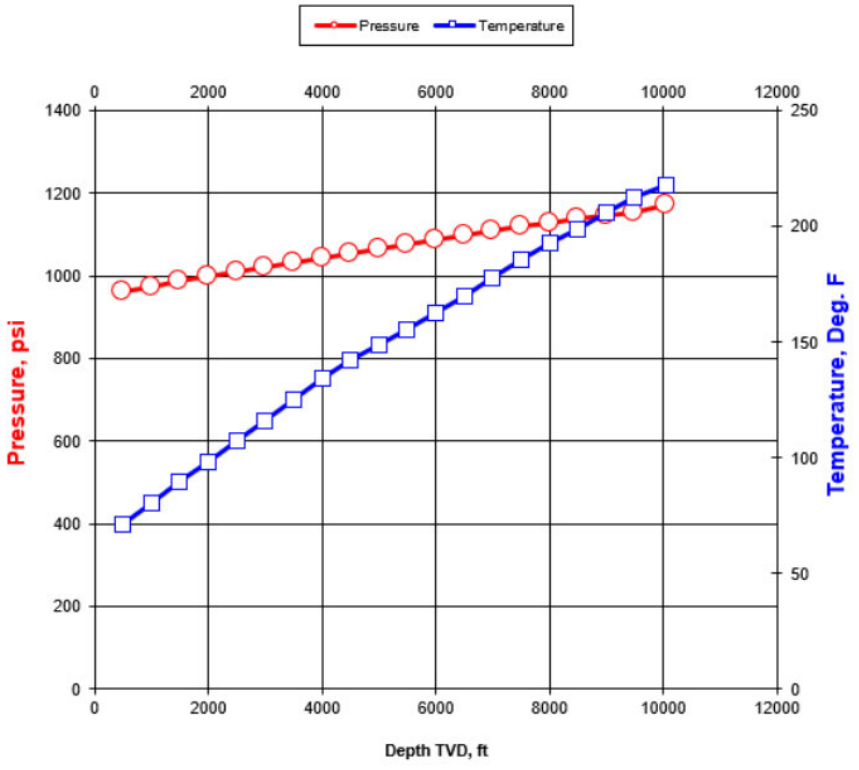

Figure A-23. POOL B-2 Pressure and Temperature Gradient

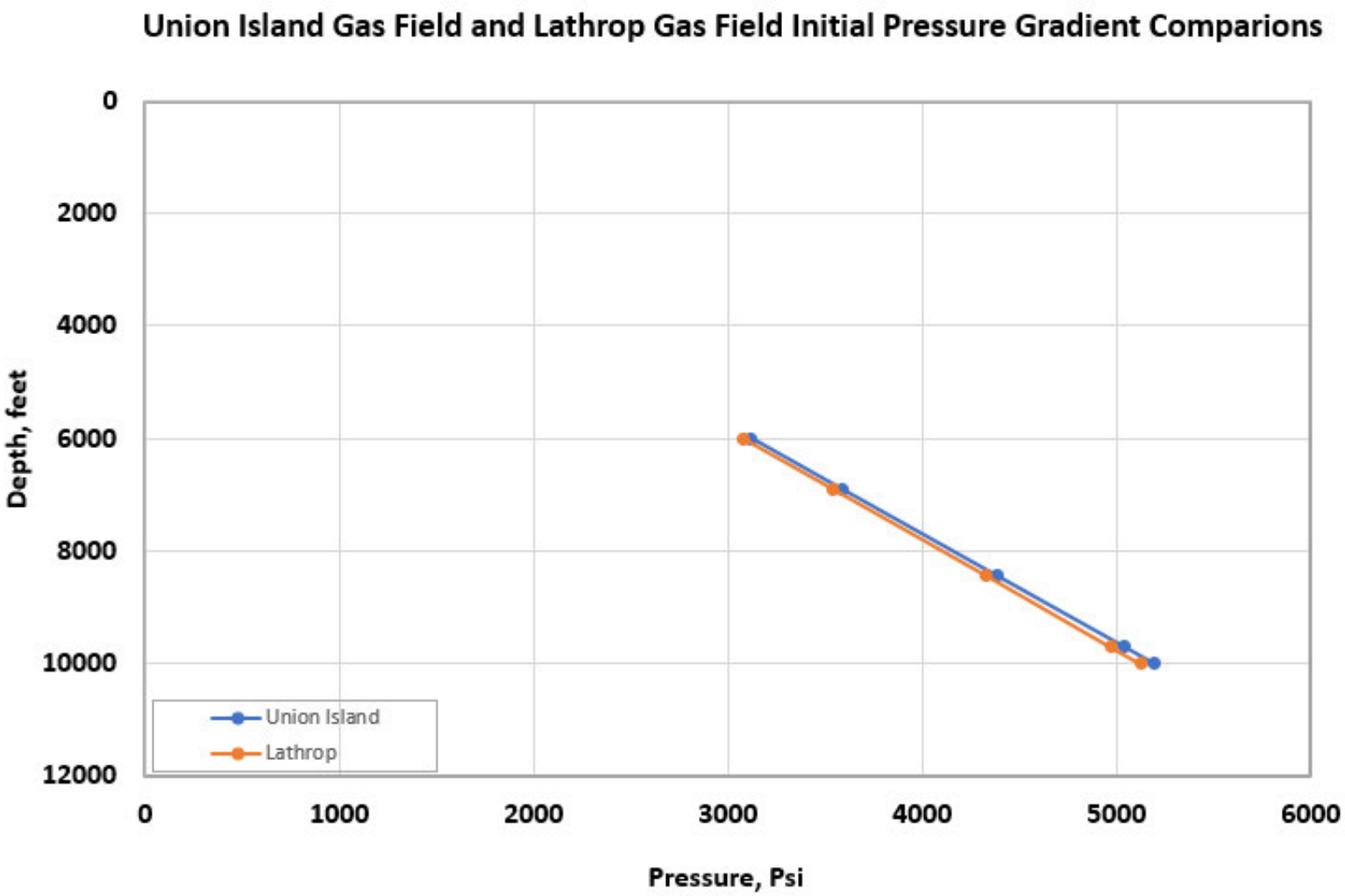

Figure A-24. Discovery pressure gradients at Union Island and Lathrop gas field.

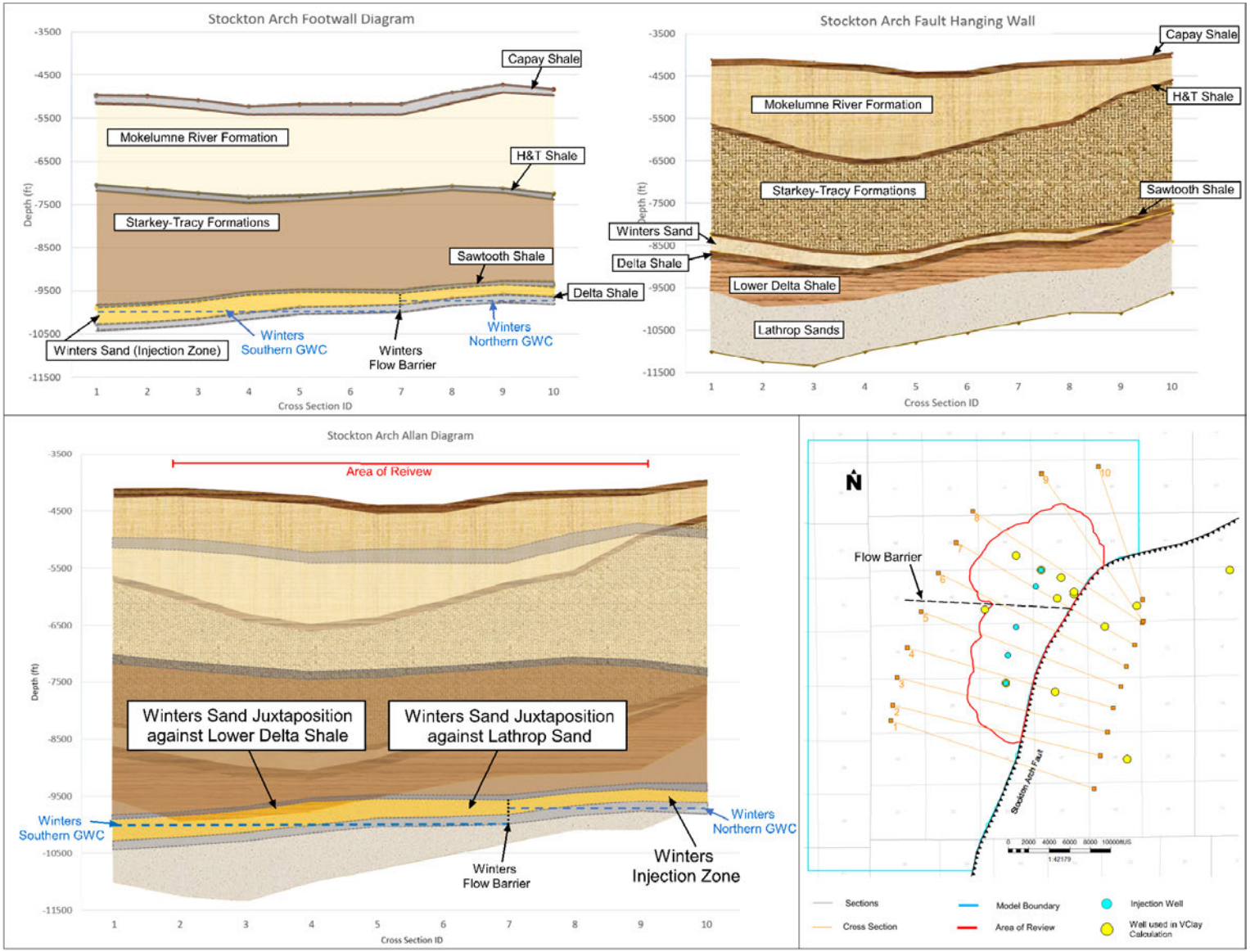

Figure A-25. Stockton Arch Fault Juxtaposition

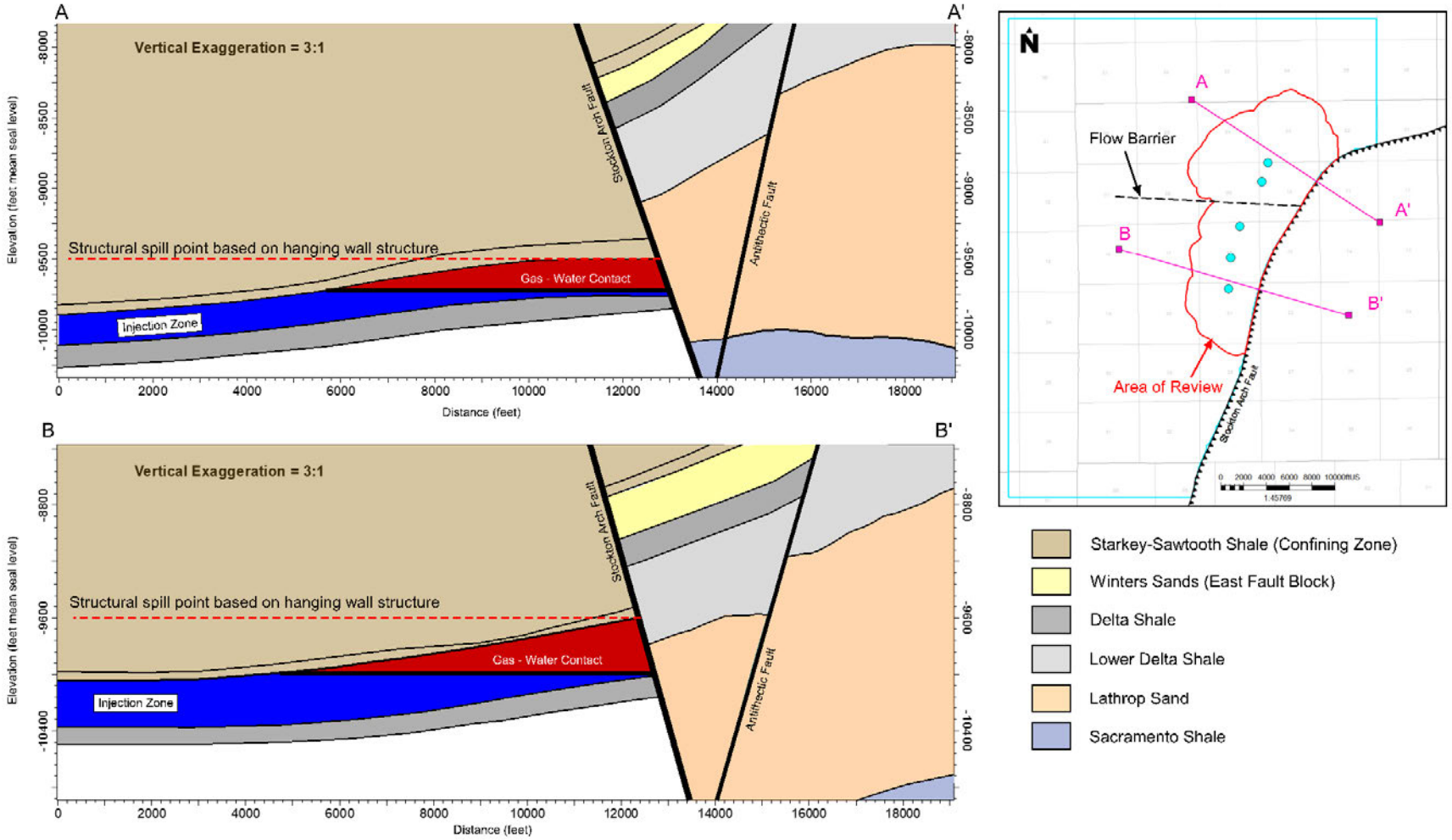

Figure A-26. Gas-water contacts and structural spill points.

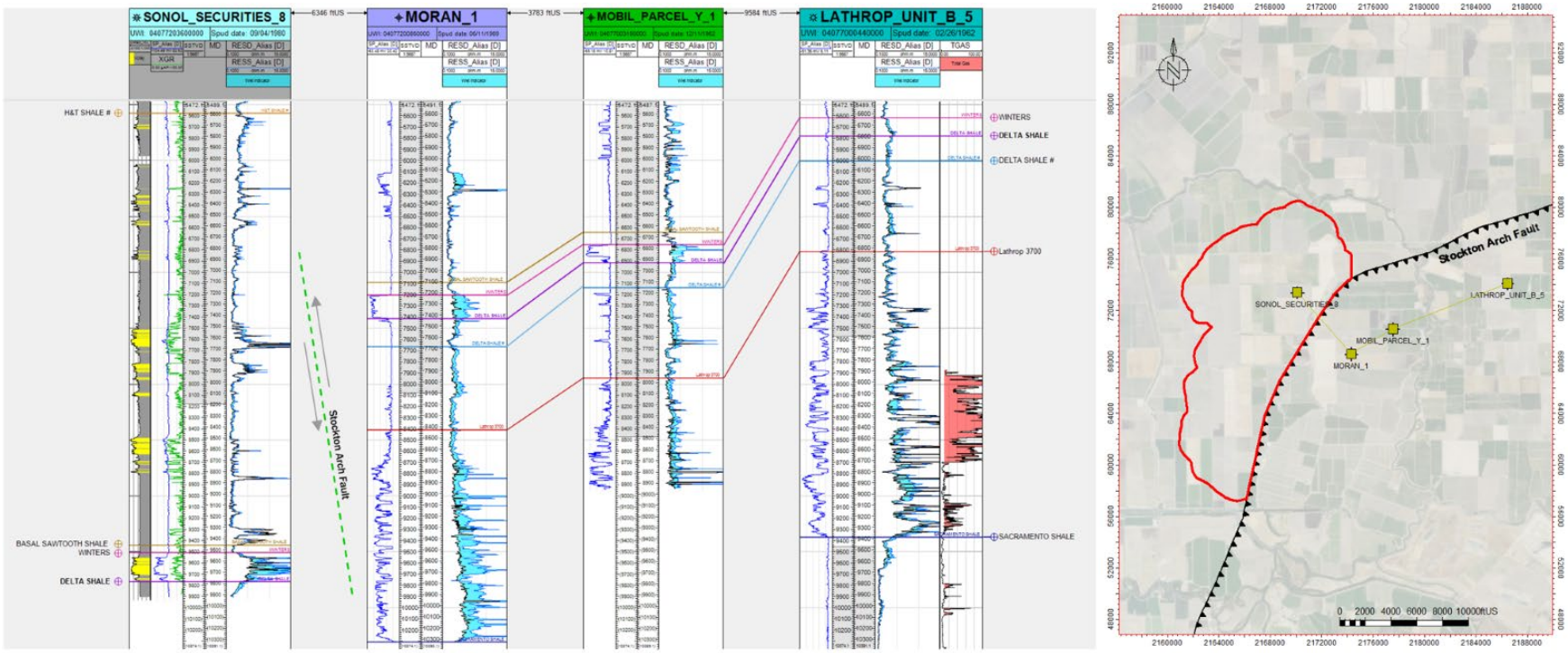

Figure A-27. Well section across the Stockton Arch Fault.

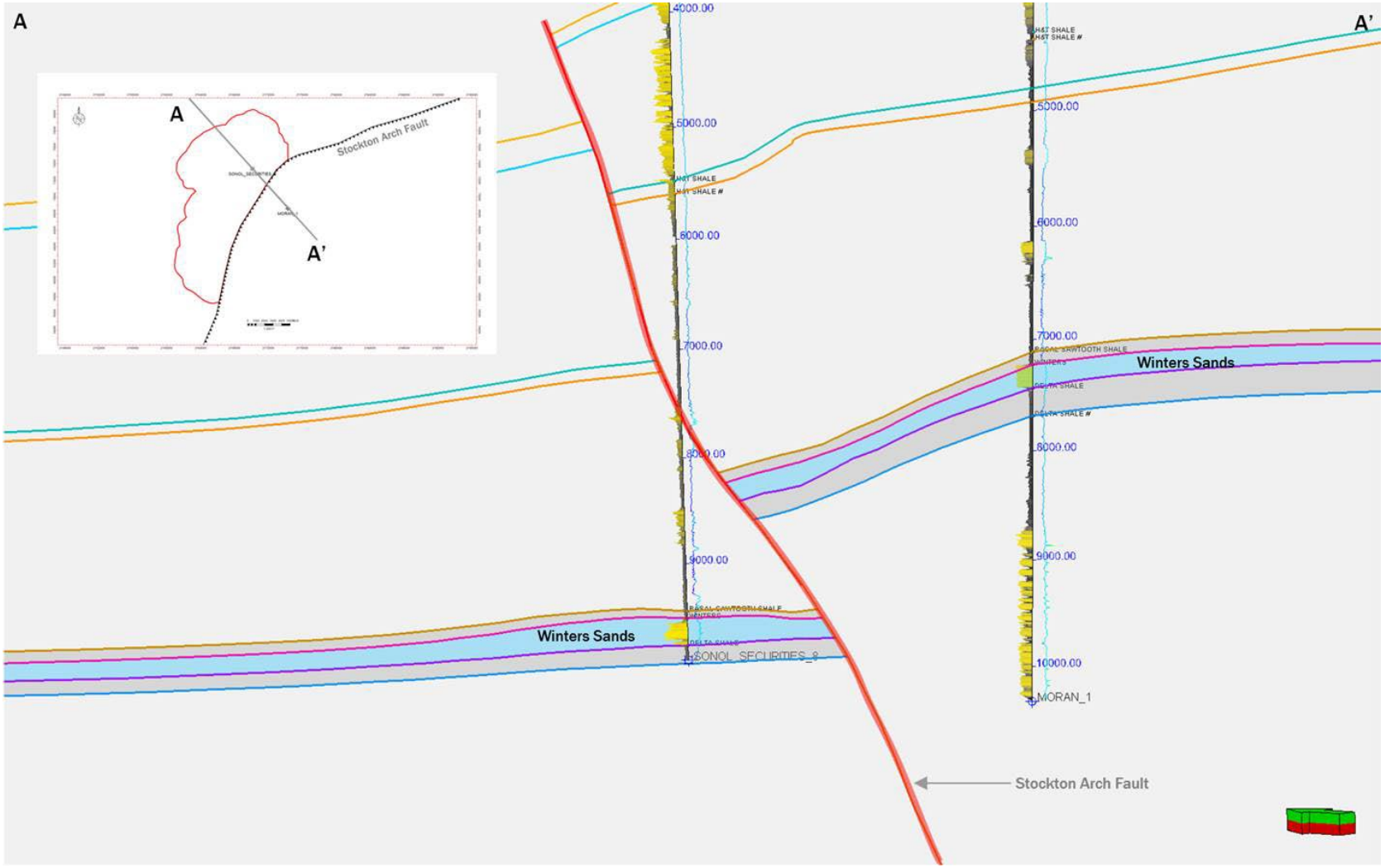

Figure A-28. Localized structural section showing a more precise location of the Stockton Arch Fault between wells Sonol_Securities_8 and Moran_1 shown in the Figure A-27 well correlation panel.

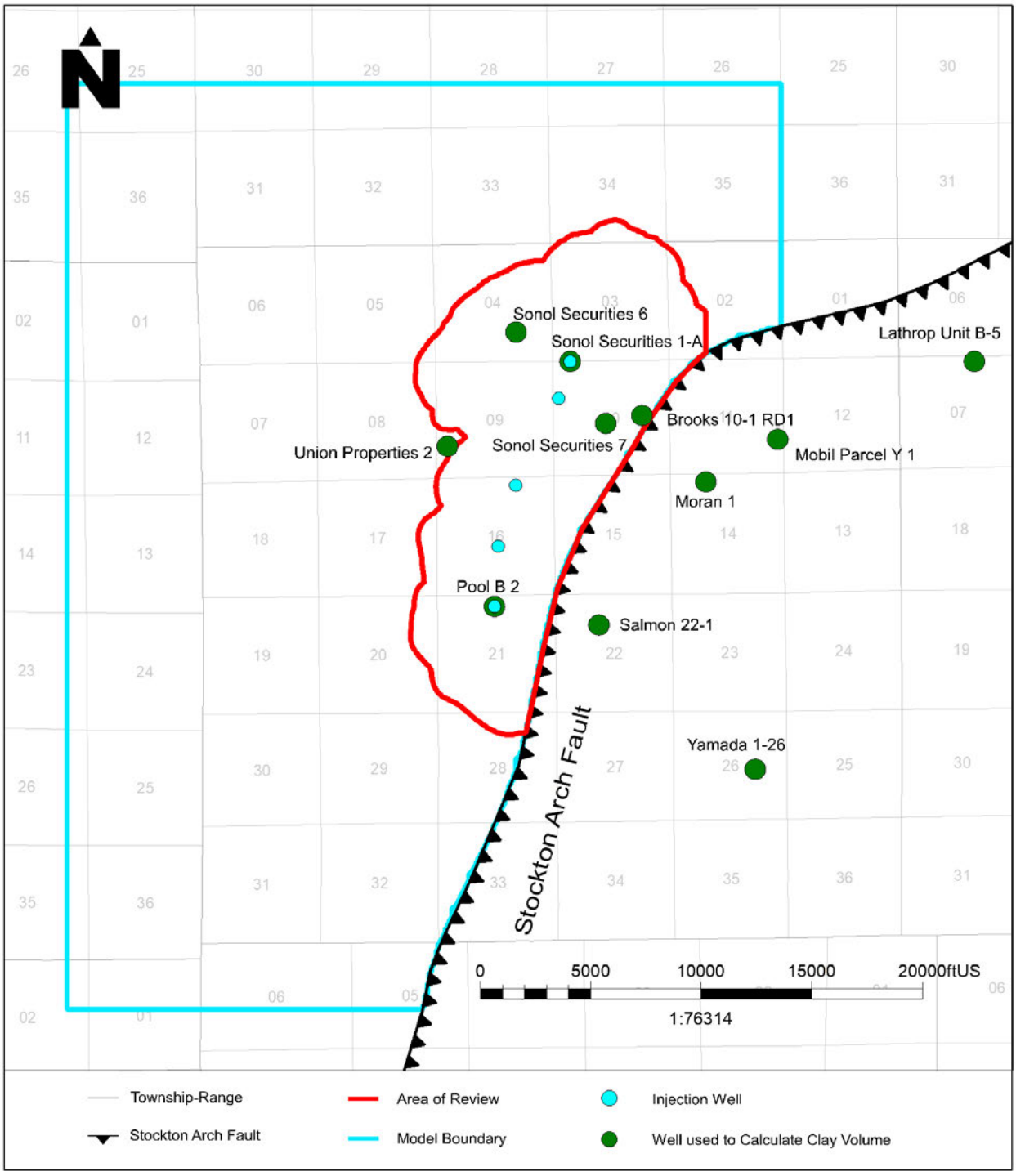

Figure A-29. Wells used to Calculate Clay Volume.

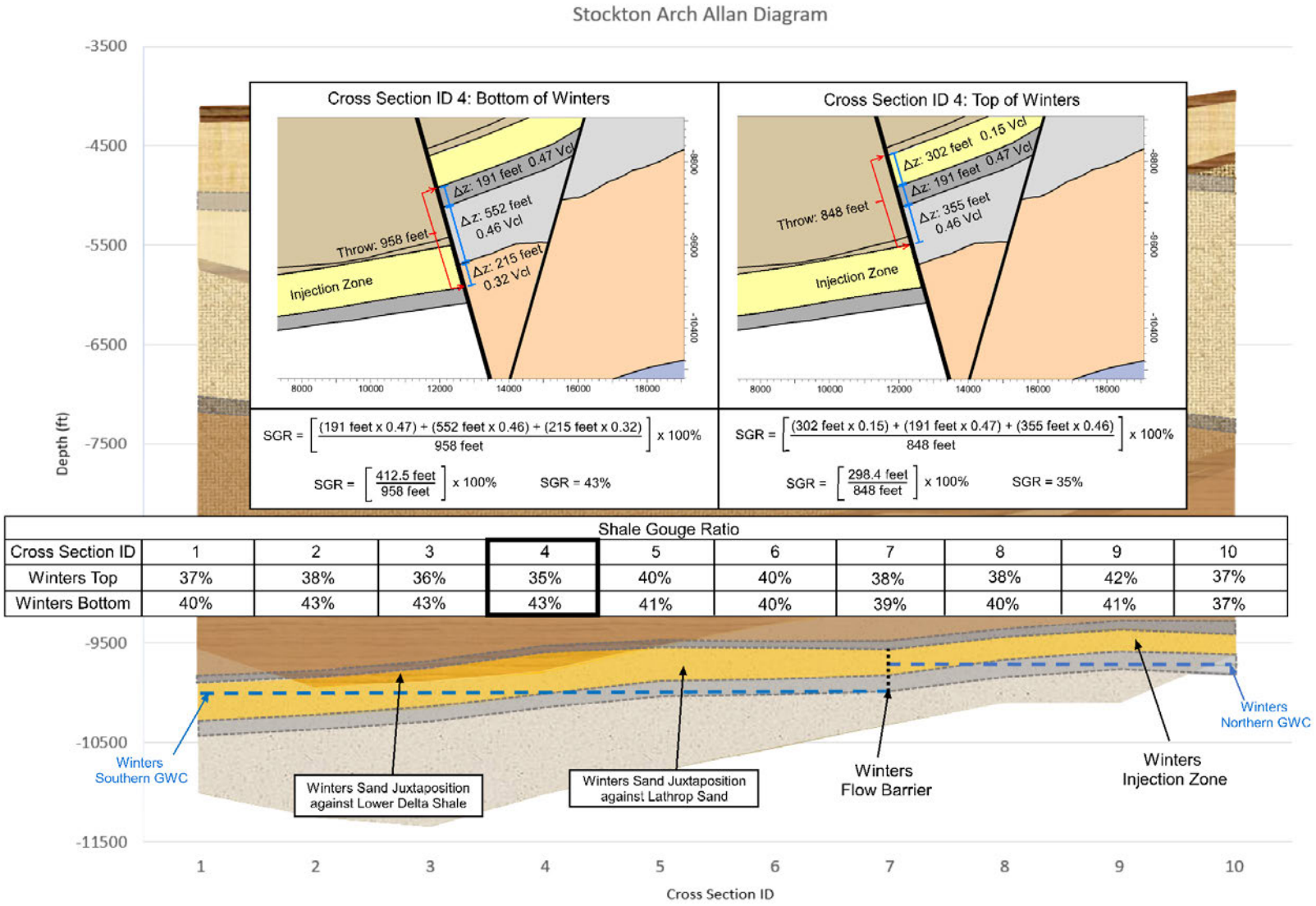

Shale Gouge Ratio

Cross Section ID	1	2	3	4	5	6	7	8	9	10
Winters Top	37%	38%	36%	35%	40%	40%	38%	38%	42%	37%
Winters Bottom	40%	43%	43%	43%	41%	40%	39%	40%	41%	37%

Figure A-30. Allan Diagram with Shale Gouge Ratio Results for the Top and Bottom of the Injection Zone.

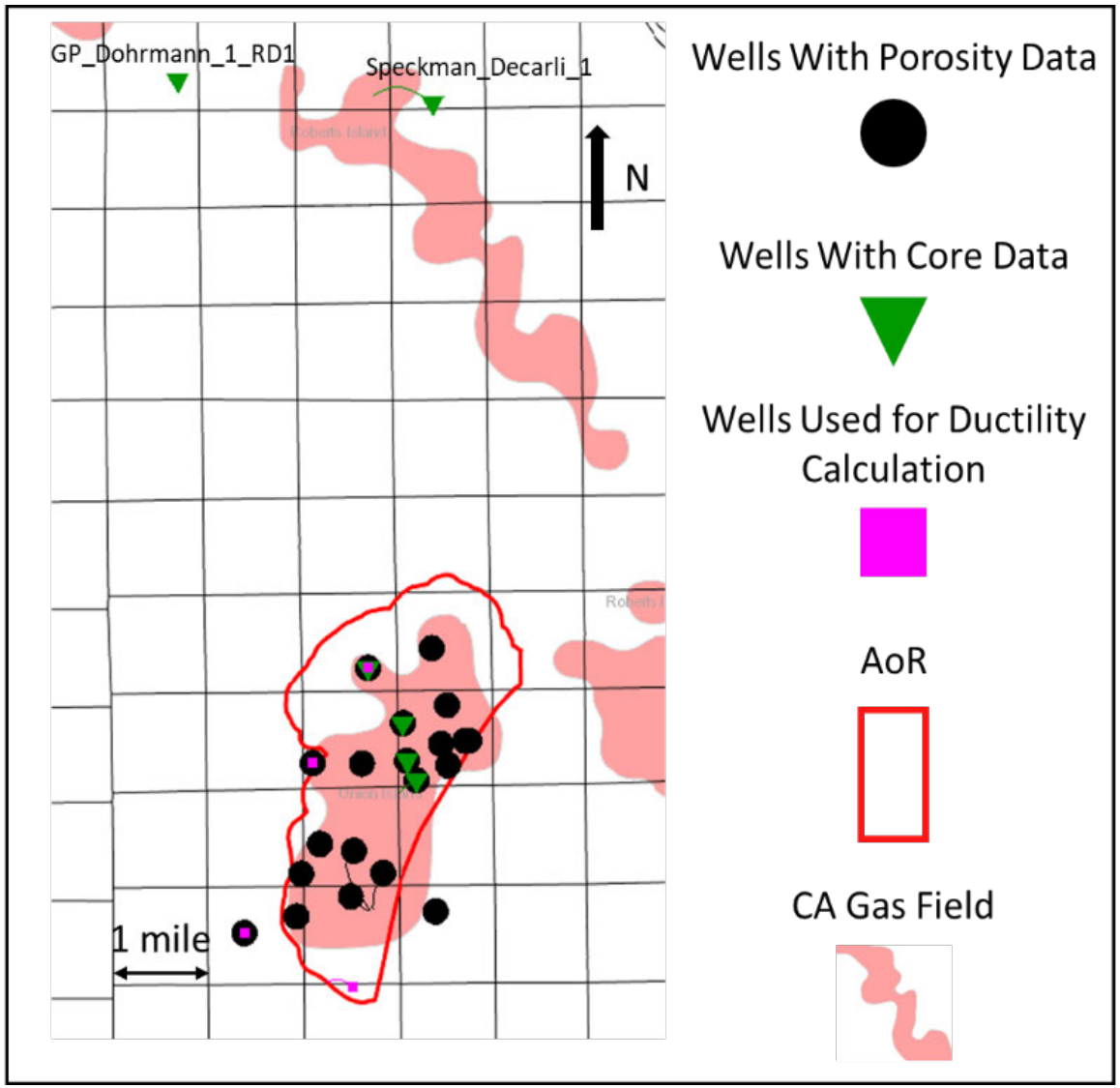

Figure A-31. Map showing location of wells with mineralogy data relative to the AoR.

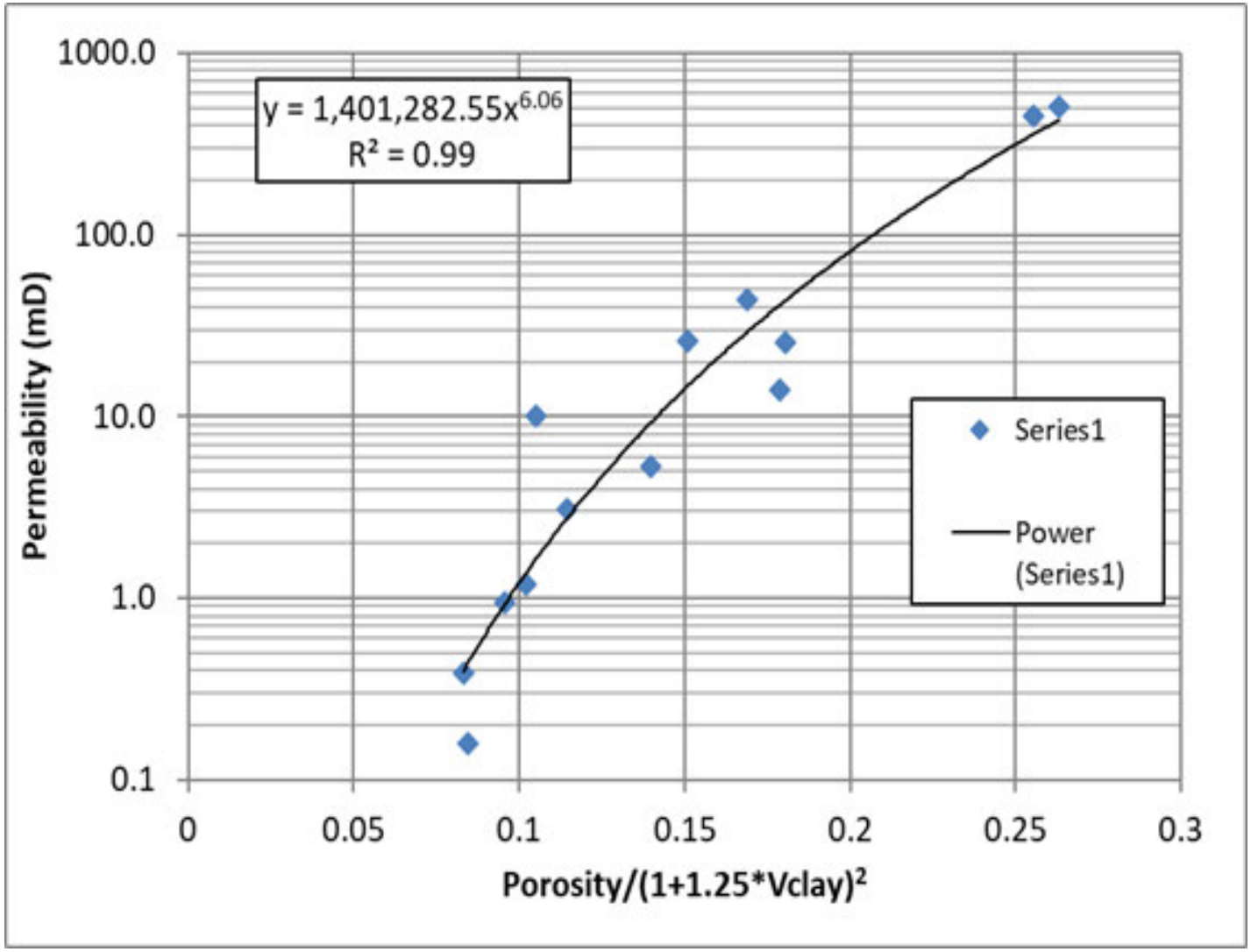

Figure A-32. Permeability transform for Sacramento basin zones.

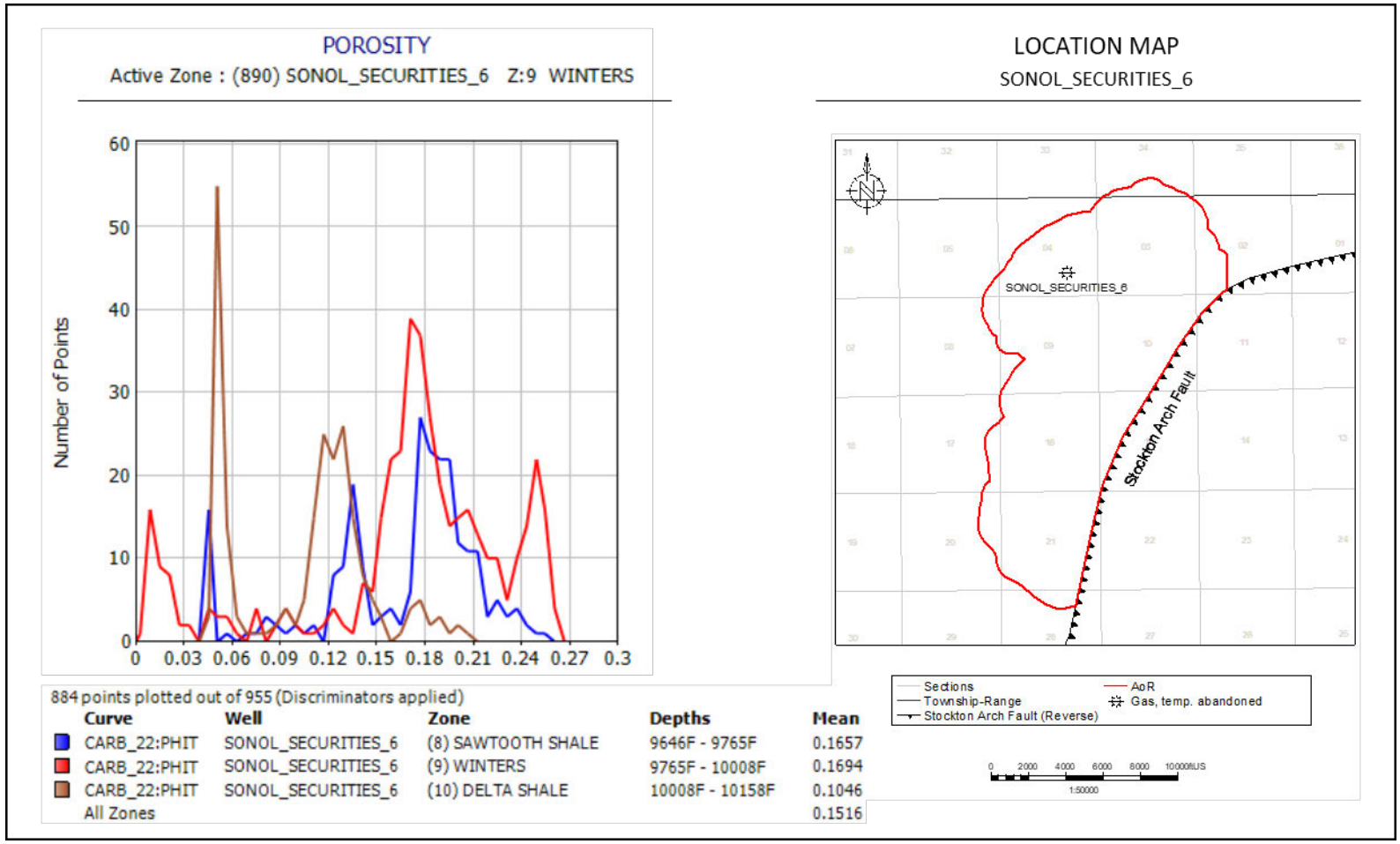

Figure A-33. Porosity histogram for well Sonol_Securities_6. In the histogram, blue represents the Sawtooth Shale, red the Winters Formation, and brown the Delta Shale. For the two shale intervals, only data with VCL>0.25 is shown, and for the Winters only data with VCL<=0.25 is shown.

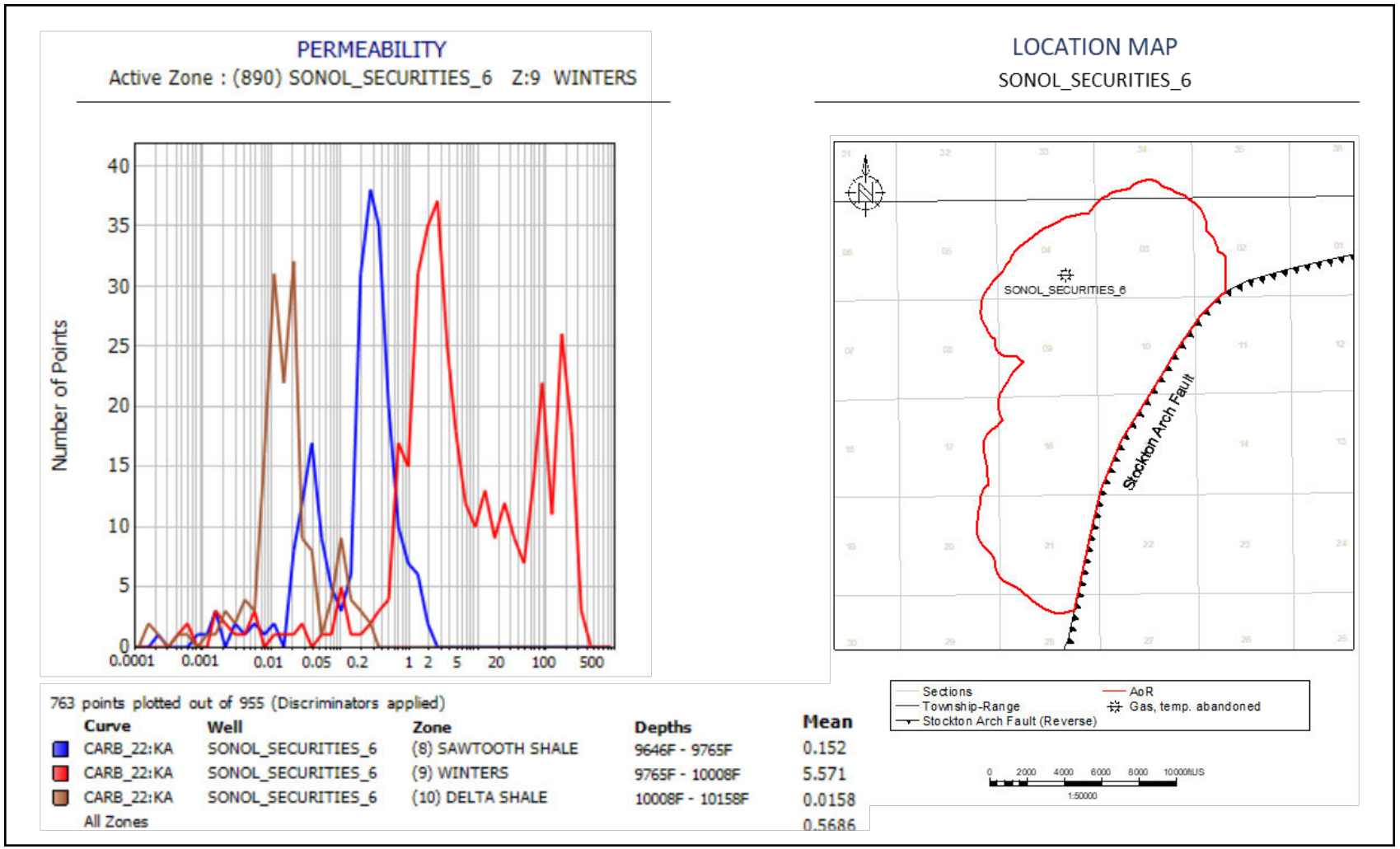

Figure A-34. Permeability histogram for well Sonol_Securities_6. In the histogram, blue represents the Sawtooth Shale, red the Winters Formation, and brown the Delta Shale. For the two shale intervals, only data with VCL>0.25 is shown, and for the Winters only data with VCL≤0.25 is shown.

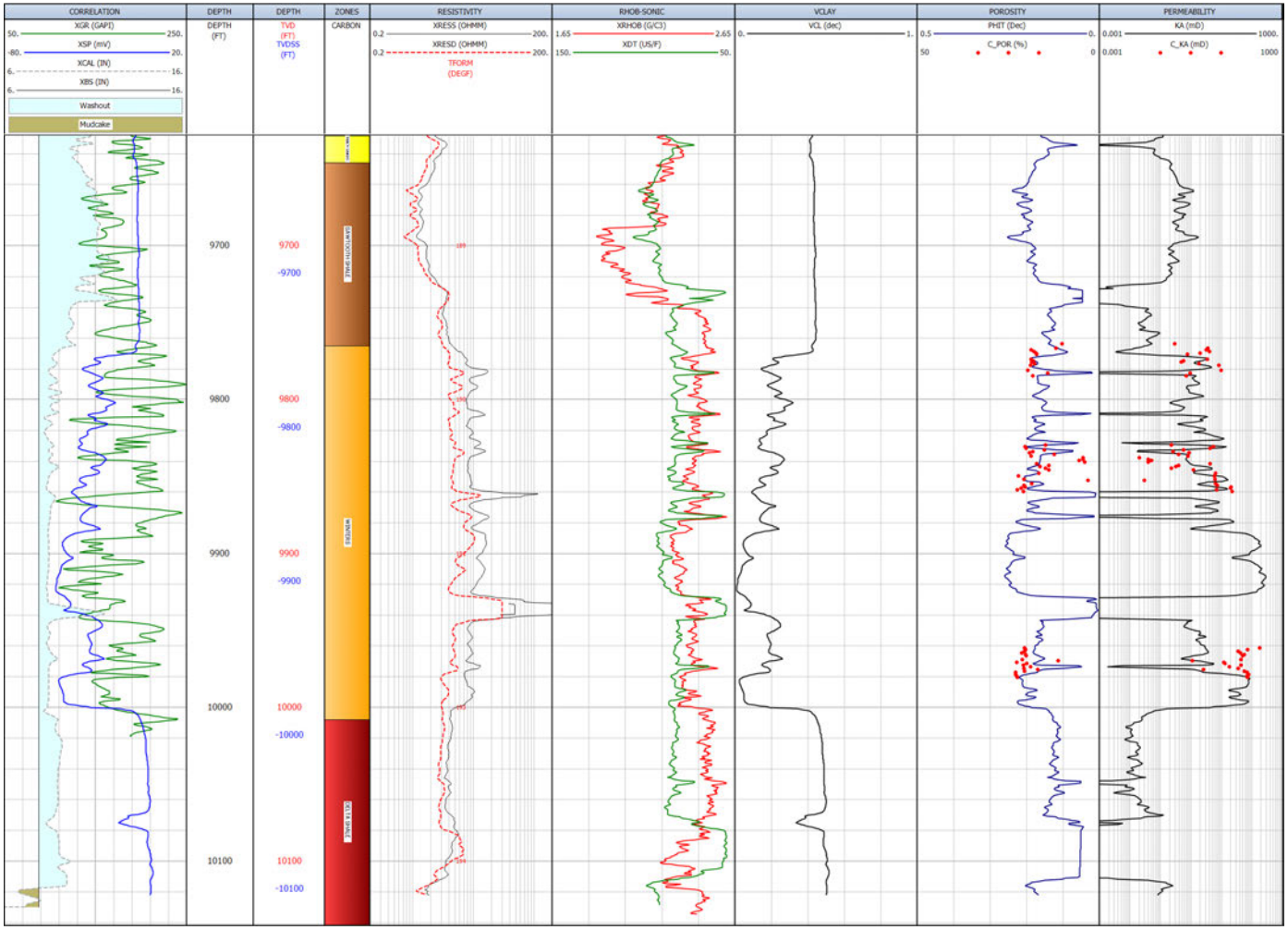

Figure A-35. Log plot for well Sonol_Securities_6, showing the log curves used as inputs into calculations of clay volume, porosity and permeability, and their outputs. Core data for porosity and permeability are shown for comparison to the log model. Track 1: Correlation and caliper logs. Track 2: Measured depth. Track 3: Vertical depth and vertical subsea depth. Track 4: Zones. Track 5: Resistivity. Track 6: Compressional sonic and density logs. Track 7: Volume of clay. Track 8: Porosity calculated from log curves and core porosity. Track 9: Permeability calculated using transform and core permeability.

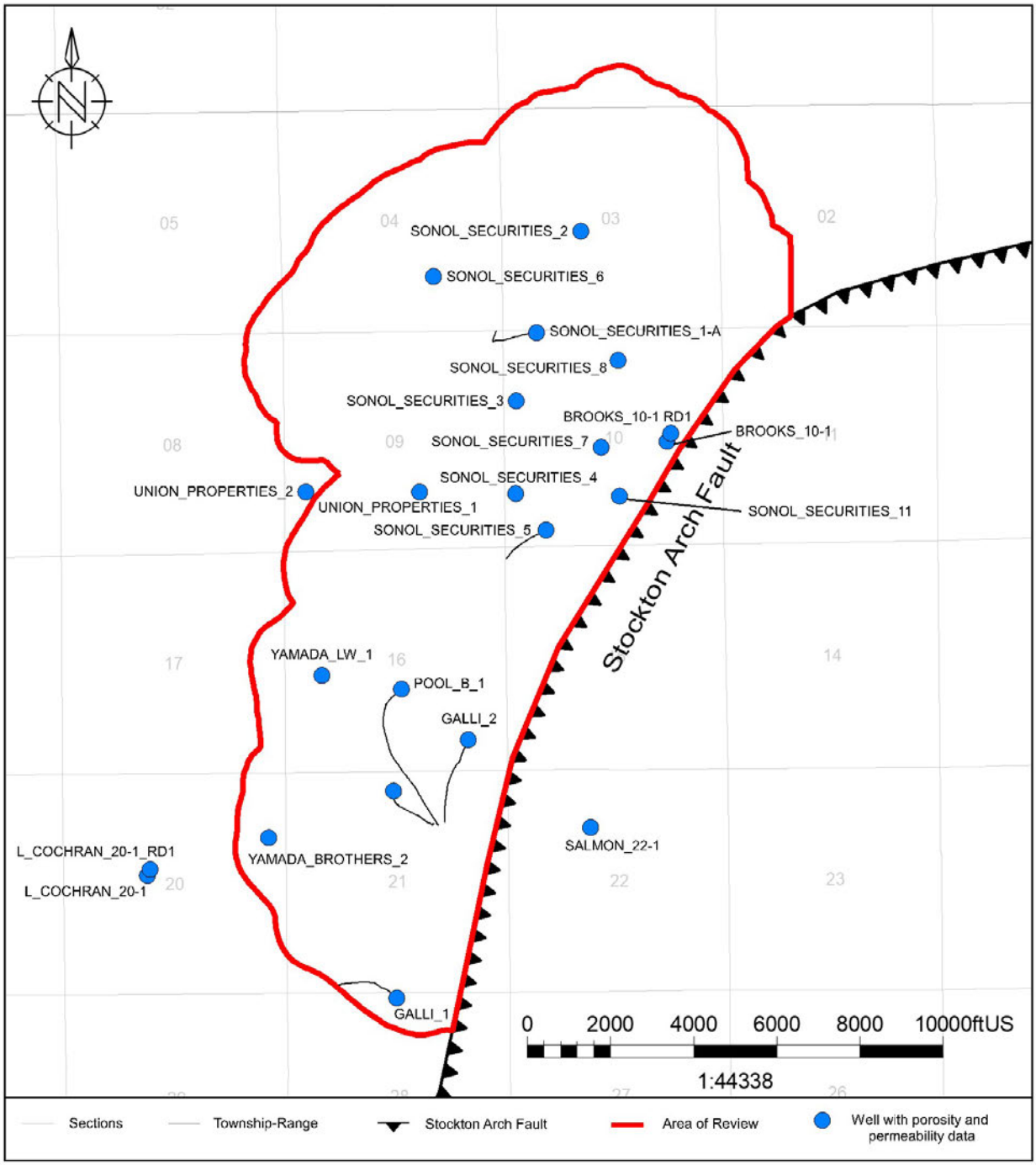

Figure A-36. Map of wells with porosity and permeability data.

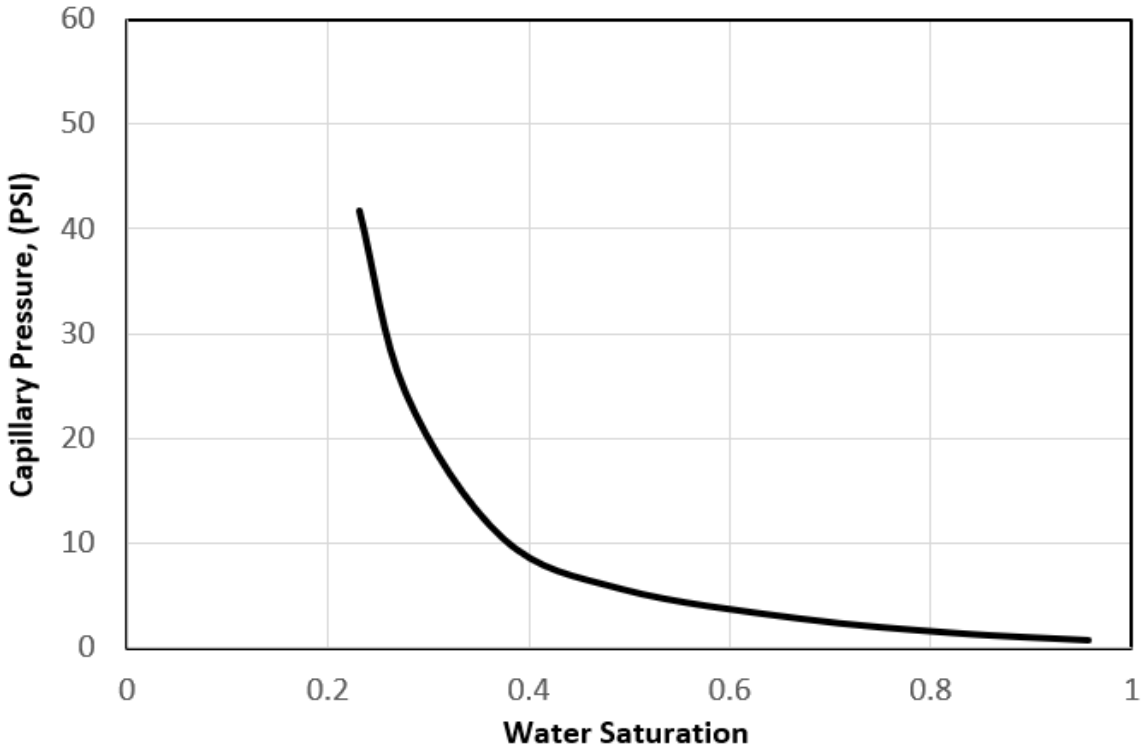

Figure A-37. Injection Zone capillary pressure curve used in computational modeling. Obtained from core sample from Sonol Securities 5 in the Union Island Gas Field.

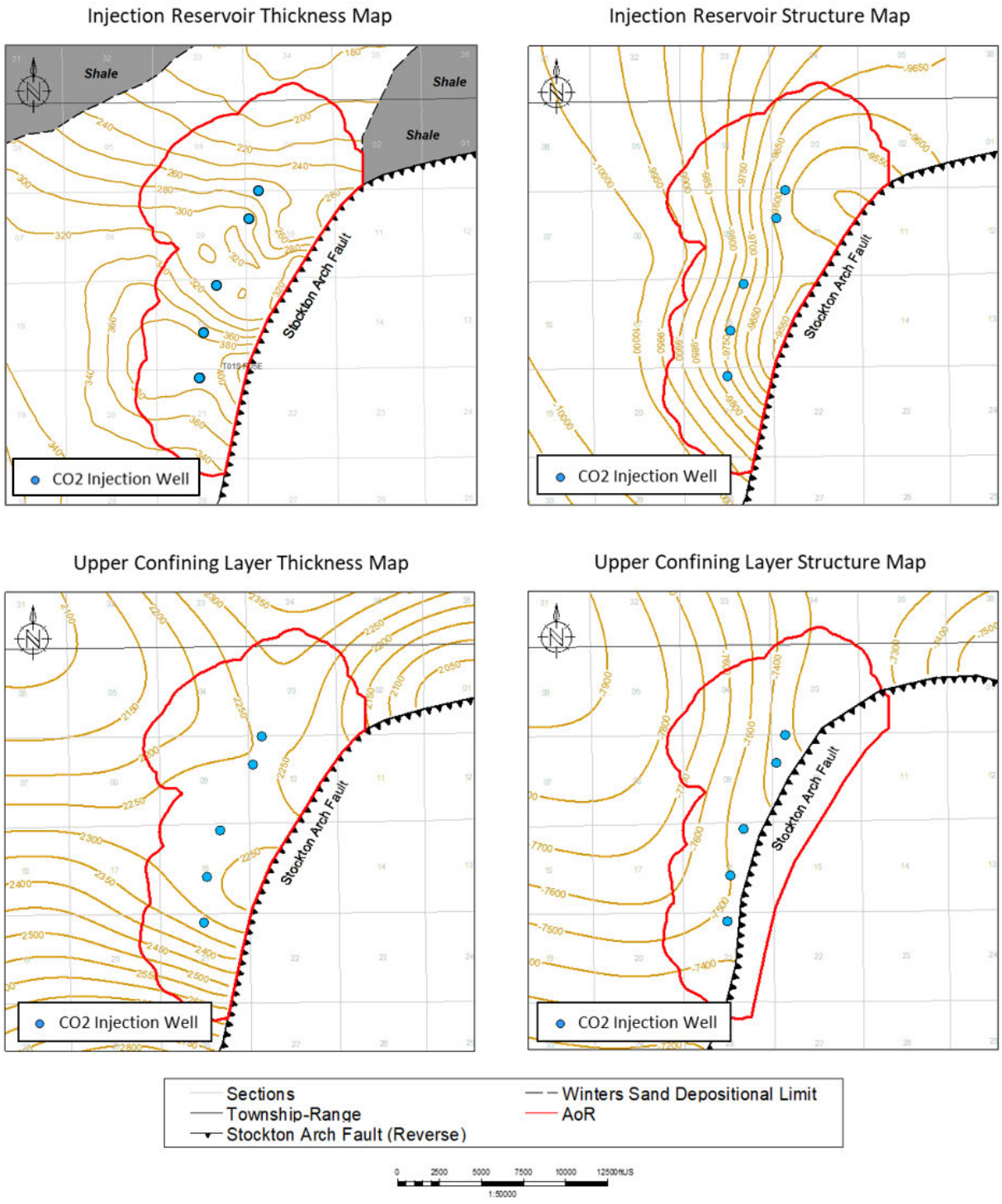

Figure A-38. Gross thickness and depth maps within the AoR for the injection reservoir and upper confining layer. The Stockton Arch Fault dips to the southeast, therefore the surface of the upper confining layer intersects the fault within the AoR boundary.

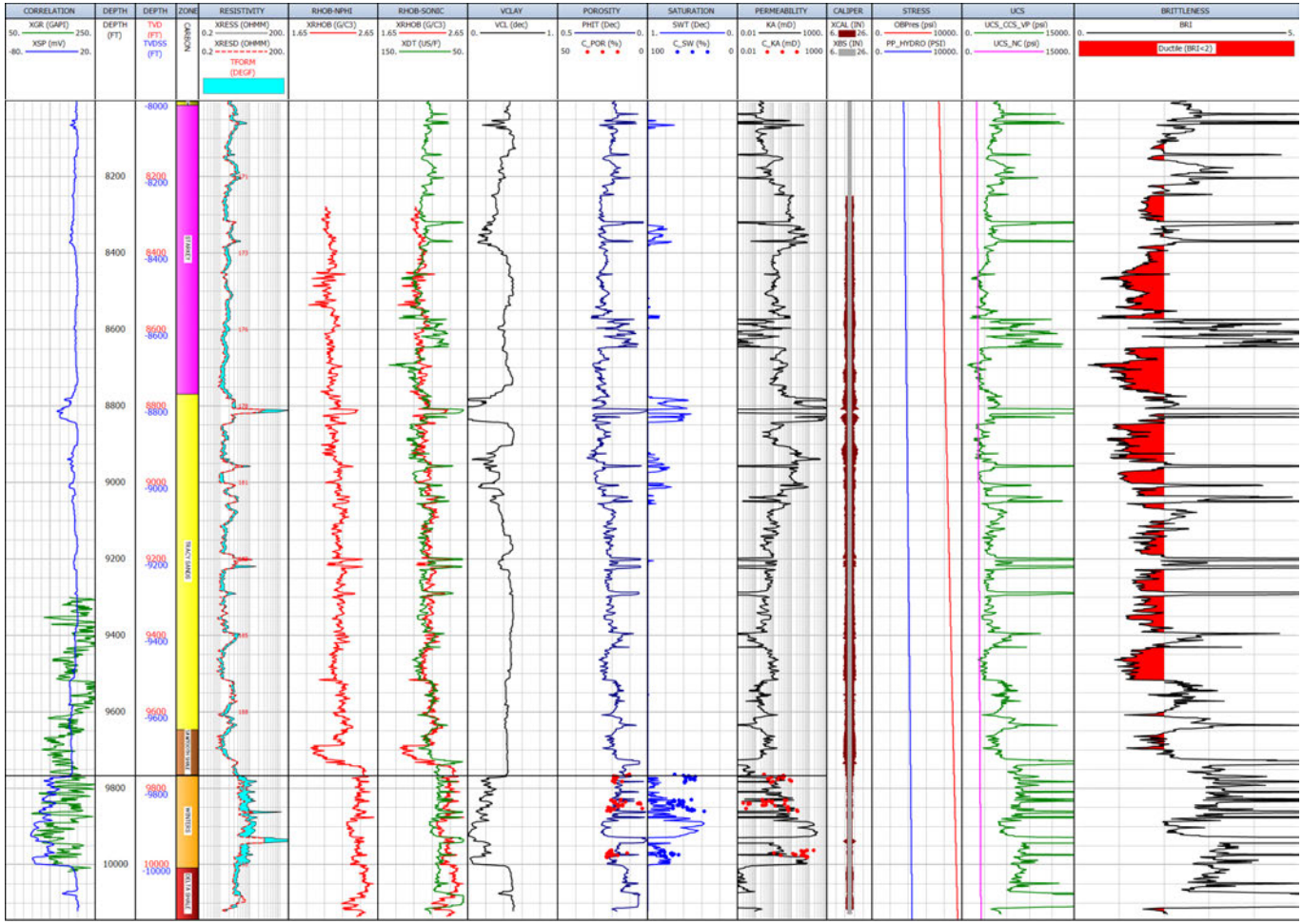

Figure A-39. Unconfined compressive strength and ductility calculations for Sonol_Securities_6. The upper confining zone ductility is less than two. Track 1: Correlation logs. Track 2: Measured depth. Track 3: Vertical depth and vertical subsea depth. Track 4: Zones. Track 5: Resistivity. Track 6: Density log. Track 7: Density and compressional sonic logs. Track 8: Volume of clay. Track 9: Porosity calculated from sonic and density. Track 10: Water saturation. Track 11: Permeability. Track 12: Caliper. Track 13: Overburden pressure and hydrostatic pore pressure. Track 14: UCS and UCS_NC. Track 15: Brittleness.

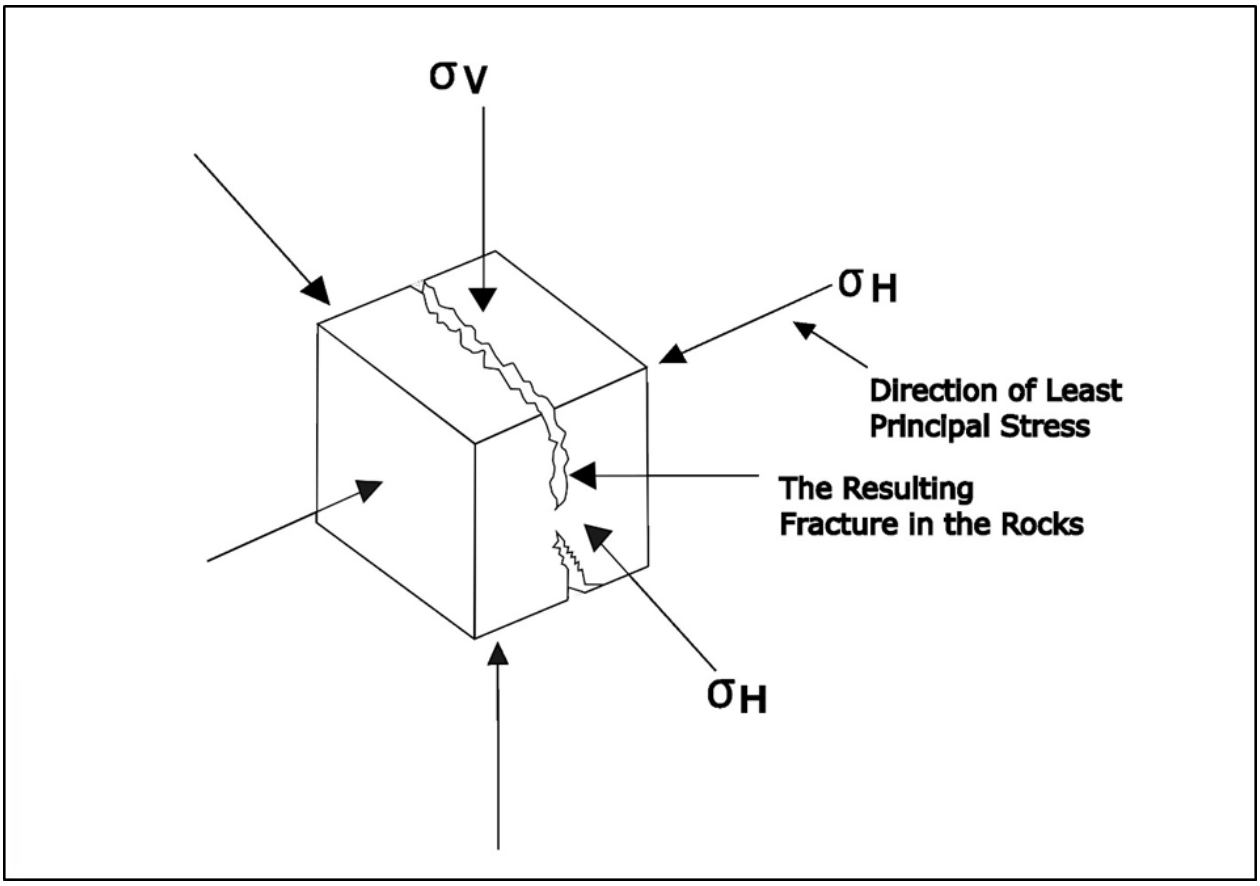

Figure A-40. Stress diagram showing the three principal stresses and the fracturing that will occur perpendicular to the minimum principal stress.

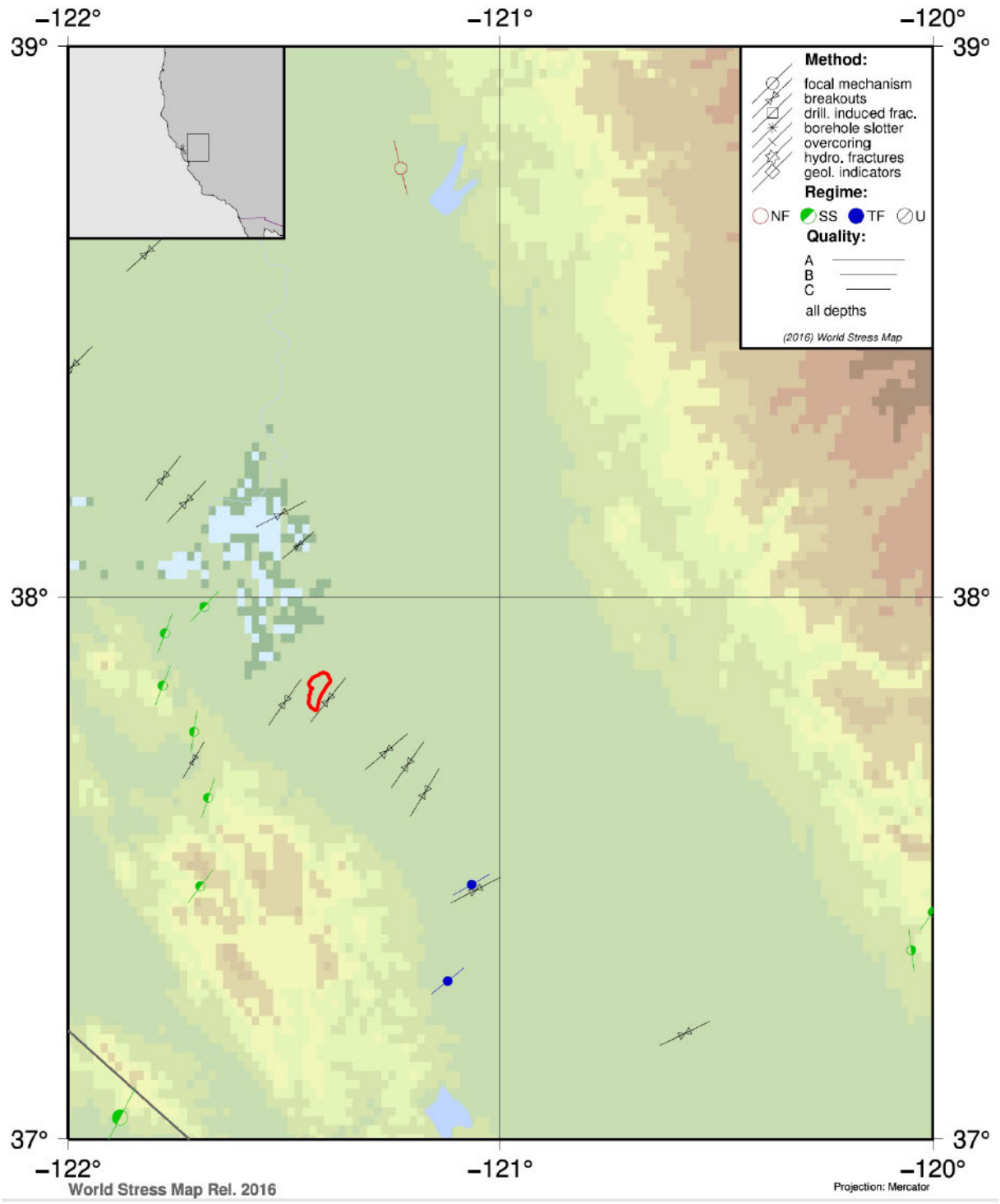

Figure A-41. World stress map output showing SHmax azimuth indicators and earthquake faulting styles in the Sacramento Basin (Heidbach et al., 2016). The red polygon is the project AoR. The background coloring represents topography.

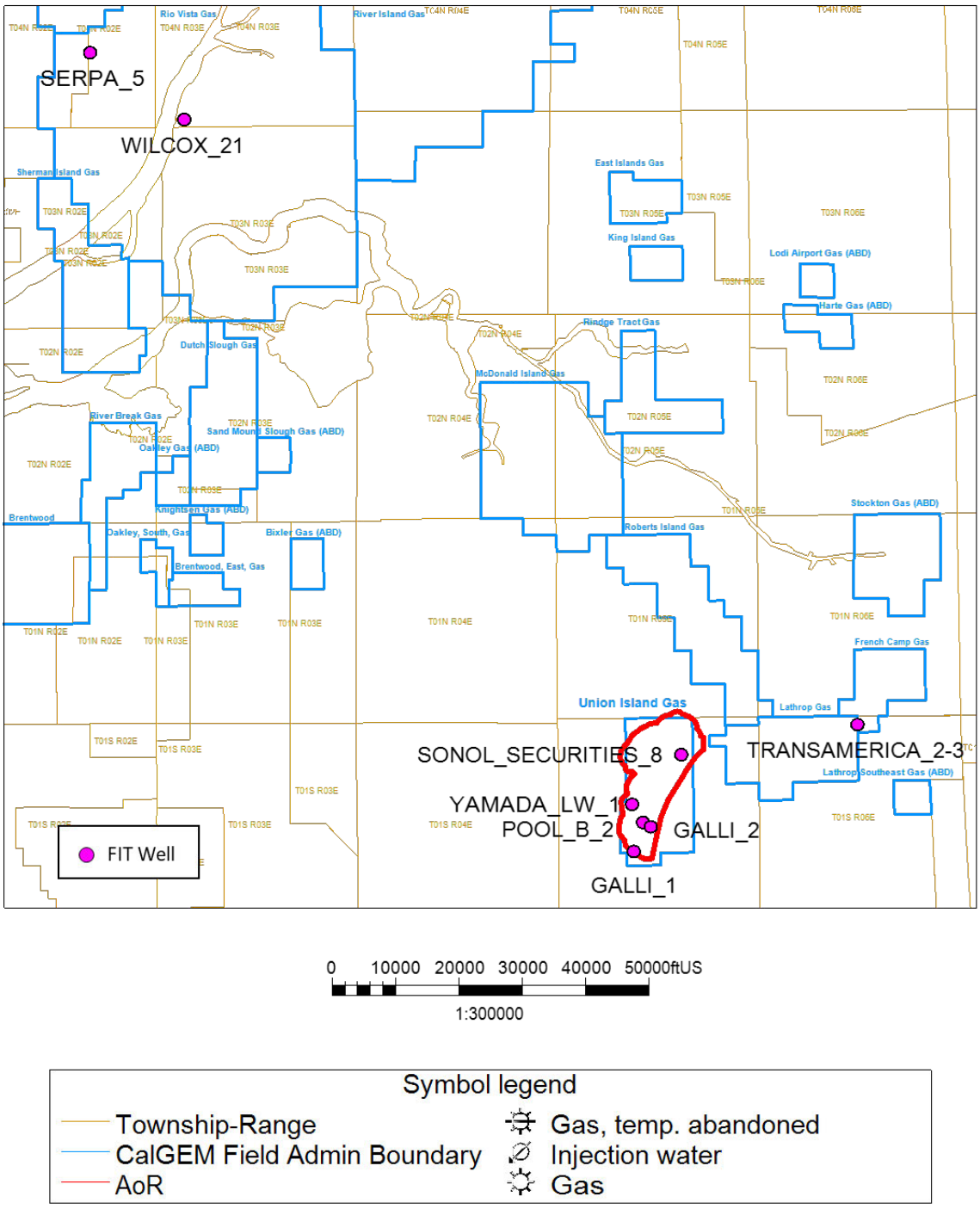

Figure A-42. Locations of wells with FIT data.

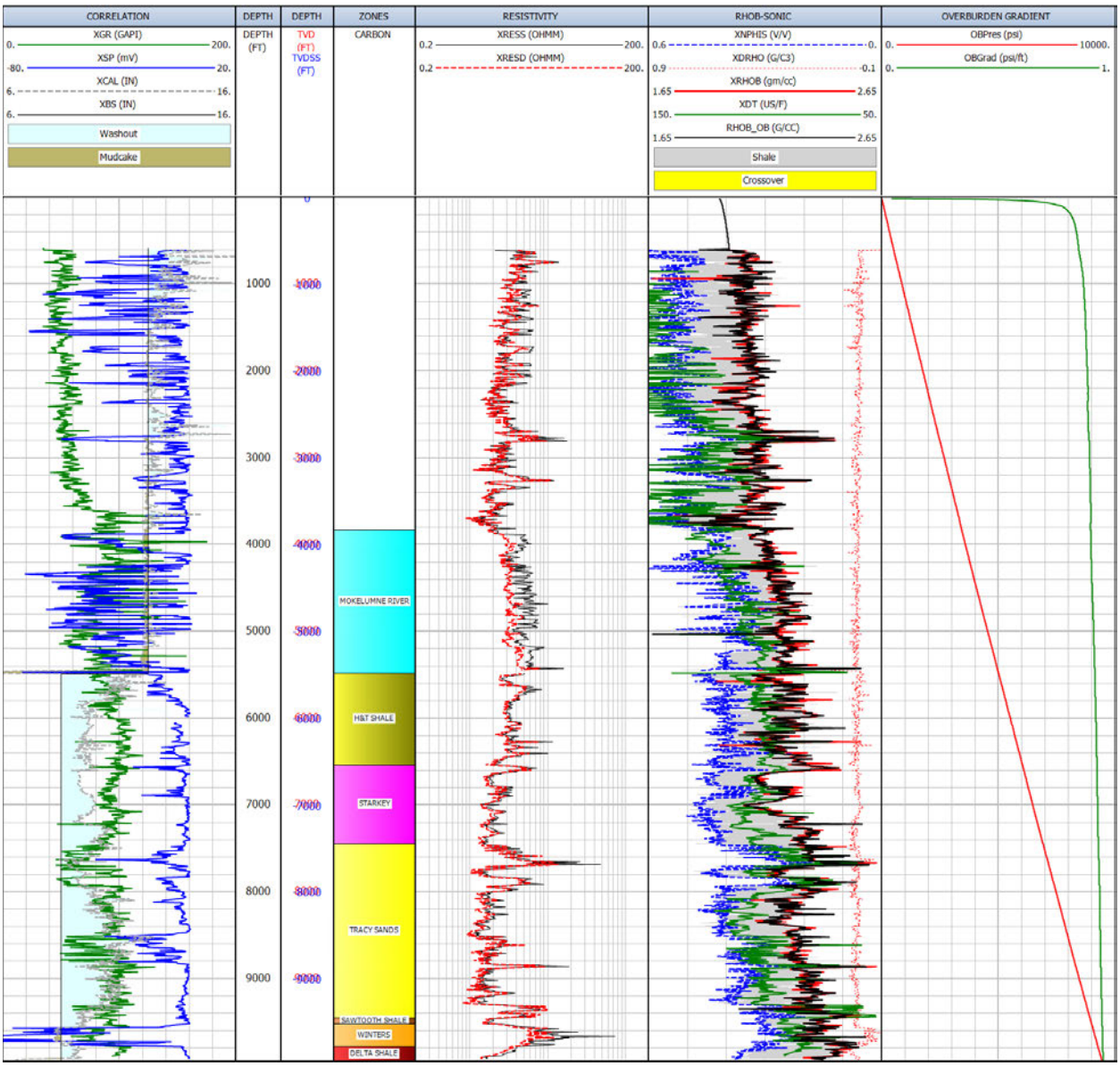

Figure A-43. Overburden gradient calculation for the SONOL_SECURITIES_8 (04077203600000). Track 1: Correlation logs and caliper log. Track 2: Measured depth. Track 3: Vertical depth and vertical subsea depth. Track 4: Zones. Track 5: Resistivity. Track 6: Density, neutron, and compressional sonic logs. The black curve shows the merged density curve with the shallow density trend as determined from nearby shallow density logs that was used for the overburden calculation. Track 7: Overburden pressure (red) and overburden gradient (green).

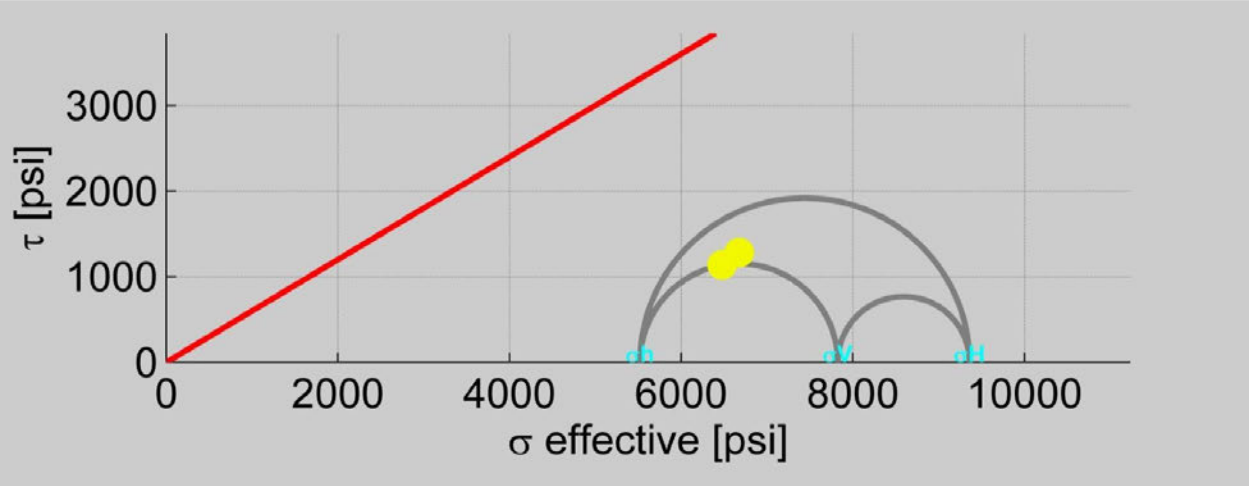

Figure A-44. Mohr circle of the Winters reservoir at present-day conditions. The normal stress (x-axis) and shear stress (y-axis) on the two Stockton Arch fault segments is represented by the two yellow dots. The red line represents the Mohr coulomb failure surface assuming a coefficient of friction of 0.6 and a fault cohesion of 0 psi.

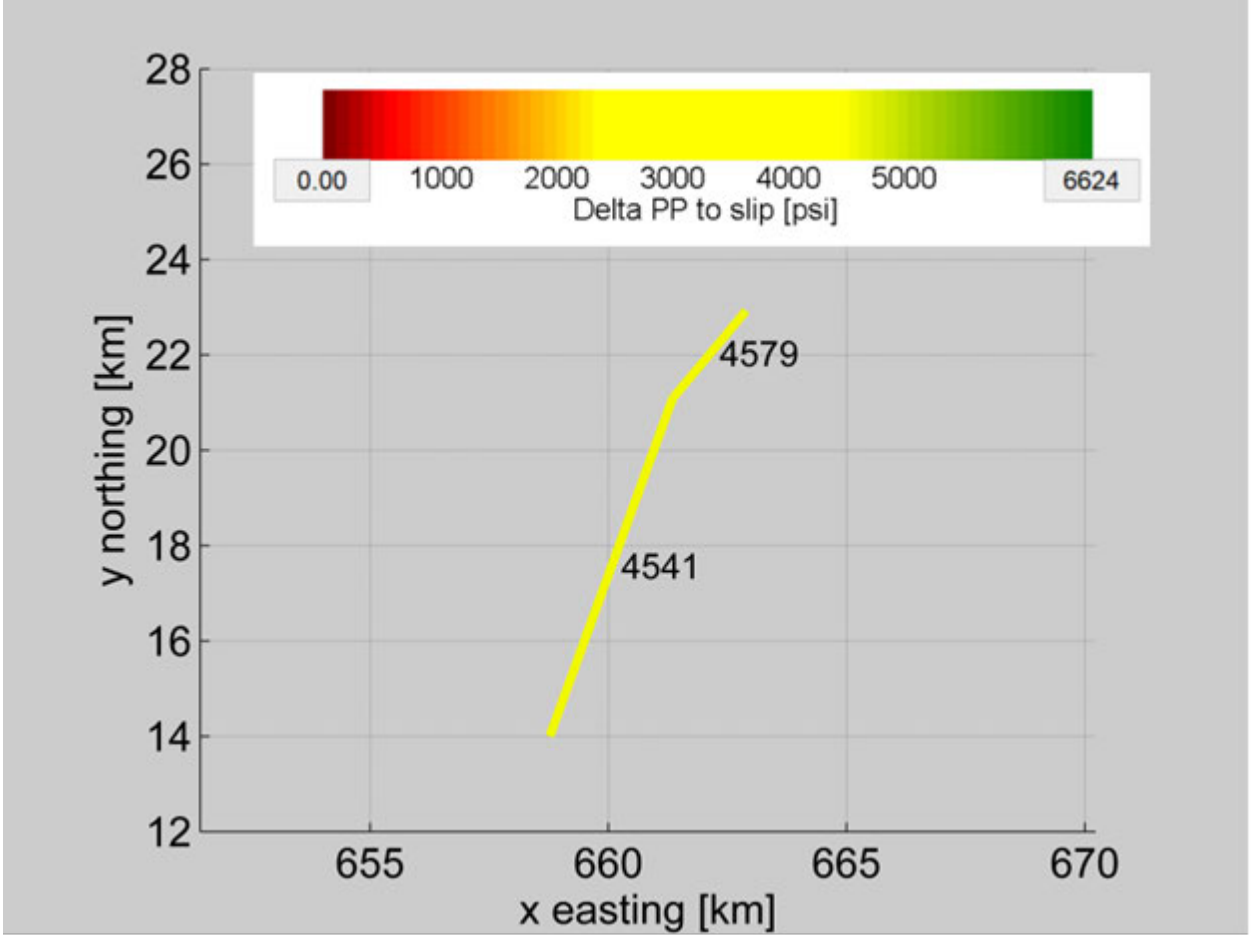

Figure A-45. Map showing the two modeled segments of the Stockton Arch Fault. The numbers on the plot represent the necessary increase in pore pressure above present-day conditions to cause failure on that fault segment.

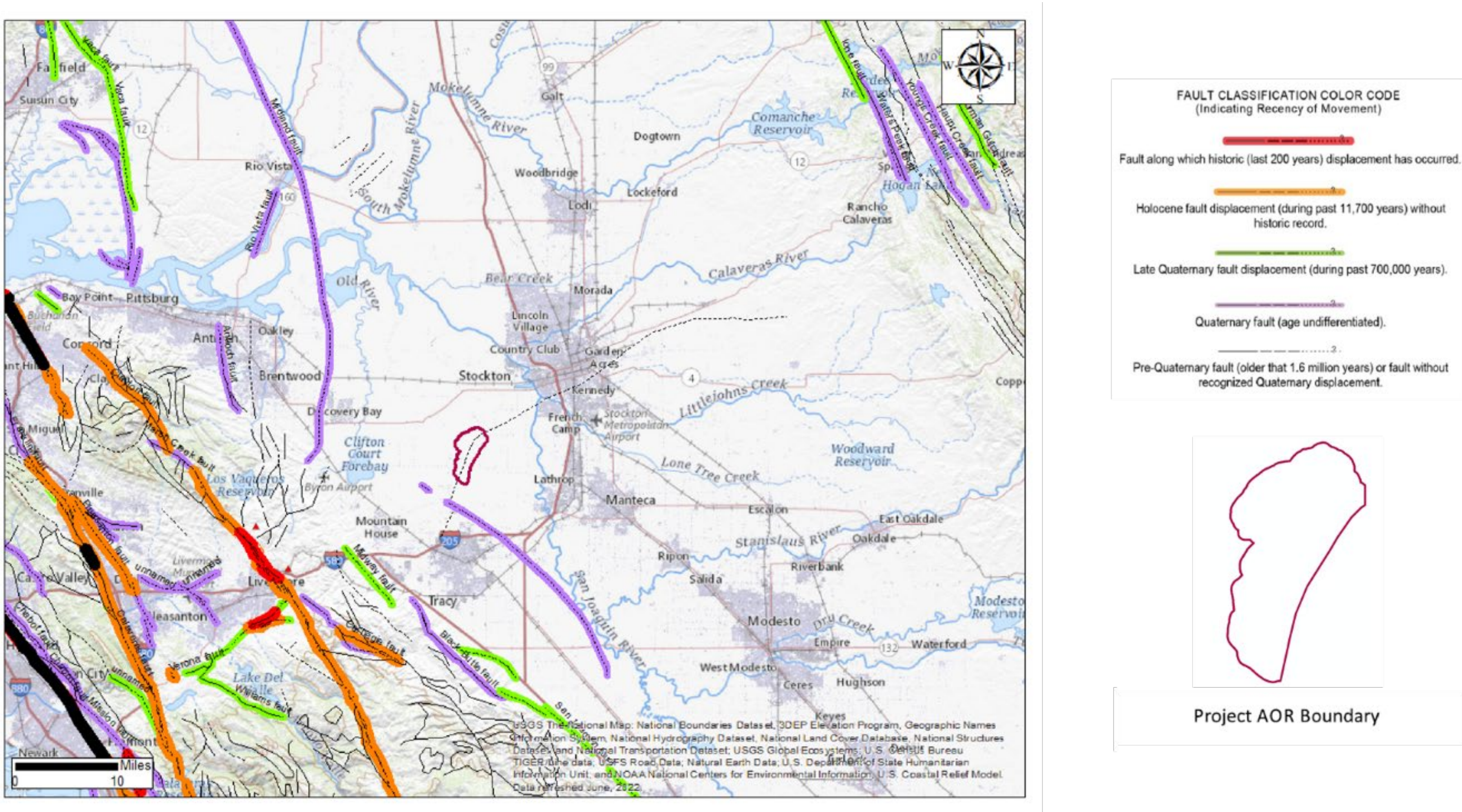

Figure A-46. Fault Activity Map from the California Geologic Survey and U.S. Geological Survey. The fault trace of the Stockton Fault shown here agrees with the 3D seismic interpretation. The fault trace is not colored indicating it is interpreted as Pre-Quaternary (older than 1.6 million years) by the California Geologic Survey. This is also in agreement with the seismic and well-based interpretation. (https://maps.conservation.ca.gov/cgs/fam/).

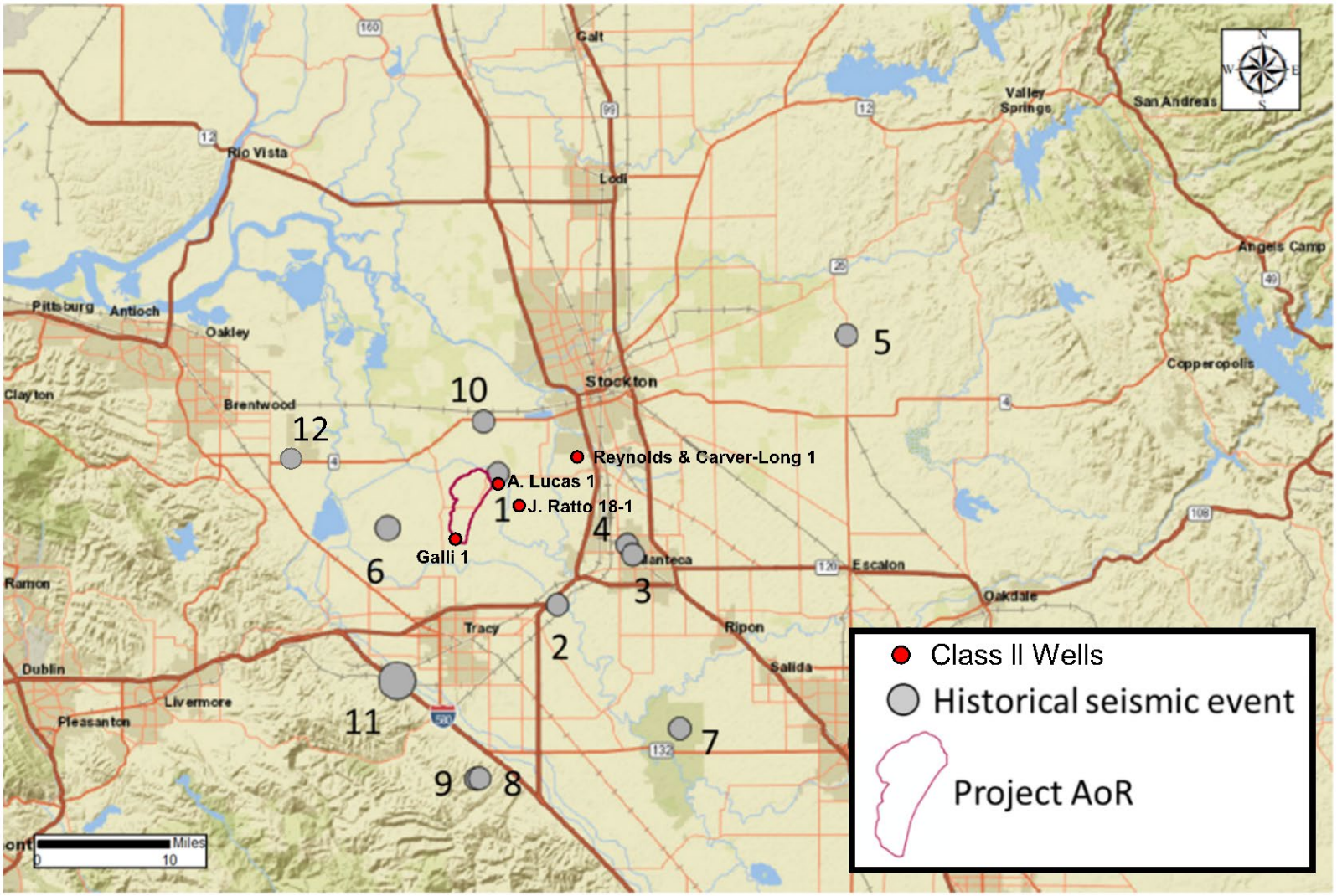

Figure A-47. Historical seismic events and Class II wells near the Area of Review. This image has been modified from USGS search results. Data from these events are compiled in Table A-12. The first column in Table A-12 shows the corresponding event # on the image. Data associated with the Class II wells is compiled in Table A-13.

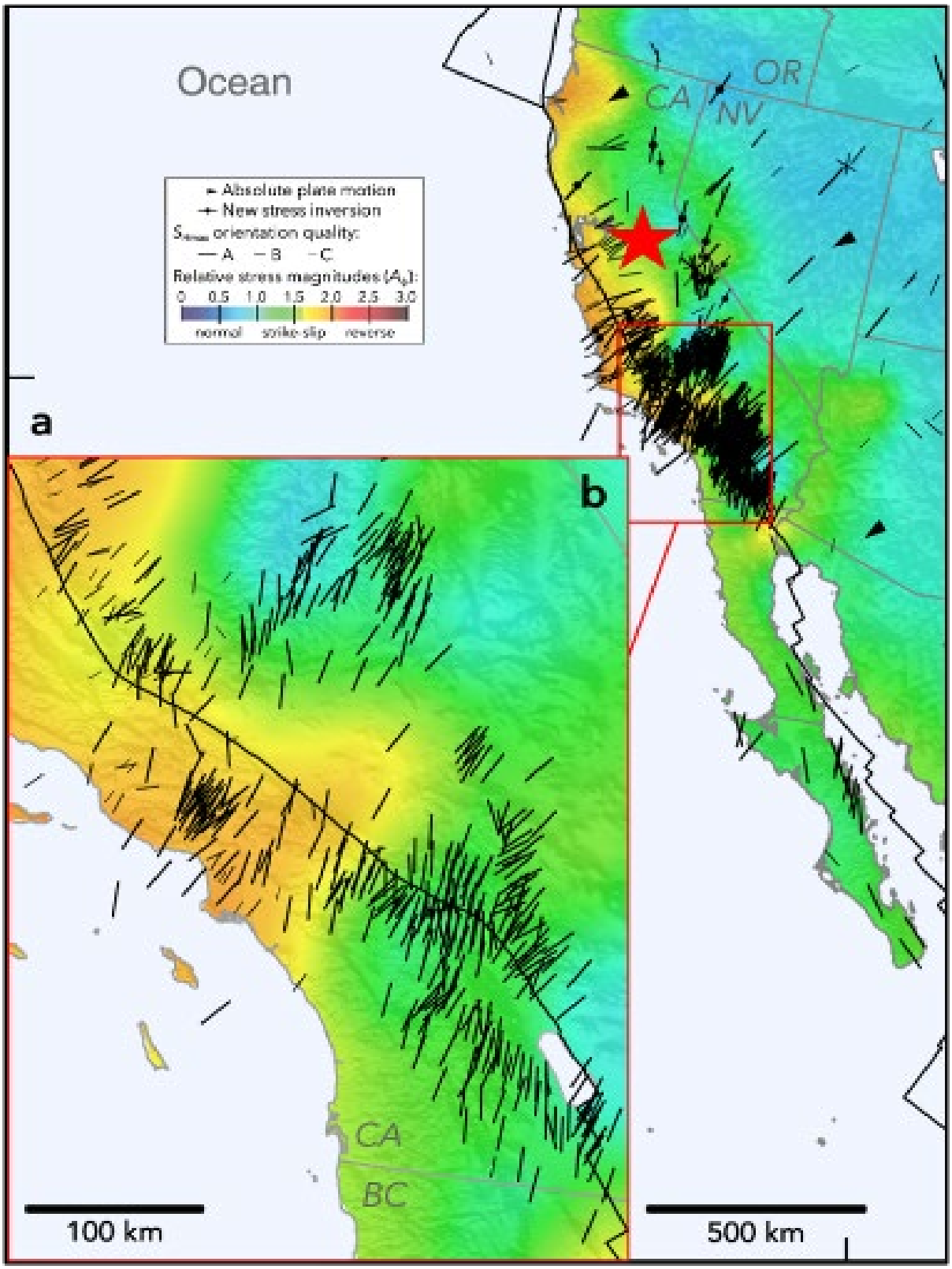

Figure A-48. Image modified from Lund Snee and Zoback (2020) showing relative stress magnitudes across California. Red star indicates CTV II project site area.

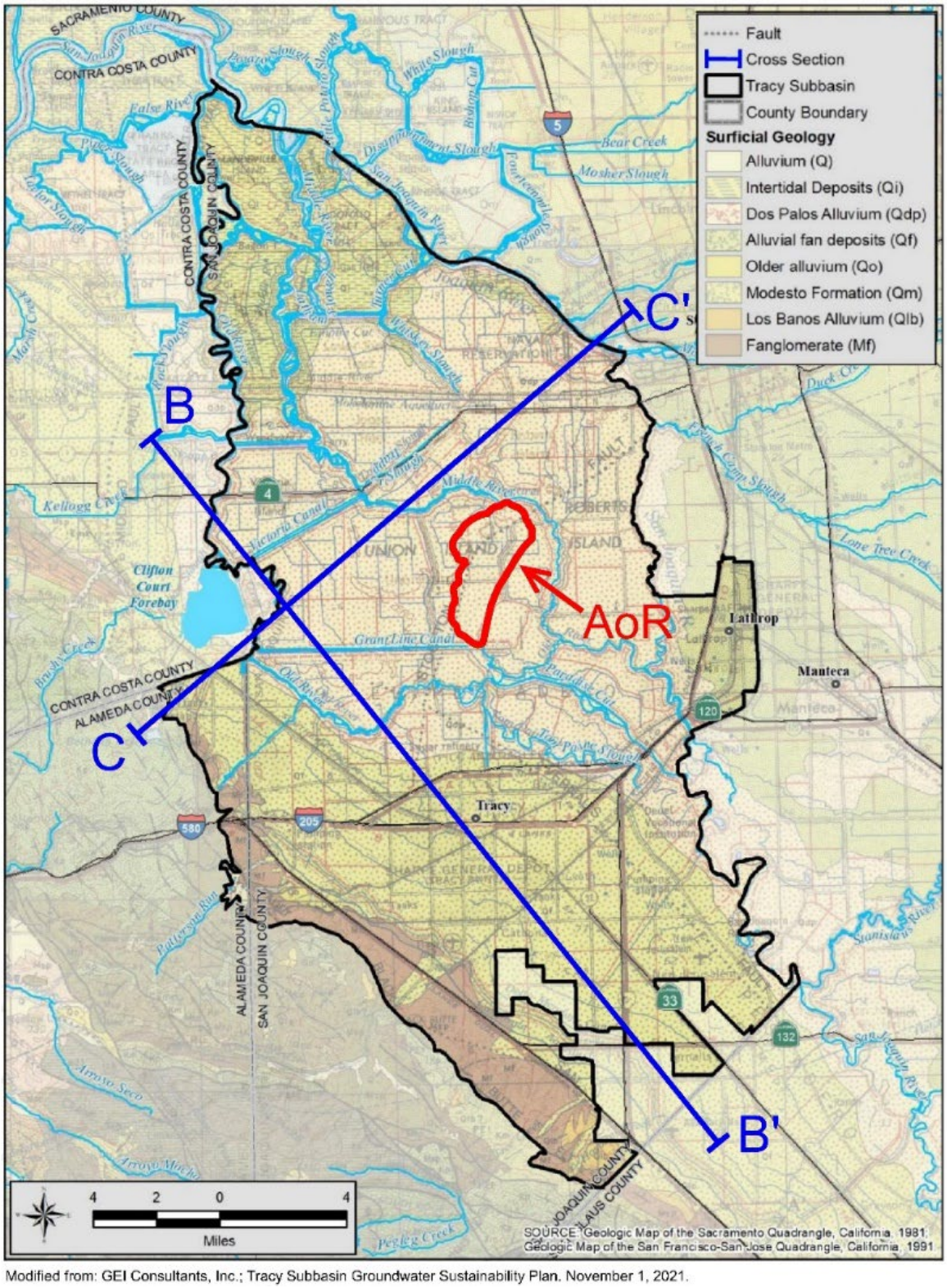

Modified from: GEI Consultants, Inc.; Tracy Subbasin Groundwater Sustainability Plan. November 1, 2021.

Figure A-49. Tracy Subbasin, surface geology, and cross section index map.

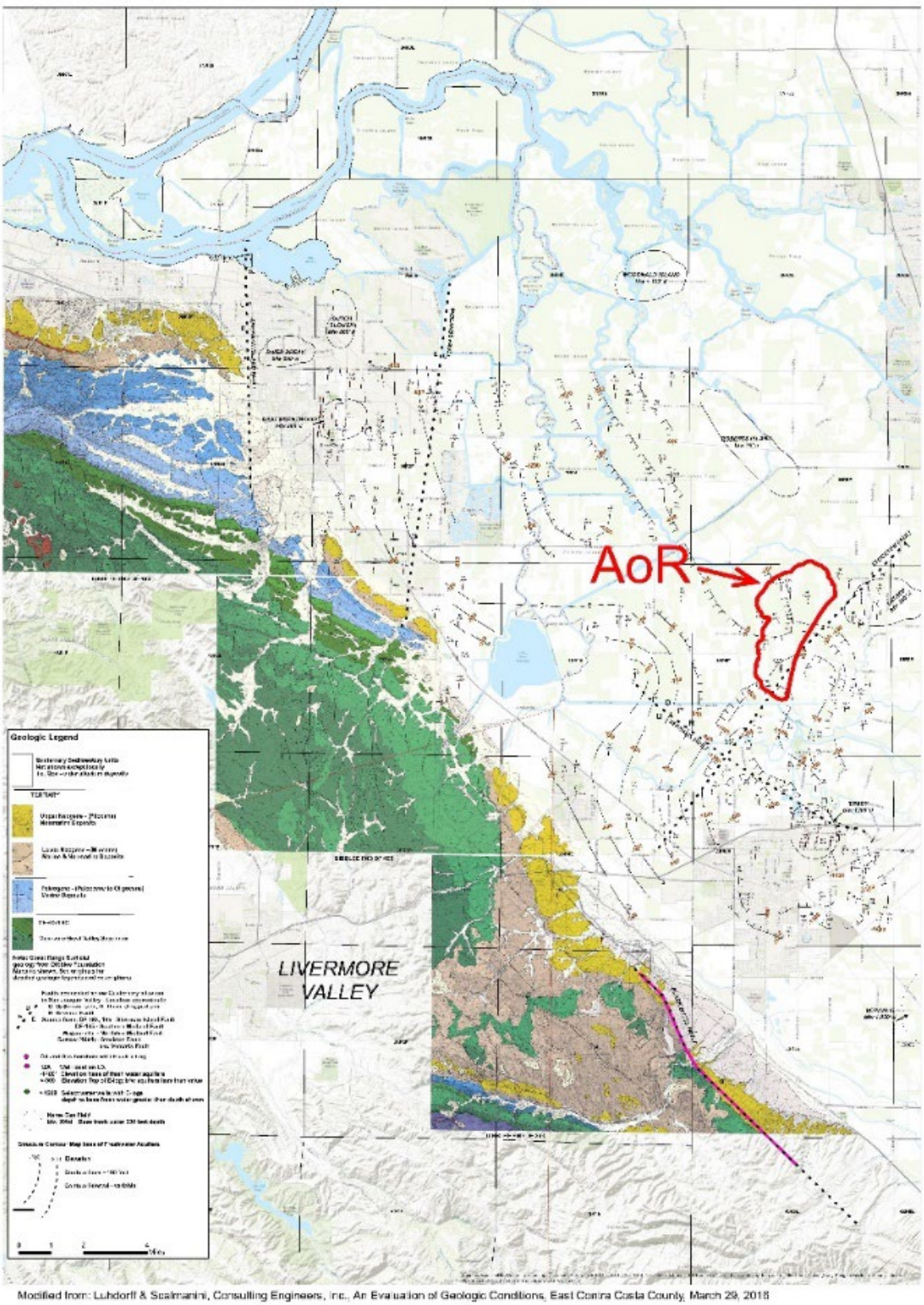

Modified from: Luhdorff & Scalmanini, Consulting Engineers, Inc., An Evaluation of Geologic Conditions, East Contra Costa County, March 29, 2018

Figure A-50. Geologic map and base of fresh water.

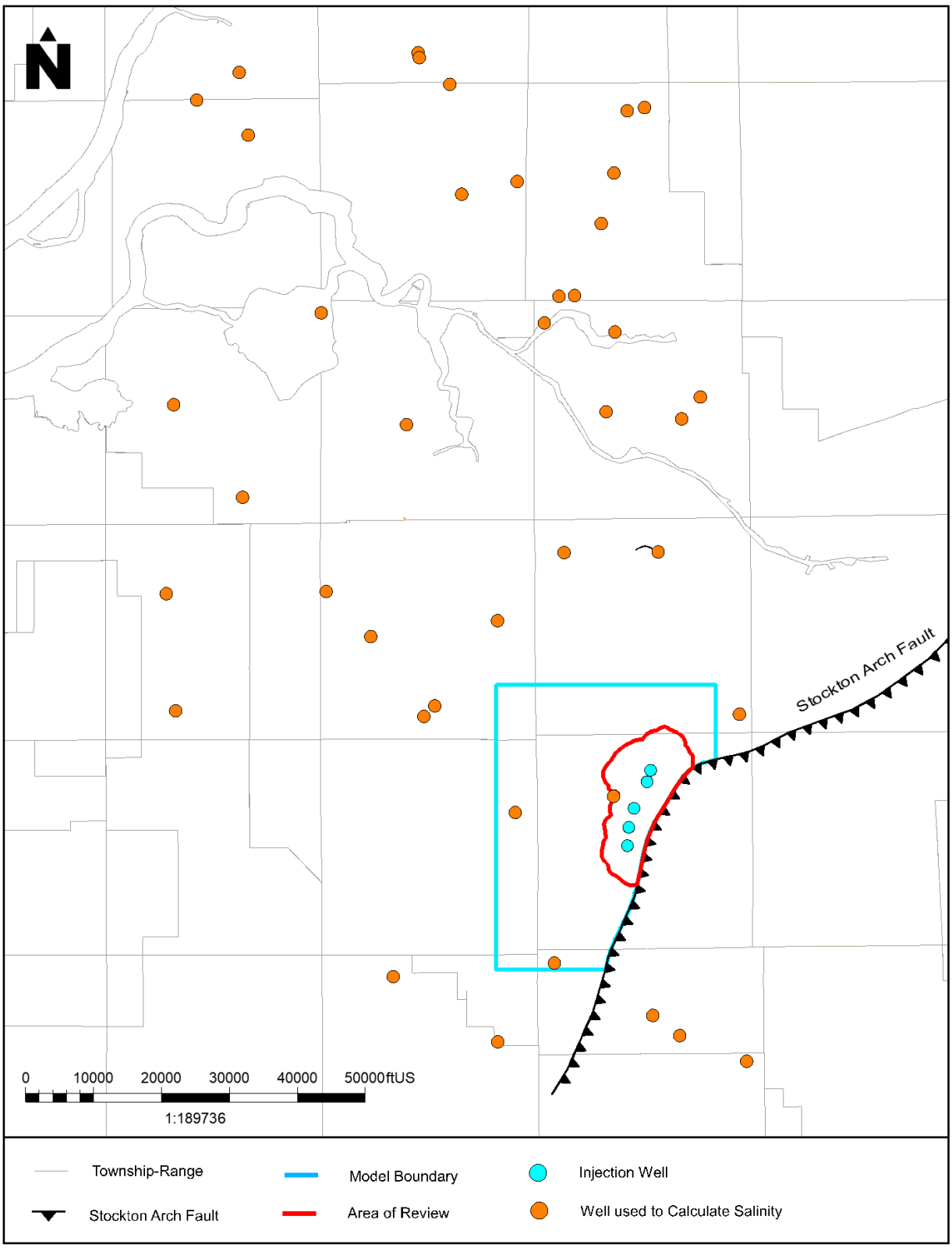

Figure A-51. Wells used in salinity calculations.

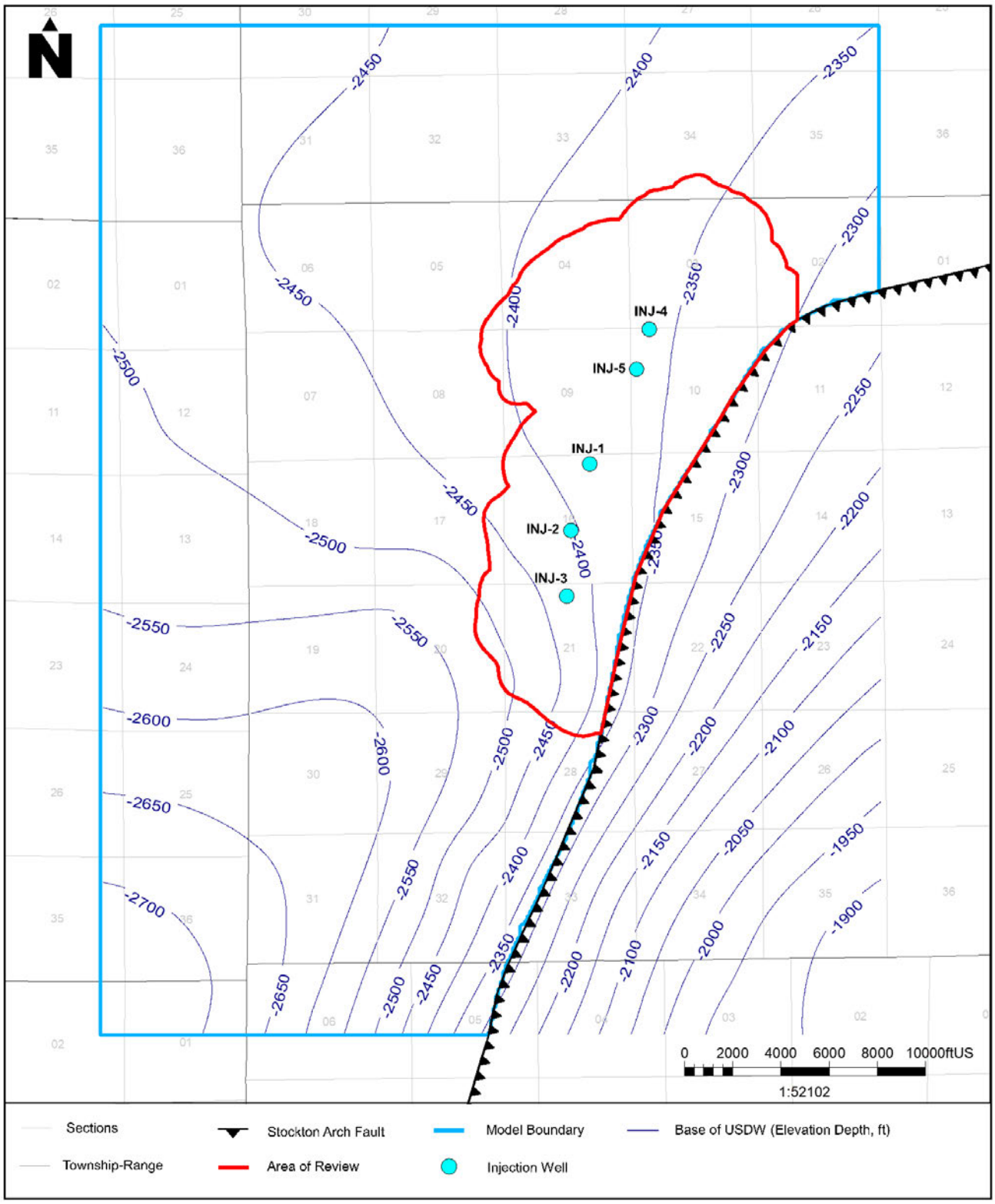

Figure A-52. Depth to the base of the lowermost USDW based on the calculation of salinity from logs (TVDSS).

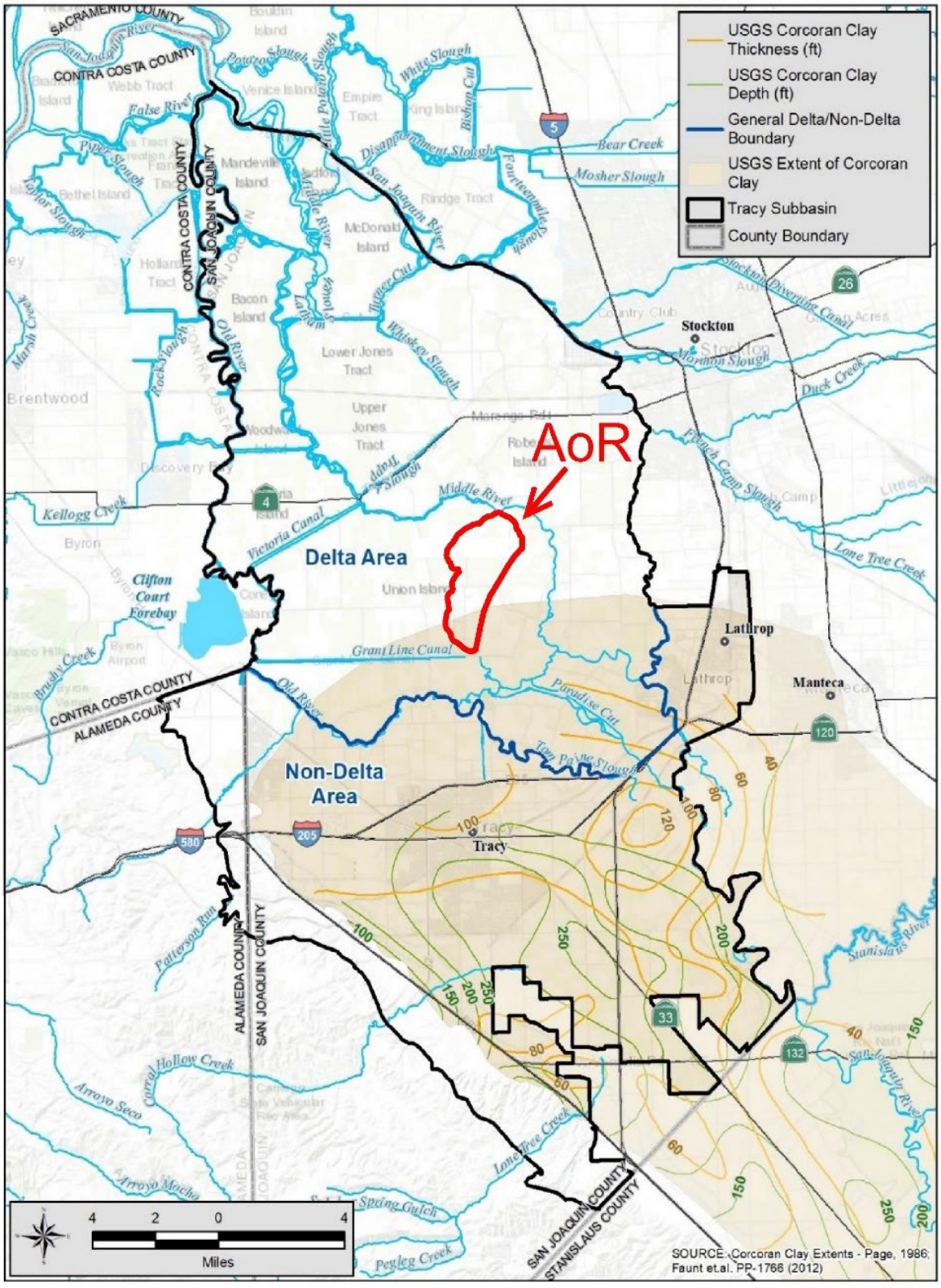

Modified from: GEI Consultants, Inc.; Tracy Subbasin Groundwater Sustainability Plan. November 1, 2021.

Figure A-53. Estimated Corcoran Clay thickness and extent.

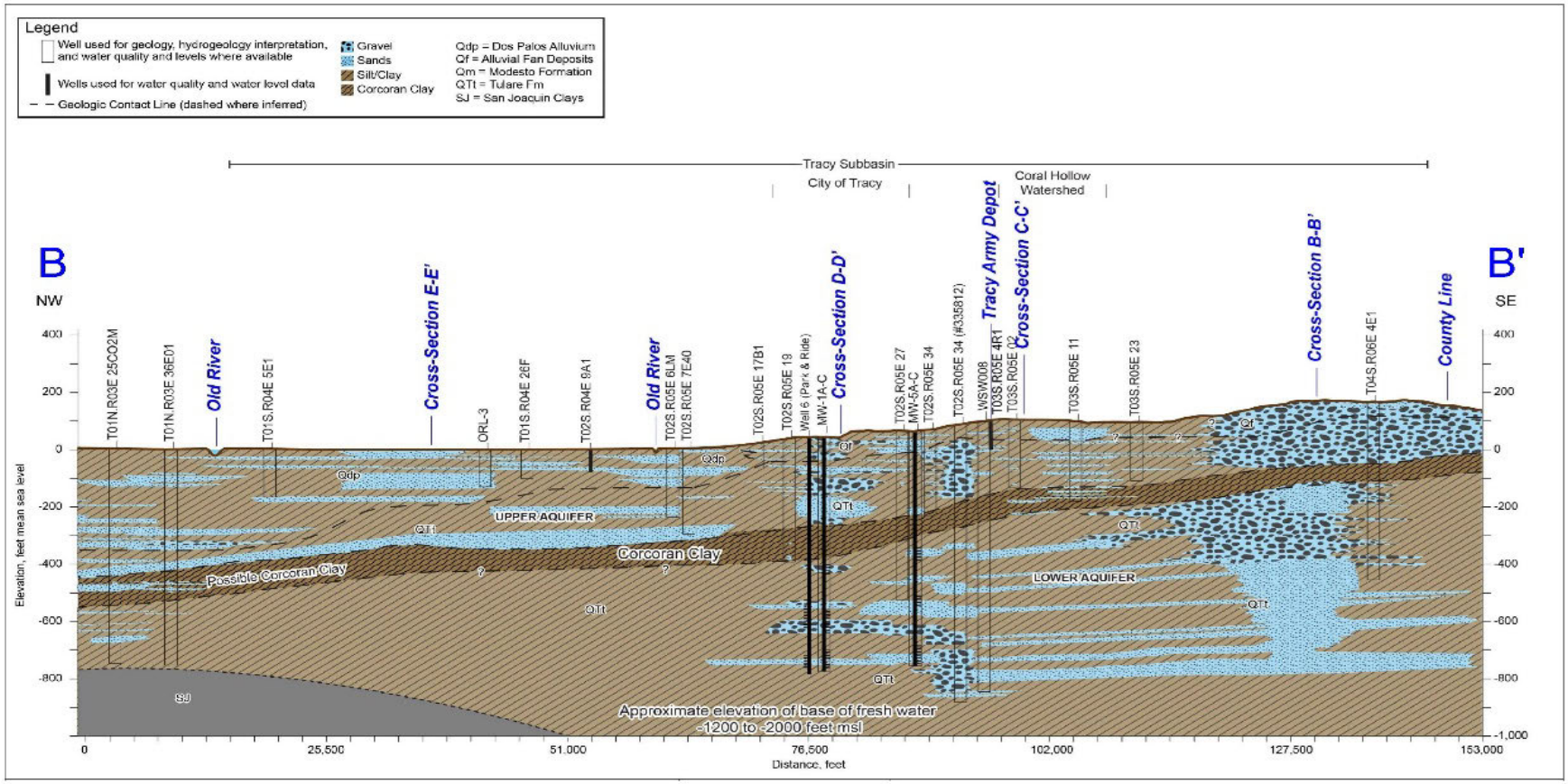

Modified from: GEI Consultants, Inc.; Tracy Subbasin Groundwater Sustainability Plan. November 1, 2021.

Figure A-54. Geologic cross section B-B'.

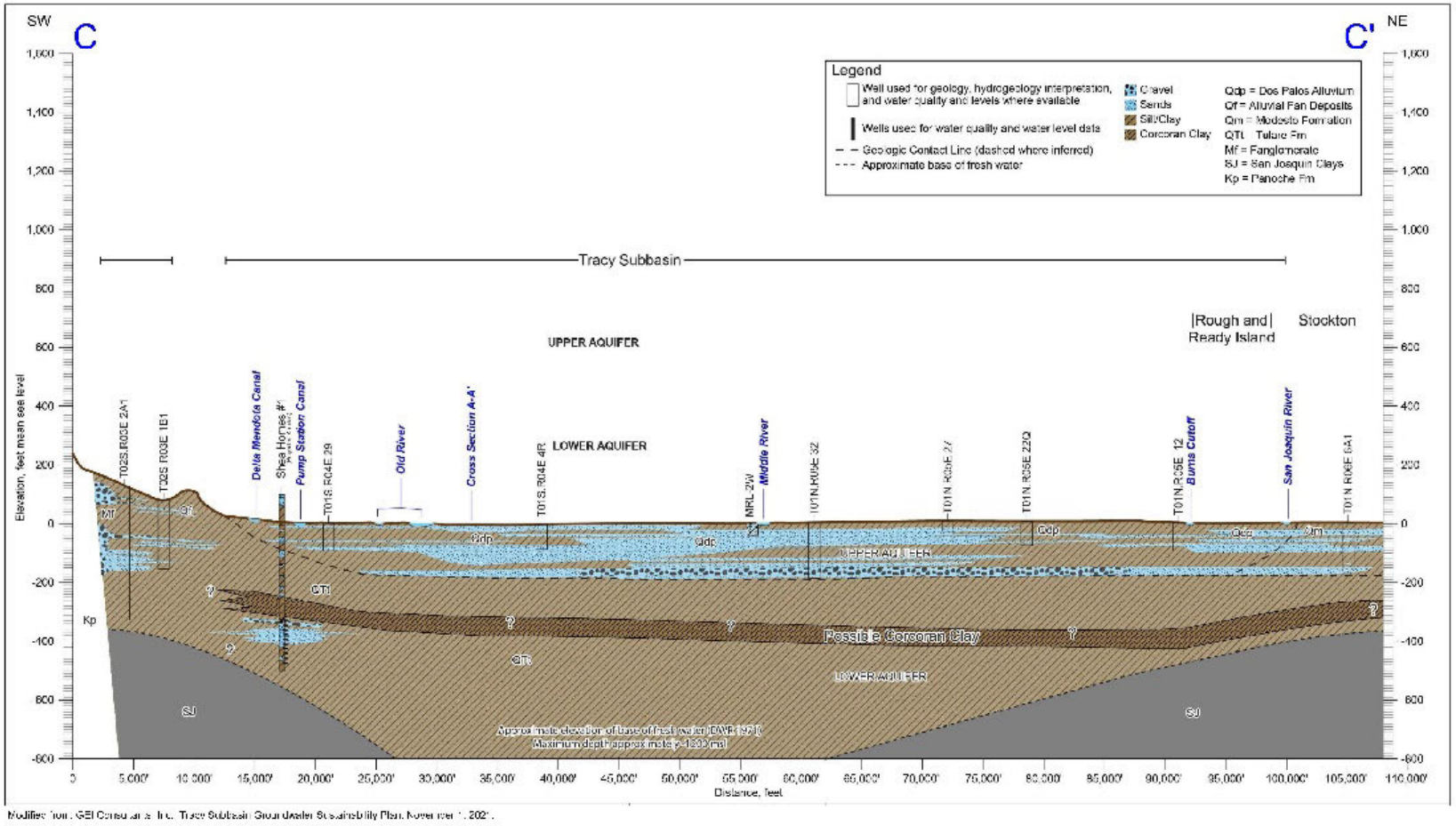

Modified from GEI Consultants Inc. Tracy Subbasin Groundwater Sustainability Plan, November 1, 2021.

Figure A-55. Geologic cross section C-C'.

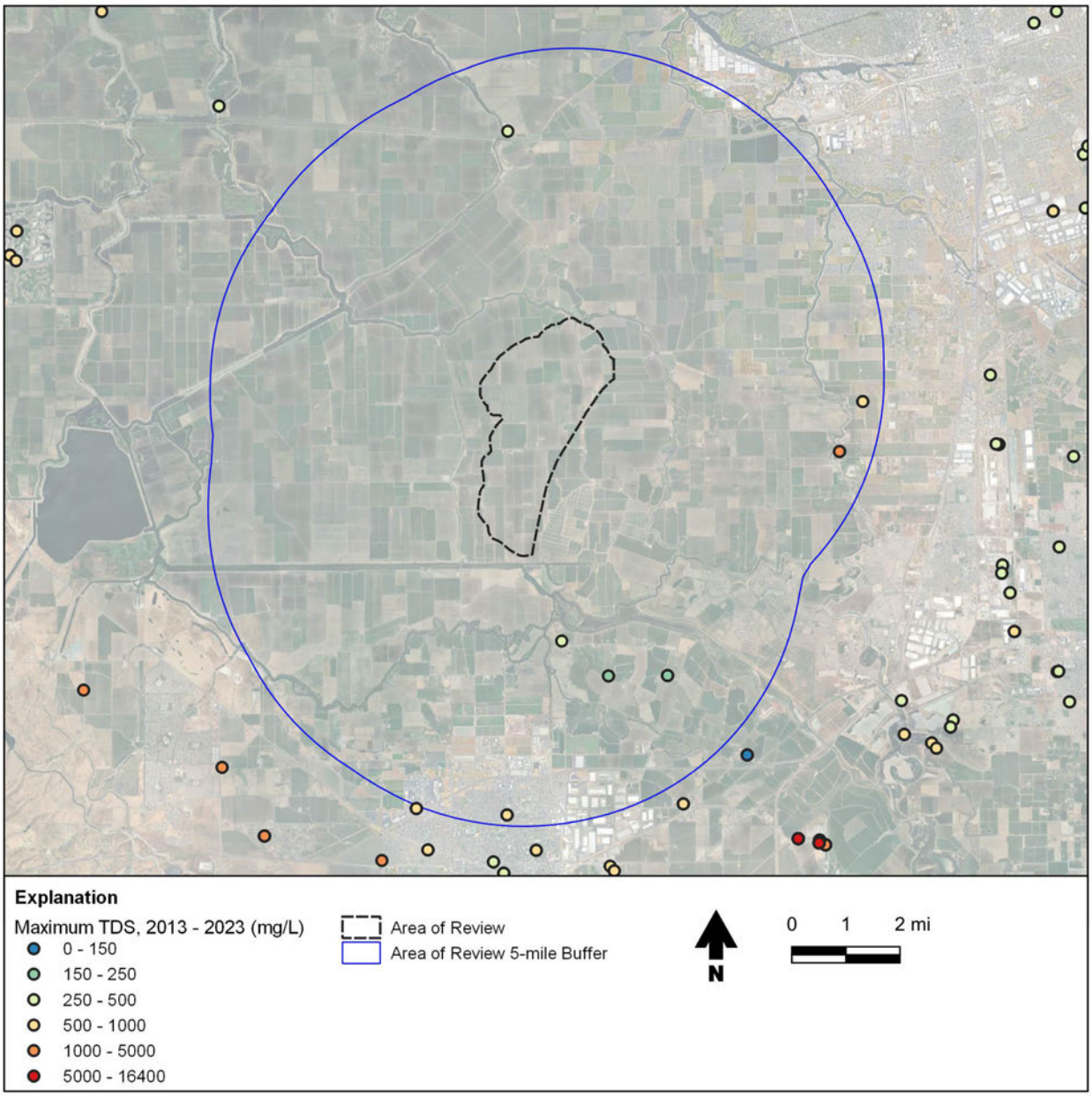

Figure A-56. Total Dissolved Solids (TDS) from water supply wells, 2013 – 2023. Data from California State Water Resources Control Board Groundwater Ambient Monitoring and Assessment (GAMA) Program. Maximum reported well depth within 5-mile AoR buffer is 732 feet.

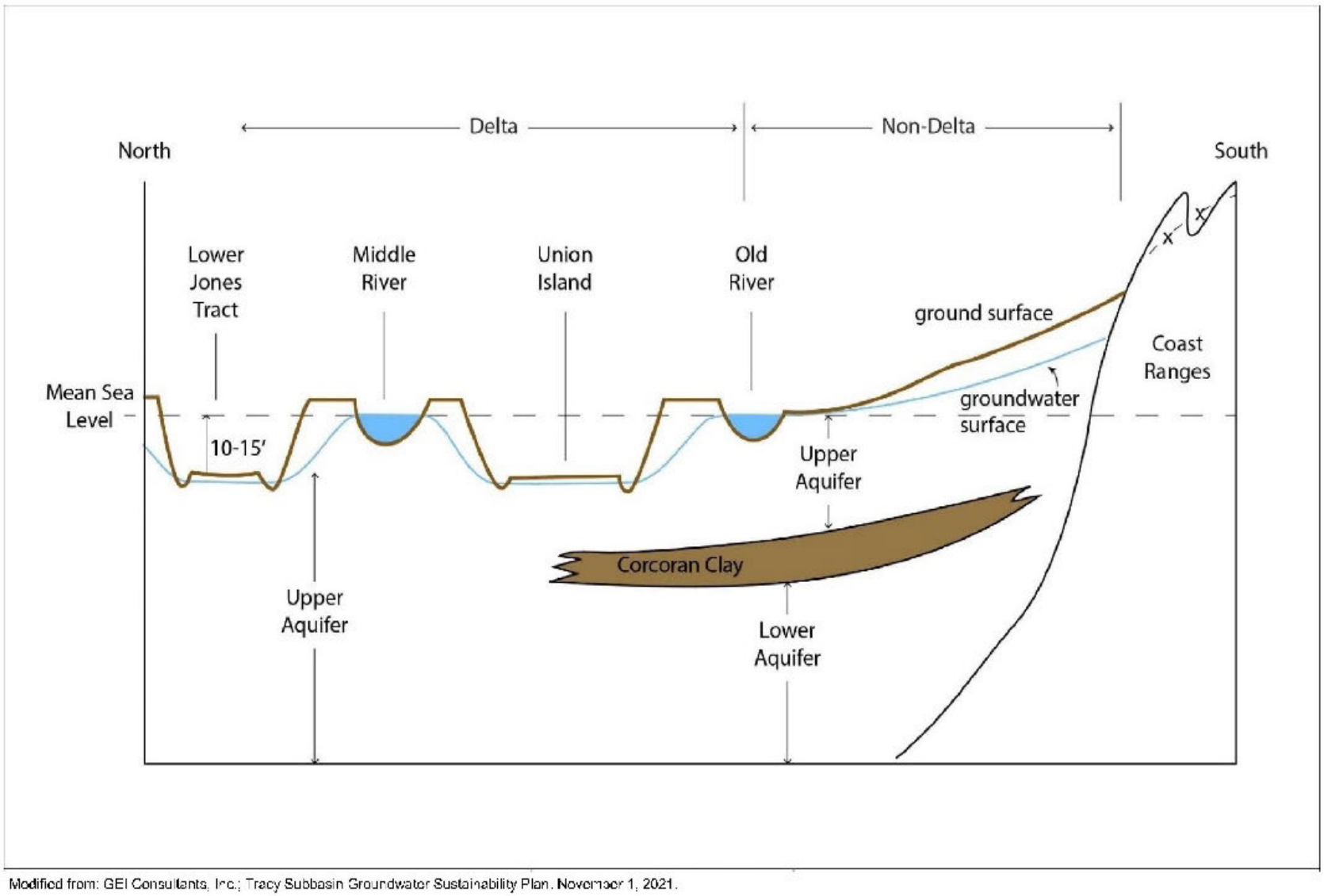

Figure A-57. Principal aquifer schematic profile.

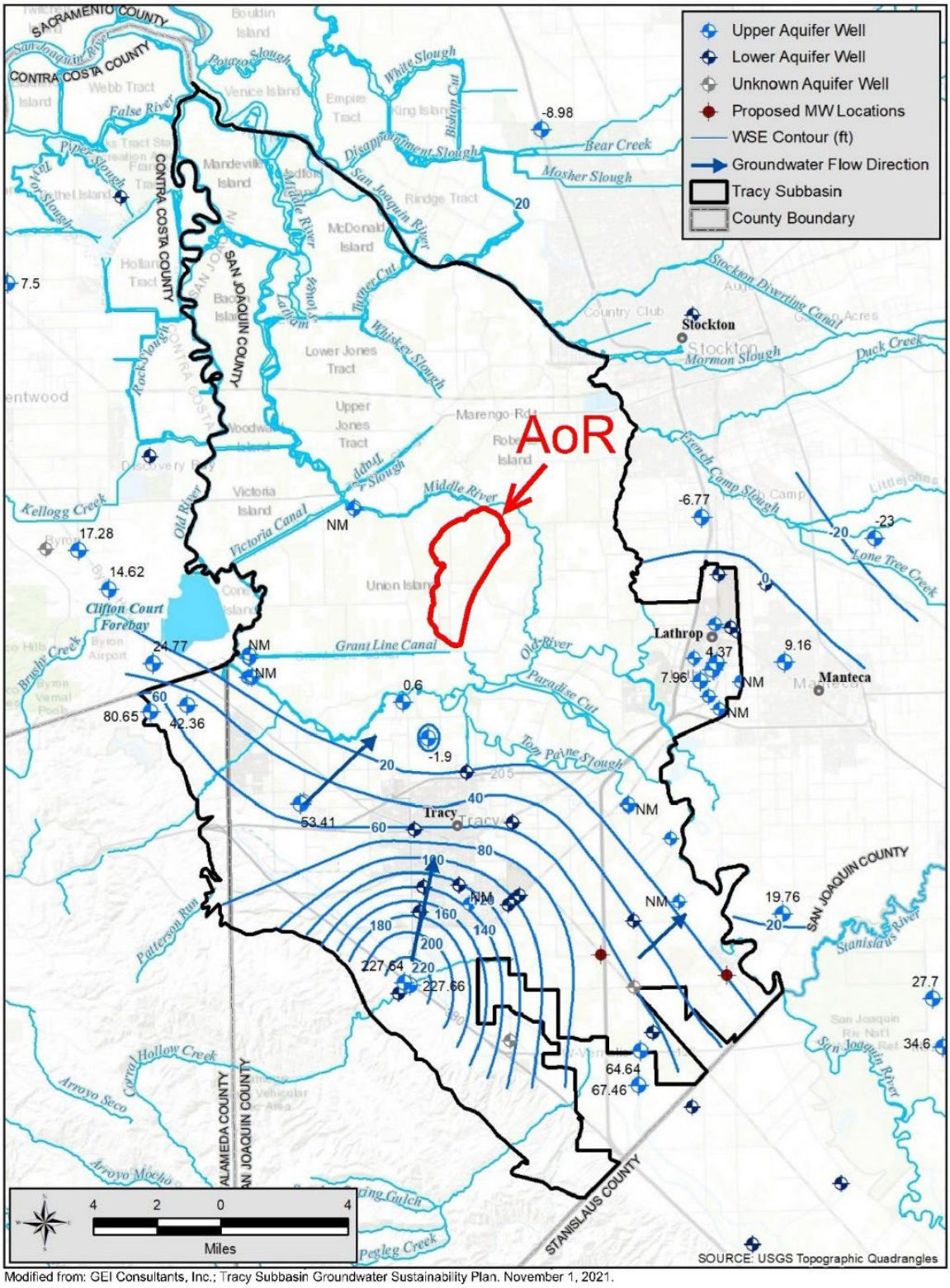

Modified from: GEI Consultants, Inc.; Tracy Subbasin Groundwater Sustainability Plan. November 1, 2021.

Figure A-58. Upper Aquifer groundwater elevations, Fall 2019.

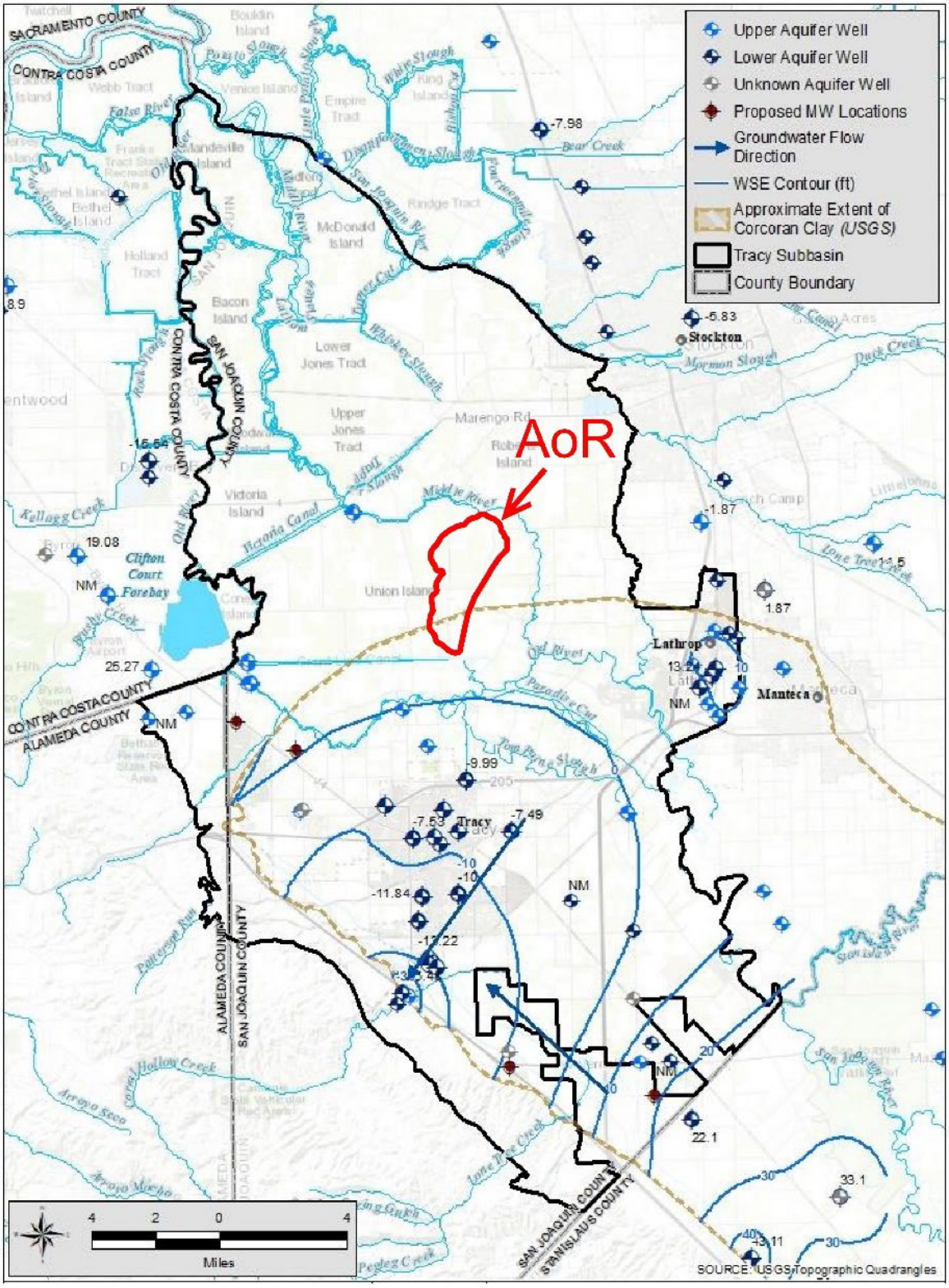

Modified from: GEI Consultants, Inc.; Tracy Subbasin Groundwater Sustainability Plan. November 1, 2021.

Figure A-59. Lower Aquifer groundwater elevations, spring 2019.

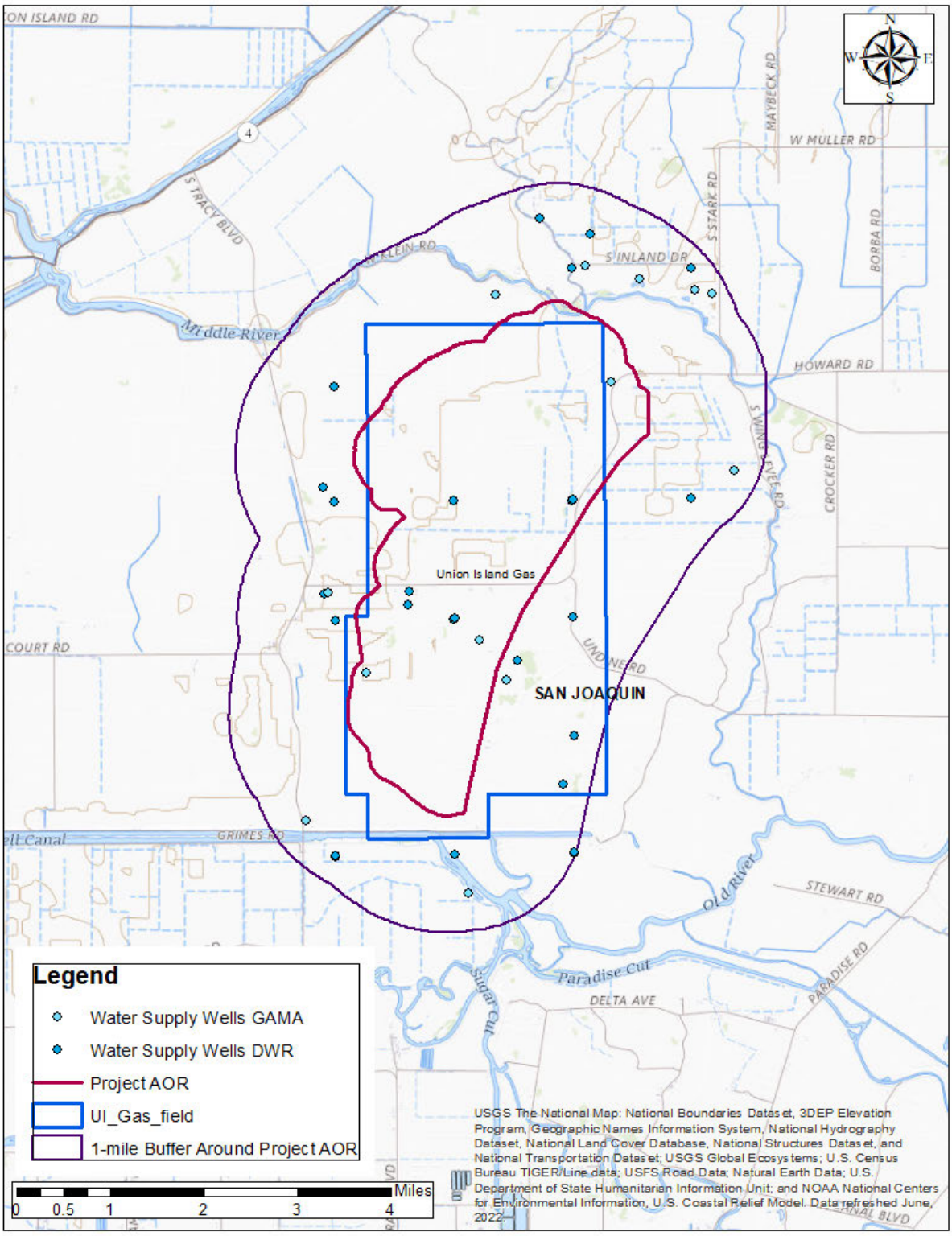

Figure A-60. Water well location map.

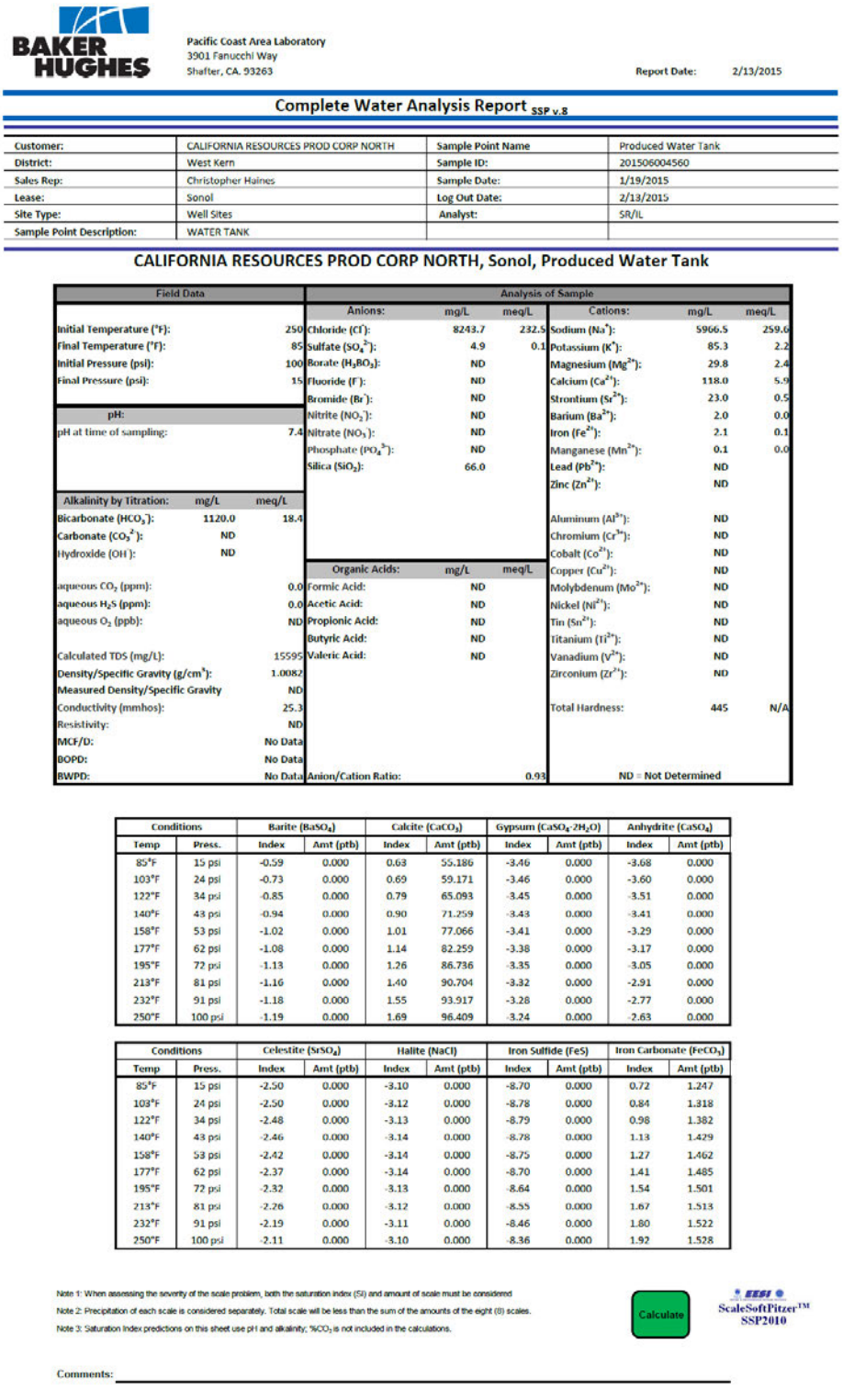

BAKER HUGHES

Pacific Coast Area Laboratory
3901 Fanucchi Way
Shafter, CA. 93263

Report Date: 2/13/2015

Complete Water Analysis Report SSP v.8

Customer:	CALIFORNIA RESOURCES PROD CORP NORTH	Sample Point Name	Produced Water Tank
District:	West Kern	Sample ID:	201506004560
Sales Rep:	Christopher Haines	Sample Date:	1/19/2015
Lease:	Sonol	Log Out Date:	2/13/2015
Site Type:	Well Sites	Analyst:	SR/IL
Sample Point Description:	WATER TANK		

CALIFORNIA RESOURCES PROD CORP NORTH, Sonol, Produced Water Tank

Field Data

Initial Temperature (°F):	250
Final Temperature (°F):	85
Initial Pressure (psi):	100
Final Pressure (psi):	15

pH:

pH at time of sampling:	7.4

Alkalinity by Titration:	mg/L	meq/L
Bicarbonate (HCO_3^-):	1120.0	18.4
Carbonate (CO_3^{2-}):	ND	
Hydroxide (OH^-):	ND	

aqueous CO_2 (ppm):	0.0
aqueous H_2S (ppm):	0.0
aqueous O_2 (ppb):	ND
Calculated TDS (mg/L):	15595
Density/Specific Gravity (g/cm³):	1.0082
Measured Density/Specific Gravity	ND
Conductivity (mmhos):	25.3
Resistivity:	ND
MCF/D:	No Data
BOPD:	No Data
BWPD:	No Data

Analysis of Sample

Anions:	mg/L	meq/L
Chloride (Cl^-):	8243.7	232.5
Sulfate (SO_4^{2-}):	4.9	0.1
Borate ($H_2BO_3^-$):	ND	
Fluoride (F^-):	ND	
Bromide (Br^-):	ND	
Nitrite (NO_2^-):	ND	
Nitrate (NO_3^-):	ND	
Phosphate (PO_4^{3-}):	ND	
Silica (SiO_2):	66.0	

Organic Acids:	mg/L	meq/L
Formic Acid:	ND	
Acetic Acid:	ND	
Propionic Acid:	ND	
Butyric Acid:	ND	
Valeric Acid:	ND	

Cations:	mg/L	meq/L
Sodium (Na^+):	5966.5	259.6
Potassium (K^+):	85.3	2.2
Magnesium (Mg^{2+}):	29.8	2.4
Calcium (Ca^{2+}):	118.0	5.9
Strontium (Sr^{2+}):	23.0	0.5
Barium (Ba^{2+}):	2.0	0.0
Iron (Fe^{2+}):	2.1	0.1
Manganese (Mn^{2+}):	0.1	0.0
Lead (Pb^{2+}):	ND	
Zinc (Zn^{2+}):	ND	
Aluminum (Al^{3+}):	ND	
Chromium (Cr^{3+}):	ND	
Cobalt (Co^{2+}):	ND	
Copper (Cu^{2+}):	ND	
Molybdenum (Mo^{2+}):	ND	
Nickel (Ni^{2+}):	ND	
Tin (Sn^{2+}):	ND	
Titanium (Ti^{2+}):	ND	
Vanadium (V^{2+}):	ND	
Zirconium (Zr^{2+}):	ND	
Total Hardness:	445	N/A

Anion/Cation Ratio: 0.93

ND = Not Determined

Conditions		Barite ($BaSO_4$)		Calcite ($CaCO_3$)		Gypsum ($CaSO_4 \cdot 2H_2O$)		Anhydrite ($CaSO_4$)	
Temp	Press.	Index	Amt (ptb)	Index	Amt (ptb)	Index	Amt (ptb)	Index	Amt (ptb)
85°F	15 psi	-0.59	0.000	0.63	55.186	-3.46	0.000	-3.68	0.000
103°F	24 psi	-0.73	0.000	0.69	59.171	-3.46	0.000	-3.60	0.000
122°F	34 psi	-0.85	0.000	0.79	65.093	-3.45	0.000	-3.51	0.000
140°F	43 psi	-0.94	0.000	0.90	71.259	-3.43	0.000	-3.41	0.000
158°F	53 psi	-1.02	0.000	1.01	77.066	-3.41	0.000	-3.29	0.000
177°F	62 psi	-1.08	0.000	1.14	82.259	-3.38	0.000	-3.17	0.000
195°F	72 psi	-1.13	0.000	1.26	86.736	-3.35	0.000	-3.05	0.000
213°F	81 psi	-1.16	0.000	1.40	90.704	-3.32	0.000	-2.91	0.000
232°F	91 psi	-1.18	0.000	1.55	93.917	-3.28	0.000	-2.77	0.000
250°F	100 psi	-1.19	0.000	1.69	96.409	-3.24	0.000	-2.63	0.000

Conditions		Celestite ($SrSO_4$)		Halite (NaCl)		Iron Sulfide (FeS)		Iron Carbonate ($FeCO_3$)	
Temp	Press.	Index	Amt (ptb)	Index	Amt (ptb)	Index	Amt (ptb)	Index	Amt (ptb)
85°F	15 psi	-2.50	0.000	-3.10	0.000	-8.70	0.000	0.72	1.247
103°F	24 psi	-2.50	0.000	-3.12	0.000	-8.78	0.000	0.84	1.318
122°F	34 psi	-2.48	0.000	-3.13	0.000	-8.79	0.000	0.98	1.382
140°F	43 psi	-2.46	0.000	-3.14	0.000	-8.78	0.000	1.13	1.429
158°F	53 psi	-2.42	0.000	-3.14	0.000	-8.75	0.000	1.27	1.462
177°F	62 psi	-2.37	0.000	-3.14	0.000	-8.70	0.000	1.41	1.485
195°F	72 psi	-2.32	0.000	-3.13	0.000	-8.64	0.000	1.54	1.501
213°F	81 psi	-2.26	0.000	-3.12	0.000	-8.55	0.000	1.67	1.513
232°F	91 psi	-2.19	0.000	-3.11	0.000	-8.46	0.000	1.80	1.522
250°F	100 psi	-2.11	0.000	-3.10	0.000	-8.36	0.000	1.92	1.528

Note 1: When assessing the severity of the scale problem, both the saturation index (SI) and amount of scale must be considered

Note 2: Precipitation of each scale is considered separately. Total scale will be less than the sum of the amounts of the eight (8) scales.

Note 3: Saturation Index predictions on this sheet use pH and alkalinity; $\%CO_2$ is not included in the calculations.

Calculate

EESI ScaleSoftPitzer™ SSP2010

Comments: _____

Figure A-61. Water geochemistry for the Sonol_Securities_4 well.

Dick Brown's Technical Service

Gas & Oilfield Measurement and Control Specialist
Design – Installation – Service

Company: CRC
Location: Sonol #5
Meter ID:
Analysis Time: 03/01/2022 15:14 Sample Type: Spot
Flowing Temp.: 80 Deg. F Flowing Pressure: 15 psig

Comp	UnNorm %	Normal %	Liquids (USgal/MCF)	Ideal (Btu/SCF)	Rel. Density
Propane	0.07668	0.07727	0.02131	1.94427	0.00118
Hydrogen Sulfide	0.00000	0.00000	0.00000	0.00000	0.00000
IsoButane	0.01738	0.01751	0.00574	0.56938	0.00035
Butane	0.02022	0.02038	0.00644	0.66485	0.00041
NeoPentane	0.00000	0.00000	0.00000	0.00000	0.00000
IsoPentane	0.01515	0.01526	0.00559	0.61062	0.00038
Pentane	0.01556	0.01568	0.00569	0.62846	0.00039
Hexane+	0.06383	0.06432	0.00000	0.00000	0.00000
Nitrogen	13.19429	13.29594	0.00000	0.00000	0.12861
Methane	84.99076	85.64405	0.00000	865.00488	0.47444
CarbonDioxide	0.20376	0.20533	0.00000	0.00000	0.00312
Ethane	0.63934	0.64426	0.17262	11.40145	0.00669
Hexane	0.00000	0.06432	0.02649	3.05896	0.00191
Heptane+	0.00000	0.00000	0.00000	0.00000	0.00000
Heptane	0.00000	0.00000	0.00000	0.00000	0.00000
Octane	0.00000	0.00000	0.00000	0.00000	0.00000
Nonane+	0.00000	0.00000	0.00000	0.00000	0.00000
Nonane	0.00000	0.00000	0.00000	0.00000	0.00000
Decane	0.00000	0.00000	0.00000	0.00000	0.00000
Undecane	0.00000	0.00000	0.00000	0.00000	0.00000
Dodecane	0.00000	0.00000	0.00000	0.00000	0.00000
Ethane-	0.00000	0.00000	0.00000	0.00000	0.00000
Propane +	0.00000	0.00000	0.00000	0.00000	0.00000
Total	99.23697	100.00000	0.24387	883.88293	0.61831

Inferior Wobbe 1109.2899 (Btu/SCF) Superior Wobbe 1128.8501 (Btu/SCF)
Compressibility 0.9983 Density 0.0473 (lbm/ft3)
Real Rel. Density 0.6183 Ideal CV 883.8829 (Btu/SCF)
Wet CV 872.2740 (Btu/SCF) Dry CV 887.4617 (Btu/SCF)
Contract Temp. 60.0000 (deg F) Contract Press. 14.7300 (psia)
Number of Cycles 2 Connected Stream 1
Atmospheric Pressure 14.73

Figure A-62. Gas chromatography for the Sonol_Securities_5 well.

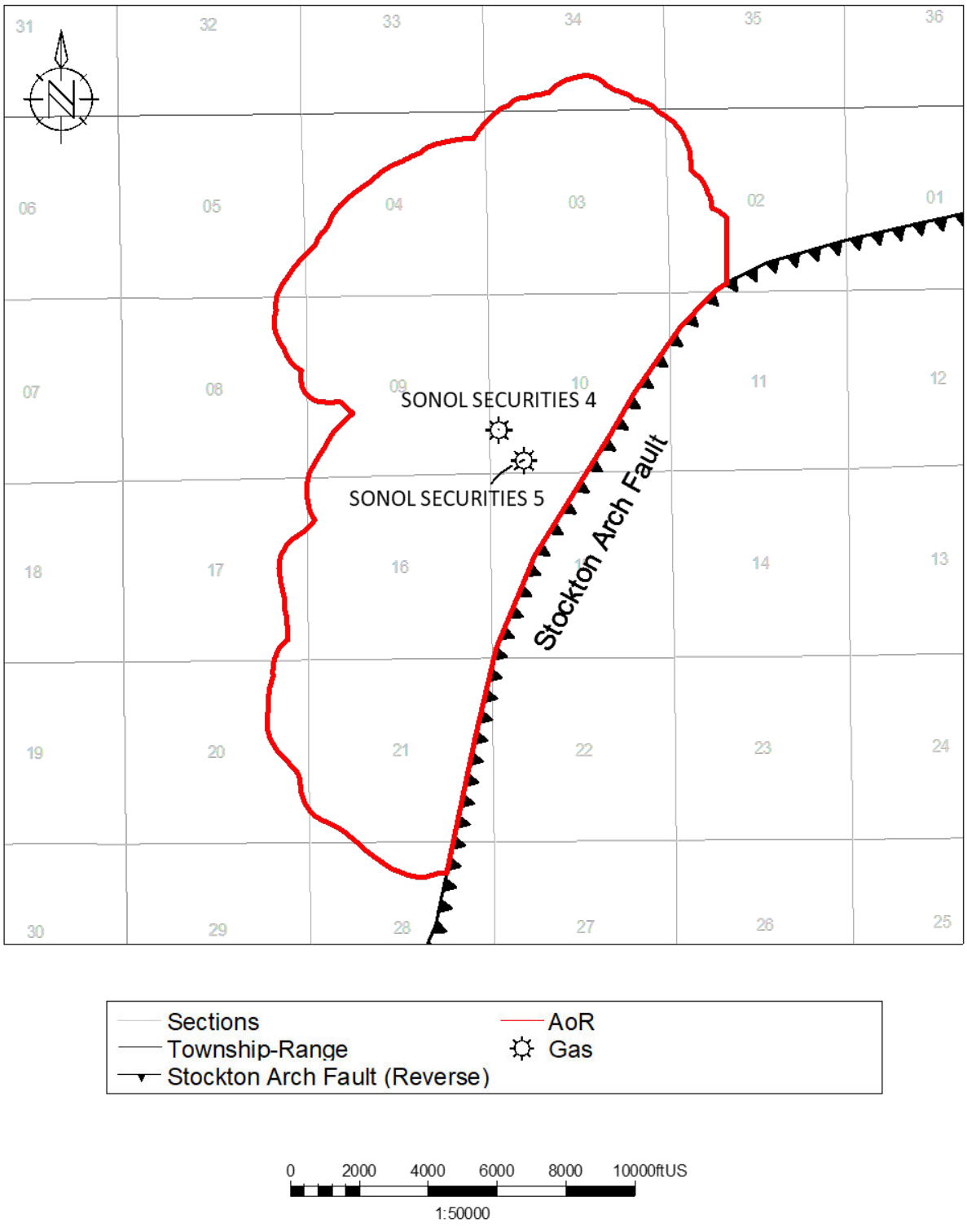

Figure A-63. Locations of wells with geochemistry data.

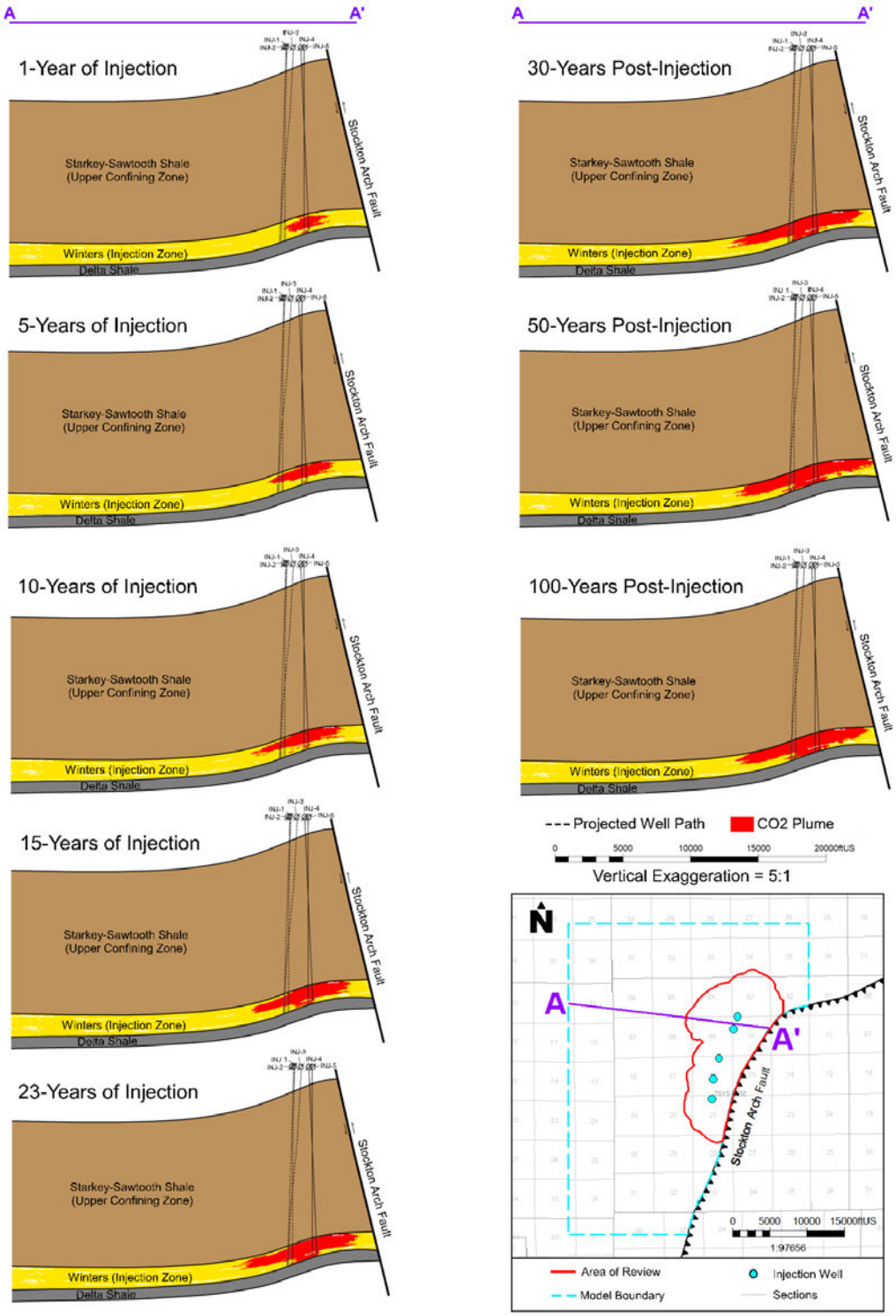

Figure A-64a. Section showing proximity of CO_2 (Injectate 1) to the Stockton Arch Fault and lateral dispersion of CO_2 throughout time and confinement under the overlying Starkey-Sawtooth through time for the five injector modeled Base scenario. As the sections show, plume growth over time is driven by the reservoir anticlinal structure, and is thus representative of the plume growth at all injector locations.

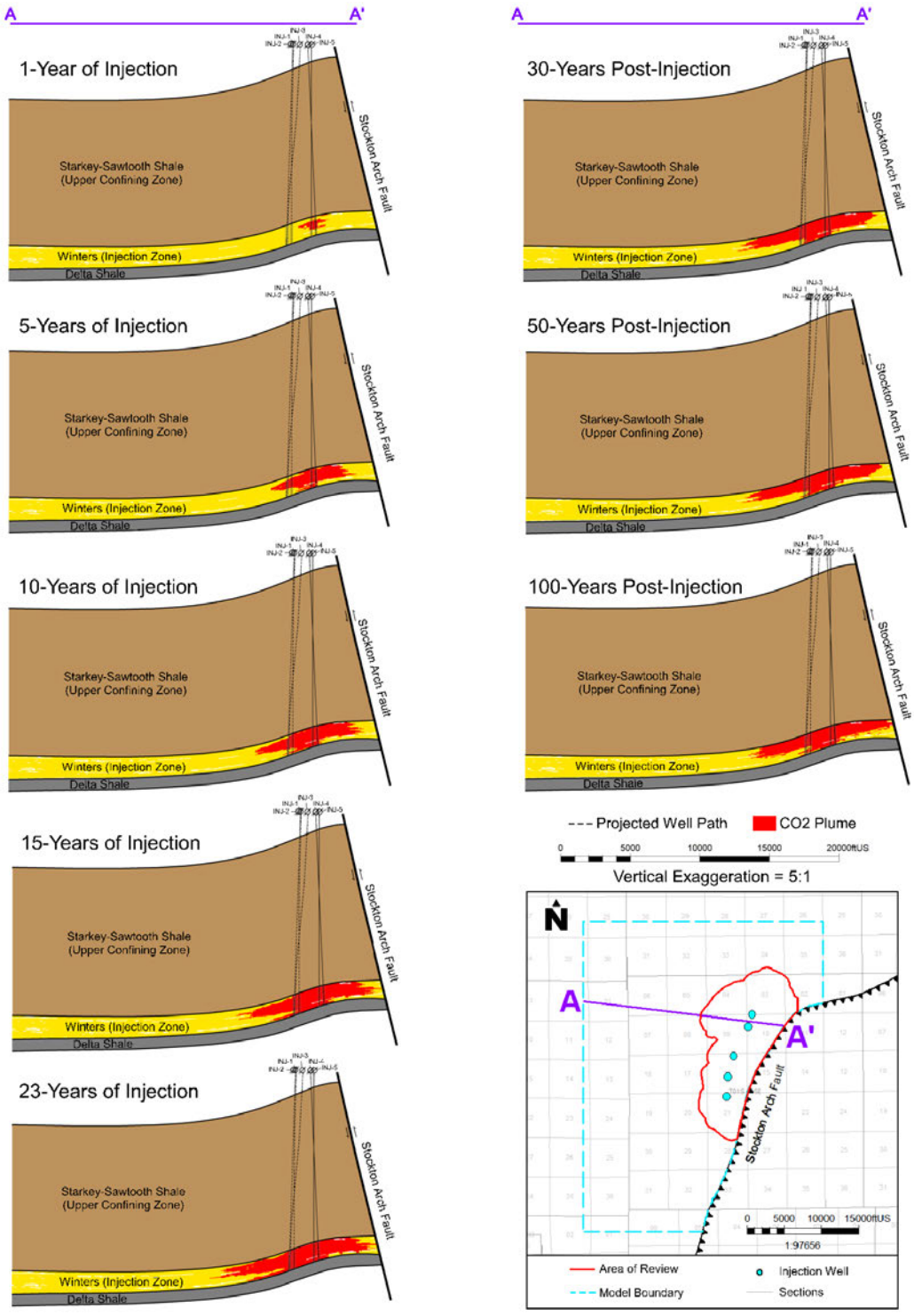

Figure A-64b. Section showing proximity of CO_2 (Injectate 2) to the Stockton Arch Fault and lateral dispersion of CO_2 throughout time and confinement under the overlying Starkey-Sawtooth through time for the five injector modeled Base scenario. As the sections show, plume growth over time is driven by the reservoir anticlinal structure, and is thus representative of the plume growth at all injector locations.

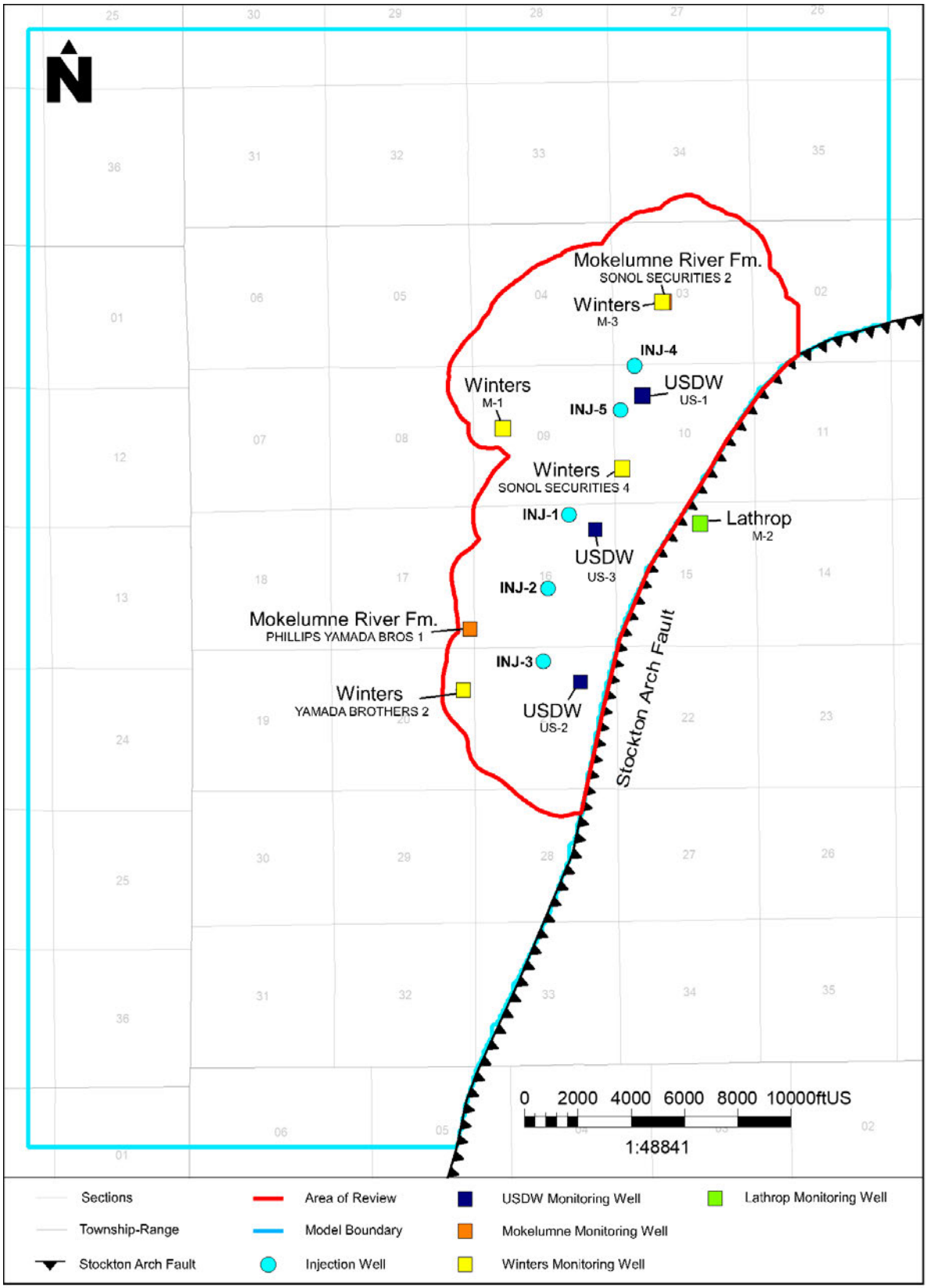

Figure A-65. Map showing the locations of injection wells and monitoring wells.

Tables

Table A-1. Oil and Gas Well Reference List based on CalGEM Data

Number	API	Lease Name	Well Number	Well Design	Well Status	Well Type	Well Type Label
1	0407720604	Bomberger	1	Bomberger 1	Plugged	DH	Dry Hole
2	0407700314	Mobil Parcel X	1	Mobil Parcel X 1	Plugged	DH	Dry Hole
3	0407720278	Galli	1	Galli 1	Idle	WD	Water Disposal
4	0407720197	Union Properties	1	Union Properties 1	Idle	DG	Dry Gas
5	0407720180	Marchini A	1	Marchini A 1	Idle	DG	Dry Gas
6	0407720254	Phillips Yamada Bros.	1	Phillips Yamada Bros. 1	Idle	DG	Dry Gas
7	0407720289	Yamada L.W.	1	Yamada L.W. 1	Idle	DG	Dry Gas
8	0407720274	Pool B	1	Pool B 1	Idle	DG	Dry Gas
9	0407720713	Sonol Securities	10	Sonol Securities 10	Idle	DG	Dry Gas
10	0407720724	Sonol Securities	11	Sonol Securities 11	Idle	DG	Dry Gas
11	0407720162	Sonol Securities	2	Sonol Securities 2	Idle	DG	Dry Gas
12	0407720287	Galli	2	Galli 2	Idle	DG	Dry Gas
13	0407720269	Yamada Brothers	2	Yamada Brothers 2	Idle	DG	Dry Gas
14	0407720360	Sonol Securities	8	Sonol Securities 8	Idle	DG	Dry Gas
15	0407720493	Brooks	10-1	Brooks 10-1	Active	DG	Dry Gas
16	0407720501	Brooks	10-2	Brooks 10-2	Active	DG	Dry Gas
17	0407720175	Sonol Securities	4	Sonol Securities 4	Active	DG	Dry Gas
18	0407720191	Sonol Securities	5	Sonol Securities 5	Active	DG	Dry Gas
19	0407720224	Sonol Securities	7	Sonol Securities 7	Active	DG	Dry Gas
20	0407720155	Sonol Securities	1	Sonol Securities 1	Plugged	DH	Dry Hole
21	0407700315	McCulloch Union Sonol Unit	1	McCulloch Union Sonol Unit 1	Plugged	DH	Dry Hole
22	0407720209	Sonol Securities	6	Sonol Securities 6	Plugged	DG	Dry Gas
23	0407720277	Marchini	M-1	Marchini M-1	Plugged	DH	Dry Hole
24	0407720159	Sonol Securities	1-A	Sonol Securities 1-A	Idle	DG	Dry Gas
25	0407720171	Sonol Securities	3	Sonol Securities 3	Idle	DG	Dry Gas
26	0407720285	Pool B	2	Pool B 2	Idle	DG	Dry Gas

Table A-2. Water Well Reference List based on DWR WCR Data

Number	WCR Number	Planned Use
27	WCR1953-000317	Water Supply Domestic
28	WCR1988-007184	Water Supply Domestic
29	WCR2004-003467	Water Supply Domestic
30	WCR0079944	Unknown
31	WCR0218619	Unknown
32	WCR2006-003520	Water Supply Domestic
33	WCR2020-010134	Water Supply Domestic

Table A-3. Water Well Reference List based on Data from GAMA

Number	Data Set	Well ID
34	WB_ILRP	AGW080018610-RANCHWELL1
35	DDW	CA3900583_001_001
36	DDW	CA3900713_001_001
37	DWR	01S05E02E002M

Table A-4. Formation Clay Volumes used in the Shale Gouge Ratio (SGR) Calculation.

Formation	Clay Volume												
	Sonol Securities 1-A	Sonol Securities 6	Pool B 2	Union Properties 2	Yamada 1-26	Salmon 22-1	Brooks 10-1 RD1	Sonol Securities 7 (EFB)	Sonol Securities 7 (WFB)	Moran 1	Mobil Parcel Y 1	Lathrop Unit B 5	Formation Average
Winters	0.14	0.14	0.18	0.16	0.13	0.13	0.16	0.10	0.17	0.08	0.22	--	0.15
Delta Shale	--	--	--	0.47	0.48	0.44	--	0.48	0.48	0.47	0.49	--	0.47
Lower Delta Shale	--	--	--	0.44	--	--	--	--	0.45	0.48	0.46	--	0.46
Lathrop Sands	--	--	--	0.35	--	--	--	--	0.34	0.25	0.34	0.30	0.32

Note:
EFB = Eastern fault block
WFB = Western fault block

Table A-5. Formation Mineralogy from X-Ray Diffraction in GP_Dohrmann_1_RD1 and XRD and Fourier Transform Infrared Spectroscopy (FTIR) in the Speckman_Decarli_1 Well

Well	Zone	Depth (ft)	Quartz	Plagioclase	K-Feldspar	Calcite	Dolomite	Siderite	Barite	Glauconite	Pyrite	Kaolinite	Chlorite	Illite & Mica	Smectite	MXL I/S	Total Clay
Speckman_Decarli_1	H&TShale	8828.0	23.0	21.0	9.0	3.0	0.0			0.0	1.0	12.0	5.0			26.0	43.0
Speckman_Decarli_1	H&TShale	8830.0	30.0	17.0	11.0	0.0	0.0			0.0	4.0	3.4	14.4	6.1	14.1		38.0
Speckman_Decarli_1	H&TShale	8909.0	20.0	20.0	13.0	0.0	0.0			2.0	2.0	5.0	3.0			35.0	43.0
Speckman_Decarli_1	H&TShale	8937.0	20.0	12.0	8.0	0.0	0.0			0.0	2.0	14.0	6.0			38.0	58.0
Speckman_Decarli_1	H&TShale	8939.0	24.0	18.0	11.0	1.0	0.0			0.0	3.0	3.0	15.5	7.7	16.8		43.0
Speckman_Decarli_1	H&TShale	8940.0	23.0	29.0	12.0	0.0	0.0			0.0	0.0	4.0	5.0			27.0	36.0
Speckman_Decarli_1	H&TShale	8942.0	23.0	15.0	10.0	0.0	0.0			0.0	2.0	12.0	5.0			33.0	50.0
Speckman_Decarli_1	H&TShale	9439.0	20.0	14.0	9.0	0.0	0.0			0.0	1.0	0.0	5.0			51.0	56.0
Speckman_Decarli_1	H&TShale	9441.0	21.0	19.0	12.0	2.0	0.0			0.0	3.0	0.0	0.0			43.0	43.0
GP_Dohrmann_1_RD1	Winters	9755.1	64.0	9.0	2.0		1.0	11.0				5.0			8.0		13.0
GP_Dohrmann_1_RD1	Winters	9758.5	70.0	12.0	4.0		1.0	2.0				5.0			6.0		11.0
GP_Dohrmann_1_RD1	Winters	9762.5	28.0	8.0	3.0		1.0	1.0			1.0	21.0	2.0	2.0	33.0		58.0
GP_Dohrmann_1_RD1	Delta Shale	10073.5	69.0	13.0	5.0		1.0	1.0				3.0	1.0	1.0	6.0		11.0
GP_Dohrmann_1_RD1	Delta Shale	10077.5	30.0	7.0	2.0	1.0		3.0			1.0	17.0	5.0	2.0	32.0		56.0
GP_Dohrmann_1_RD1	Delta Shale	10082.5	70.0	13.0	3.0		1.0	1.0				3.0	2.0	2.0	5.0		12.0
GP_Dohrmann_1_RD1	Delta Shale	10090.5	51.0	8.0	2.0		1.0				2.0	8.0	4.0	3.0	21.0		36.0
GP_Dohrmann_1_RD1	Delta Shale	10096.2	72.0	13.0	3.0		1.0		1.0			3.0	1.0	2.0	4.0		10.0
GP_Dohrmann_1_RD1	Delta Shale	10070.5	69.0	14.0	4.0		1.0	1.0				4.0	1.0		6.0		11.0

Well locations shown in Figure A-26.

Table A-6. Core Samples Within the Injection Zone

Well	Sample Depth (feet)	Porosity (%)	Permeability Horizontal (mD)	Permeability Vertical (mD)	Oil Saturation (%)	Water Saturation (%)	Grain Density (g/cc)
Sonol_Securities_6	9763.5	10.3	0.29	—	0	70	—
Sonol_Securities_6	9766.5	11.9	3.6	—	0	60.3	—
Sonol_Securities_6	9767.5	18.8	3.1	—	0	54.8	—
Sonol_Securities_6	9768.5	18	4	—	0	47.2	—
Sonol_Securities_6	9769.5	17.5	2	—	0	53.2	—
Sonol_Securities_6	9770.5	17.2	0.75	—	0	56.4	—
Sonol_Securities_6	9773.5	18.8	3.4	—	0	58	—
Sonol_Securities_6	9774.5	18.2	0.57	—	0	49.4	—
Sonol_Securities_6	9775.5	18.6	0.49	—	0	50.6	—
Sonol_Securities_6	9776.5	17.9	1.8	—	0	52.5	—
Sonol_Securities_6	9777.5	18.9	8.2	—	0	47.7	—
Sonol_Securities_6	9780.75	19.7	9.8	—	0	57.5	—
Sonol_Securities_6	9782.5	14.3	0.95	—	0	58.7	—
Sonol_Securities_6	9784.5	18.4	0.71	—	0	59.2	—
Sonol_Securities_6	9829.5	14.9	0.23	—	0	51.8	—
Sonol_Securities_6	9830.5	20.4	5.4	—	0	65.4	—
Sonol_Securities_6	9831.5	20.1	4.2	—	0	70.7	—
Sonol_Securities_6	9832.5	15.1	0.58	—	0	60.9	—
Sonol_Securities_6	9833.5	18.4	0.26	—	0	72.9	—
Sonol_Securities_6	9834.5	19.3	0.88	—	0	69.9	—
Sonol_Securities_6	9835.5	12.4	0.39	—	0	60.5	—
Sonol_Securities_6	9836.5	18.8	0.8	—	0	64.4	—
Sonol_Securities_6	9837.5	4.5	0.02	—	0	77.8	—
Sonol_Securities_6	9838.5	4.6	0.04	—	0	76.2	—

Table A-6 (cont.)

Well	Sample Depth (feet)	Porosity (%)	Permeability Horizontal (mD)	Permeability Vertical (mD)	Oil Saturation (%)	Water Saturation (%)	Grain Density (g/cc)
Sonol_Securities_6	9839.5	5.6	0.05	—	0	75.4	—
Sonol_Securities_6	9840.5	4.1	0.04	—	0	76	—
Sonol_Securities_6	9841.5	17.3	4.3	—	0	64.7	—
Sonol_Securities_6	9842.5	14	0.39	—	0	60.7	—
Sonol_Securities_6	9843.5	16.3	0.32	—	0	67.1	—
Sonol_Securities_6	9844.5	14.9	0.23	—	0	65	—
Sonol_Securities_6	9845.5	14	1.2	—	0	72.3	—
Sonol_Securities_6	9847.5	16.6	6.4	—	0	60.9	—
Sonol_Securities_6	9849.5	22.2	5.9	—	0	56.8	—
Sonol_Securities_6	9851.5	20.8	6.1	—	0	55.8	—
Sonol_Securities_6	9852.5	3.2	0.03	—	0	72	—
Sonol_Securities_6	9854.5	18.7	6.3	—	0	50.8	—
Sonol_Securities_6	9855.5	20.7	7.2	—	0	56.1	—
Sonol_Securities_6	9856.5	20.4	21	—	0	53.5	—
Sonol_Securities_6	9857.5	21.5	20	—	0	48.3	—
Sonol_Securities_6	9858.5	22.6	6.9	—	0	51	—
Sonol_Securities_6	9859.5	20.9	22	—	0	37.4	—
Sonol_Securities_6	9961.5	20.6	184	148	0	85.1	—
Sonol_Securities_6	9962.5	20.3	73	—	0	82.8	—
Sonol_Securities_6	9963.5	20.6	36	—	0	82.5	—
Sonol_Securities_6	9964.5	21.3	42	—	0	85.7	—
Sonol_Securities_6	9965.5	20.3	57	48	0	84.8	—
Sonol_Securities_6	9966.5	20.1	49	—	0	81.5	—

Table A-6 (cont.)

Well	Sample Depth (feet)	Porosity (%)	Permeability Horizontal (mD)	Permeability Vertical (mD)	Oil Saturation (%)	Water Saturation (%)	Grain Density (g/cc)
Sonol_Securities_6	9968.8	21.2	44	—	0	87.8	—
Sonol_Securities_6	9969.5	11.4	1.1	—	0	73	—
Sonol_Securities_6	9970.5	22.7	12	5.9	0	74.3	—
Sonol_Securities_6	9971.5	20	13	—	0	71.3	—
Sonol_Securities_6	9972.5	20.9	44	—	0	70.6	—
Sonol_Securities_6	9973.5	19	18	—	0	65.8	—
Sonol_Securities_6	9974.5	20.8	36	37	0	72.8	—
Sonol_Securities_6	9975.5	16.9	2.6	—	0	81.6	—
Sonol_Securities_6	9976.5	20.6	57	—	0	85.2	—
Sonol_Securities_6	9977.25	23	69	—	0	80	—
Sonol_Securities_6	9978.65	23	79	78	0	80.5	—
Sonol_Securities_6	9979.5	22.8	70	—	0	80.7	—
Sonol_Securities_6	9980.5	22.6	71	77	0	79.7	—
Sonol_Securities_4	9658.7	28.9	4.4	—	0	70	2.67
Sonol_Securities_4	9659.4	27.9	16	—	0	70	2.66
Sonol_Securities_4	9660.4	23.9	4.7	—	0	69.4	2.64
Sonol_Securities_4	9661	21.9	11	—	0	68.9	2.63
Sonol_Securities_4	9662.6	27.6	28	14	0	69.6	2.63
Sonol_Securities_4	9663.4	27.2	27	—	0	69.5	2.64
Sonol_Securities_4	9664	214	3.6	—	0	67.3	2.64
Sonol_Securities_4	9665	23.2	69	—	0	55.6	2.61
Sonol_Securities_4	9666	27.4	104	107	0	68.9	2.65
Sonol_Securities_4	9666.8	29.9	173	—	0	69	2.65

Table A-6 (cont.)

Well	Sample Depth (feet)	Porosity (%)	Permeability Horizontal (mD)	Permeability Vertical (mD)	Oil Saturation (%)	Water Saturation (%)	Grain Density (g/cc)
Sonol_Securities_4	9667.7	29.8	152	—	0	68.5	2.65
Sonol_Securities_4	9668.8	30.3	182	104	0	69	2.65
Sonol_Securities_4	9669.5	28	145	—	0	69	2.64
Sonol_Securities_4	9670.5	28.3	142	—	0	69	2.64
Sonol_Securities_4	9672	32.2	161	—	0	69	2.65
Sonol_Securities_4	9672.5	31.8	160	—	0	70.4	2.65
Sonol_Securities_4	9673.5	32.4	124	101	0	70.3	2.65
Sonol_Securities_4	9674.4	31.1	102	—	0	70.5	2.64
Sonol_Securities_4	9675.5	6.3	0.5	—	0	79.4	2.66
Sonol_Securities_4	9676.5	6.2	0.3	—	0	74.2	2.67
Sonol_Securities_4	9677.3	4.7	0.3	0.2	0	75.6	2.68
Sonol_Securities_4	9678	3.6	0.5	—	0	58.2	2.7
Sonol_Securities_4	9679.3	48	0.3	—	0	77.3	2.66
Sonol_Securities_4	9680.8	24.4	133	—	0	62	2.65
Sonol_Securities_4	9681.5	24	128	81	0	63	2.65
Sonol_Securities_4	9683.5	24	117	—	0	65.5	2.65
Sonol_Securities_5	9834.2	22.4	413	—	—	—	—
Sonol_Securities_5	9980.75	20.2	40	—	—	—	—
Sonol_Securities_5	9972	15.3	9.2	—	—	—	—

Table A-7. Core Samples Within the Delta Shale

Well	Sample Depth (feet)	Porosity (%)	Permeability Horizontal (mD)	Permeability Vertical (mD)	Oil Saturation (%)	Water Saturation (%)	Grain Density (g/cc)
GP_Dohrmann_1_RD1	10075.5	14.4	0.04	—	0	99.7	2.66
GP_Dohrmann_1_RD1	10076.5	14	0.7	—	0	99.5	2.66
GP_Dohrmann_1_RD1	10077.5	13.9	0.79	—	0	99.5	2.65
GP_Dohrmann_1_RD1	10078.5	13.6	0.04	—	0	99.5	2.65
GP_Dohrmann_1_RD1	10079.5	13.7	0.04	—	0	99.9	2.65
GP_Dohrmann_1_RD1	10080.6	16.3	0.67	—	0	98.1	2.65
GP_Dohrmann_1_RD1	10085.5	13.8	0.05	—	0	99.3	2.66
GP_Dohrmann_1_RD1	10086.5	14.7	0.03	—	0	99.1	2.67
GP_Dohrmann_1_RD1	10087.5	13.1	0.07	—	0	98.9	2.65
GP_Dohrmann_1_RD1	10068.5	13.6	0.06	—	0	99.5	2.64
GP_Dohrmann_1_RD1	10092.5	13.5	0.04	—	0	98.9	2.65
GP_Dohrmann_1_RD1	10093.5	13.6	0.04	—	0	99.5	2.65
GP_Dohrmann_1_RD1	10094.5	14.3	0.05	—	0	99	2.64
GP_Dohrmann_1_RD1	10095.5	14.5	0.04	—	0	99.2	2.65
GP_Dohrmann_1_RD1	10252.5	11.3	0.18	—	0	99.3	2.66
GP_Dohrmann_1_RD1	10253.5	10	0.06	—	0	99.4	2.66
GP_Dohrmann_1_RD1	10254.5	10.5	0.07	—	0	98.9	2.66
GP_Dohrmann_1_RD1	10255.5	10.7	0.07	—	0	98.6	2.65
GP_Dohrmann_1_RD1	10256.5	10.3	0.08	—	0	99.3	2.65
GP_Dohrmann_1_RD1	10257.5	10.2	0.06	—	0	99.9	2.66
GP_Dohrmann_1_RD1	10256.5	10.5	0.06	—	0	99.3	2.66
GP_Dohrmann_1_RD1	10259.5	10.7	1.3	—	0	98.6	2.67
GP_Dohrmann_1_RD1	10274.5	10.7	0.08	—	0	98.4	2.65

Table A-7 (cont.)

Well	Sample Depth (feet)	Porosity (%)	Permeability Horizontal (mD)	Permeability Vertical (mD)	Oil Saturation (%)	Water Saturation (%)	Grain Density (g/cc)
GP_Dohrmann_1_RD1	10288.6	10.4	0.1	—	0	99.8	2.66
GP_Dohrmann_1_RD1	10289.6	11.1	0.07	—	0	99.6	2.65

Table A-8. Starkey-Sawtooth Shale and Winters Formation Gross Thickness and Depth within the AoR

Zone	Property	Low	High	Mean
Upper Confining Zone *Starkey-Sawtooth Shale*	Thickness (feet)	2,158	2,637	2,288
	Depth (feet TVD)	7,208	7,776	7,457
Reservoir *Winters Formation Sandstone*	Thickness (feet)	120	365	256
	Depth (feet TVD)	9,492	9,995	9,713

Table A-9. Wells with Data for Fracture Gradient Determination

UWI	Well	Field	Zone	Date	Test Type	Depth (feet)	Fracture Gradient (feet)
04077203600000	Sonol_Securities_8	Union Island	H&T Shale	09/14/1980	LOT	5504	0.809
04077202890000	Yamada_Line_Well_1	Union Island	Mokelumne	10/23/1976	FIT	6042	0.76
04077202870000	Galli_2	Union Island	H&T Shale	09/01/1976	FIT	6178	0.76
04077202850000	Pool_B_2	Union Island	H&T Shale	07/29/1976	FIT	6186	0.76
04077202780000	Galli_1	Union Island	Mokelumne	05/26/1976	FIT	6207	0.75
04077207070000	TRANSAMERICA 2-3	French Camp	Lathrop	10/12/2007	FIT	9367	0.882
04077207070000	TRANSAMERICA 2-3	French Camp	Lathrop	10/13/2007	FIT	9728	0.873
04077207070000	TRANSAMERICA 2-3	French Camp	Lathrop	10/13/2007	FIT	9940	0.868
04077207070000	TRANSAMERICA 2-3	French Camp	Lathrop	10/14/2007	FIT	10200	0.881
04095213280000	SERPA 5	Rio Vista	Peterson	10/18/2012	FIT	10930	0.831
04067205160000	WILCOX 21	Rio Vista	Peterson	01/28/2012	FIT	11025	0.781
04067205160000	WILCOX 21	Rio Vista	Peterson	01/29/2012	FIT	11037	0.780

FIT = formation integrity tests
LOT = leak off tests

Table A-10. Wells Used for the Overburden Stress Gradient Calculation

Well Name	API	UWI
SONOL_SECURITIES_7	04077202240000	04077202240000
SONOL_SECURITIES_11	04077207240000	04077207240000
L_COCHRAN_20_1	04077204100000	04077204100000
SONOL_SECURITIES_2	04077201620000	04077201620000
SONOL_SECURITIES_6	04077202090000	04077202090000
GALLI_1	04077202780000	04077202780000
SONOL_SECURITIES_1_A	04077201590000	04077201590000
UNION_PROPERTIES_2	04077203220000	04077203220000

Table A-11. Input Parameters Used for the Mohr Circle Analysis Based on Present-Day Conditions in the Injection Zone

Parameter	Present-Day Conditions
Pore Pressure (psi)	1,200
Overburden Stress Gradient (psi/ft)	0.94
Minimum Horizontal Stress Gradient (psi/ft)	0.7
Maximum Horizontal Stress Gradient (psi/ft)	1.1
Coefficient of Friction	0.6
Fault Cohesion (psi)	0

Table A-12. Data from USGS Earthquake Catalog for Faults in the Region of CTV II

#	Date	Latitude	Longitude	Depth (km)	Magnitude	Last Updated	Location
12	3/1/2024	37.89	-121.62	2.2	2.9	3/1/2024	3 km SW of Discovery Bay, California
1	10/15/2010	37.88	-121.39	14.6	3.1	1/23/2017	9 km WSW of Taft Mosswood, California
2	2/10/1992	37.77	-121.32	14.6	3.1	2/9/2016	8 km SSW of Lathrop, California
3	2/4/1991	37.81	-121.24	7.7	3.1	12/18/2016	2 km NW of Manteca, California
4	2/3/1991	37.82	-121.24	9.4	3.1	12/18/2016	2 km E of Lathrop, California
5	1/27/1980	38	-121	6	3.3	4/2/2016	8 km ESE of Linden, California
6	8/6/1979	37.83	-121.51	6	4.3	4/1/2016	6 km NNE of Mountain House, California
7	2/2/1979	37.66	-121.19	18	3.5	4/1/2016	10 km WSW of Salida, California
8	10/6/1976	37.61	-121.41	2.9	3.3	12/15/2016	13 km S of Tracy, California
9	9/5/1976	37.61	-121.41	6.5	3.5	12/15/2016	13 km S of Tracy, California
10	2/2/1944	37.93	-121.4	6	3.8	1/28/2016	7 km SW of Country Club, California
11	7/15/1866	37.7	-121.5		6	1/30/2021	Southwest of Stockton, California

Table A-13. Class II Wells near Area of Review

API	Designation	Operator Name	Current Type	Current Status	Field	TVDSS (ft)	Latitude	Longitude	Spud Date	Idle Start Date	Abandoned Date
0407720278	Galli 1	California Resources Production Corporation	Water Disposal	Idle	Union Island Gas	10,298	37.82554	-121.4354	5/15/1976	11/1/2014	—
0407720438	J. Ratto 18-1	California Resources Production Corporation	Water Disposal	Idle	Lathrop Gas	10,074	37.8549	-121.365	7/10/1984	6/1/2007	—
0407720033	Reynolds & Carver-Long 1	Laymac Corporation	Water Disposal	Plugged & Abandoned	French Camp Gas	7,634	37.89606	-121.2999	12/1/1967	2/1/1992	4/17/2020
0407720259	A. Lucas 1	TXO Production Corp.	Water Disposal	Plugged & Abandoned	Lathrop Gas	11,503	37.87362	-121.3882	—	—	4/25/1988

Table A-14. Wells Used for Salinity Calculation

Well Name	UWI
1	04077203560000
AMERADA_HONEGGER_1-34	04013000010000
ARNAUDO_BROS_1	04077206240000
BACCHETTI_1	04077201380000
BANK_OF_STOCKTON_1	04077206270000
BANTA_UNIT_WELL_1A	04077203440000
BORDEN_1	04077004250000
BOULDIN_DEVELOPMENT_CO_1	04077202170000
COLDANI_1	04077206660000
DELL_ARINGA_1-31	04077204860000
DELTA_1	04077202760000
EBERHARDT_1	04077206260000
EBERHARDT_2	04077206450000
HAYES_1-7	04013202760000
HOLLY_SUGAR_1	04077206010000
JACKSON_1	04077206300000
KLEIN_1-36	04077206330000
M_C_FONG_1	04077205070000
MANDEVILLE_2	04077205590000
MANTELLI_1	04077201450000
NGC_STENZEL_1	04013201780000
NUSS_1	04077206650000
OHLENDORF_UNIT_1_1	04077203480000
PACIFIC_1	04077206440000
PACIFIC_2	04077206960000
PEREIRA_ET_AL_UNIT_1	04077203710000
PODESTA_1	04077200280000
R_M_FARMS_1	04077206810000
RIPKEN_21-1	04077205660000
ROCHA_ET_AL_UNIT_1	04077203350000
RVGU_14	04067000510000
RVGU_19	04067000760000
RVGU_25	04067001040000
SPECKMAN_DECARLI_1	04077206490000
STEVENS_16-1	04077205120000
TRACT_1_1-7	04013200820000
UNION_PROPERTIES_2	04077203220000
VICTORIA_ISLAND_FARMS_1	04077206780000

Table A-14 (cont.)

Well Name	UWI
WESTERN_ENOS_NUNN_1	04013201560000
WOODWARD_ISLAND_UNIT_20-1	04013002740000
ZUCKERMAN_1-21	04077201570000

Table A-15. Water Supply Well Information

Data Source	WCR Number	Wells from GAMA	Legacy Log Number	Planned Use or Former Use	LAT (DWR)	LONG (DWR)	LAT & LONG Accuracy (DWR)	LAT (GAMA)	LONG (GAMA)	T	R	S	APN	Date Work Ended	Total Completed Depth	Top of Perforated Interval	Bottom of Perforated Interval	Static Water Level
DWR	WCR1953-000314	NA	39-1016	Water Supply Domestic	37.89012	-121.4081	Centroid of Section	NA	NA	01N	05E	34	NA	9/2/1953	32	22	25	NA
DWR	WCR2013-001675	NA	e0200322	Monitoring	37.89444	-121.4053		NA	NA	01N	05E	34	131-310-3	10/28/2013	85	70	80	
DWR	WCR0079890	NA			37.89012	-121.4081	Centroid of Section	NA	NA	01N	05E	34	NA	NA	NA	NA	NA	NA
DWR	WCR2013-001674	NA	e0200320	Monitoring	37.89639	-121.4131		NA	NA	01N	05E	34	131-310-2	10/30/2013	45	35	40	NA
DWR	WCR2013-001673	NA	e0200318	Monitoring	37.89639	-121.4131		NA	NA	01N	05E	34	131-310-2	10/27/2013	90	75	85	NA
DWR	WCR0256937	NA			37.89022	-121.3897	Centroid of Section	NA	NA	01N	05E	35	NA	NA	NA	NA	NA	NA
DWR	WCR1950-000581	NA	39-1018	Water Supply Domestic	37.89022	-121.3897	Centroid of Section	NA	NA	01N	05E	35	NA	6/27/1950	60	40	45	NA
DWR	WCR2001-002697	NA	736784	Water Supply Domestic	37.89022	-121.3897	Centroid of Section	NA	NA	01N	05E	35	131-320-2	10/11/2001	45	33	43	12
DWR	WCR2008-000742	NA	944033	Water Supply Domestic	37.89022	-121.3897	Centroid of Section	NA	NA	01N	05E	35	NA	9/15/2008	52	30	50	10
DWR	WCR2008-000743	NA	944034	Other Unused	37.89022	-121.3897	Centroid of Section	NA	NA	01N	05E	35	NA	9/14/2008	NA	NA	NA	NA
DWR	WCR1950-000580	NA	39-1017	Water Supply Domestic	37.89022	-121.3897	Centroid of Section	NA	NA	01N	05E	35	NA	6/14/1950	62	NA	NA	NA
DWR	WCR1974-000848	NA	98960	Water Supply Domestic	37.87549	-121.4449	Centroid of Section	NA	NA	01S	05E	5	NA	3/5/1974	70	57	67	NA
DWR	WCR0192144	NA			37.87549	-121.4449	Centroid of Section	NA	NA	01S	05E	5	NA	NA	NA	NA	NA	NA
DWR	WCR0259899	NA			37.86116	-121.4448	Centroid of Section	NA	NA	01S	05E	8	NA	NA	NA	NA	NA	NA
DWR	WCR2020-000218	NA		Water Supply Domestic	37.86301	-121.4466		NA	NA	01S	05E	8	19328022	12/12/2019	300	260	300	NA
DWR	WCR1956-000052	NA	21463	Water Supply Domestic	37.86116	-121.4448	Centroid of Section	NA	NA	01S	05E	8	NA	6/6/1956	32	NA	NA	NA
DWR	WCR1953-000317	NA	39-1173	Water Supply Domestic	37.86132	-121.4263	Centroid of Section	NA	NA	01S	05E	9	NA	4/30/1953	35	NA	NA	NA
DWR	WCR0244683	NA			37.86132	-121.4263	Centroid of Section	NA	NA	01S	05E	9	NA	NA	NA	NA	NA	NA
DWR	WCR0059123	NA	64879	Water Supply Domestic	37.86149	-121.408	Centroid of Section	NA	NA	01S	05E	10	NA	4/28/1987	60	40	60	NA
DWR	WCR2004-003467	NA	926292	Water Supply Domestic	37.86149	-121.408	Centroid of Section	NA	NA	01S	05E	10	NA	7/1/2004	55	41	51	9
DWR	WCR1991-010920	NA	433872	Water Supply Domestic	37.86139	-121.4081		NA	NA	01S	05E	10	189-210-19	9/29/1991	106	78	98	NA

Table A-15 (cont.)

Data Source	WCR Number	Wells from GAMA	Legacy Log Number	Planned Use or Former Use	LAT (DWR)	LONG (DWR)	LAT & LONG Accuracy (DWR)	LAT (GAMA)	LONG (GAMA)	T	R	S	APN	Date Work Ended	Total Completed Depth	Top of Perforated Interval	Bottom of Perforated Interval	Static Water Level
DWR	WCR0218619	NA			37.86149	-121.408	Centroid of Section	NA	NA	01S	05E	10	NA	NA	NA	NA	NA	NA
DWR	WCR1987-008304	NA	64879	Water Supply Domestic	37.86149	-121.408	Centroid of Section	NA	NA	01S	05E	10	NA	4/28/1987	97	NA	NA	NA
DWR	WCR1992-009665	NA	488363	Water Supply Domestic	37.86165	-121.3896	Centroid of Section	NA	NA	01S	05E	11	189-220-11	9/23/1992	80	45	65	NA
DWR	WCR0274319	NA			37.86165	-121.3896	Centroid of Section	NA	NA	01S	05E	11	NA	NA	NA	NA	NA	NA
DWR	WCR1953-000319	NA	39-1175	Water Supply Domestic	37.86165	-121.3896	Centroid of Section	NA	NA	01S	05E	11	NA	6/1/1953	49	46	49	NA
DWR	WCR1994-005899	NA	569345	Water Supply Domestic	37.84694	-121.4079	Centroid of Section	NA	NA	01S	05E	15	189-160-9	5/30/1994	187	115	125	
DWR	WCR1952-000293	NA	39-1177	Other Unused	37.84694	-121.4079		NA	NA	01S	05E	15	NA	5/16/1952	NA	NA	NA	NA
DWR	WCR1983-001903	NA	243982	Water Supply Domestic	37.84694	-121.4079	Centroid of Section	NA	NA	01S	05E	15	NA	6/6/1983	110	NA	NA	NA
DWR	WCR2008-000103	NA	940591	Water Supply Irrigation - Agriculture	37.84694	-121.4079	Centroid of Section	NA	NA	01S	05E	15	NA	1/13/2008	85	60	80	NA
DWR	WCR0034671	NA			37.84694	-121.4079	Centroid of Section	NA	NA	01S	05E	15	NA	NA	NA	NA	NA	NA
DWR	WCR2020-006687	NA		Water Supply Domestic	37.84149	-121.4165		NA	NA	01S	05E	15	189-160-20	5/19/2020	100	80	100	12
DWR	WCR0079944	NA			37.84674	-121.4263	Centroid of Section	NA	NA	01S	05E	16	NA	NA	NA	NA	NA	NA
DWR	WCR1987-005878	NA	251137	Water Supply Irrigation - Agriculture	37.84674	-121.4263	Centroid of Section	NA	NA	01S	05E	16	NA	6/2/1987	98	NA	NA	NA
DWR	WCR1975-000098	NA	111941	Water Supply Domestic	37.84674	-121.4263	Centroid of Section	NA	NA	01S	05E	16	NA	12/1/1975	482	258	278	NA
DWR	WCR1988-007184	NA	284293	Water Supply Domestic	37.84667	-121.4264		NA	NA	01S	05E	16	NA	9/15/1988	230	NA	NA	NA
DWR	WCR2006-003520	NA	e0938241	Water Supply Domestic	37.84674	-121.4263	Centroid of Section	NA	NA	01S	05E	16	NA	11/7/2006	50	30	40	7
DWR	WCR1951-000470	NA	39-1178	Water Supply Domestic	37.84674	-121.4263	Centroid of Section	NA	NA	01S	05E	16	NA	3/20/1951	36	33	36	
DWR	WCR0020139	NA	938241	Water Supply Domestic	37.8484	-121.4335	>50 FT	NA	NA	01S	05E	16	NA	11/7/2006	40	30	40	7
DWR	WCR2020-010134	NA		Water Supply Domestic	37.85004	-121.4333	Unknown	NA	NA	01S	05E	16	189-160-140	7/21/2020	80	60	80	10
DWR	WCR1952-000294	NA	39-1179	Water Supply Domestic	37.84674	-121.4263	Centroid of Section	NA	NA	01S	05E	16	NA	10/10/1952	43	24	28	NA
DWR	WCR1954-000381	NA	21451	Water Supply Domestic	37.84674	-121.4263	Centroid of Section	NA	NA	01S	05E	16	NA	5/20/1954	39	36	39	NA

Table A-15 (cont.)

Data Source	WCR Number	Wells from GAMA	Legacy Log Number	Planned Use or Former Use	LAT (DWR)	LONG (DWR)	LAT & LONG Accuracy (DWR)	LAT (GAMA)	LONG (GAMA)	T	R	S	APN	Date Work Ended	Total Completed Depth	Top of Perforated Interval	Bottom of Perforated Interval	Static Water Level
DWR	WCR1978-001522	NA	128682	Water Supply Domestic	37.84654	-121.4448	Centroid of Section	NA	NA	01S	05E	17	NA	5/18/1978	98	48	98	NA
DWR	WCR1993-006062	NA	495202	Water Supply Industrial	37.84654	-121.4448	Centroid of Section	NA	NA	01S	05E	17	NA	8/11/1993	250	130	175	NA
DWR	WCR2016-015880	NA	E0299807		37.84972	-121.4464	Unknown	NA	NA	01S	05E	17	18917005	2/4/2016	NA	NA	NA	NA
DWR	WCR1984-002263	NA	178094	Water Supply Public	37.84654	-121.4448	Centroid of Section	NA	NA	01S	05E	17	NA	7/19/1984	90	23	73	NA
DWR	WCR0316821	NA			37.84654	-121.4448	Centroid of Section	NA	NA	01S	05E	17	NA	NA	NA	NA	NA	NA
DWR	WCR1953-000321	NA	39-1180	Water Supply Domestic	37.84654	-121.4448	Centroid of Section	NA	NA	01S	05E	17	NA	4/28/1953	28	25	28	NA
DWR	WCR2016-015881	NA	E0299805		37.84972	-121.4464	Unknown	NA	NA	01S	05E	17	18917005	2/4/2016	NA	NA	NA	NA
DWR	WCR2022-009653	NA		Water Supply Domestic	37.82617	-121.4096	>50 Ft	NA	NA	01S	05E	22	189-200-060	3/24/2022	60	40	60	10
DWR	WCR1999-006661	NA	814148	Water Supply Irrigation - Agriculture	37.83219	-121.4078	Centroid of Section	NA	NA	01S	05E	22	189-200-6	1/12/1999	160	120	160	NA
DWR	WCR0089724	NA			37.81768	-121.4078	Centroid of Section	NA	NA	01S	05E	27	NA	NA	NA	NA	NA	NA
DWR	WCR1979-000974	NA	86184	Water Supply Domestic	37.81768	-121.4078	Centroid of Section	NA	NA	01S	05E	27	NA	7/1/1979	97	36	46	
DWR	WCR1952-000295	NA	39-1181	Water Supply Domestic	37.81768	-121.4078	Centroid of Section	NA	NA	01S	05E	27	NA	5/23/1952	85	74	78	NA
DWR	WCR1990-012688	NA	370320	Water Supply Domestic	37.81778	-121.4078		NA	NA	01S	05E	27	189-230-17	6/27/1990	184	NA	NA	NA
DWR	WCR1776-000538	NA	39-1182		37.81747	-121.4261	Centroid of Section	NA	NA	01S	05E	28	NA	NA	79	NA	NA	NA
DWR	WCR0045687	NA			37.81747	-121.4261	Centroid of Section	NA	NA	01S	05E	28	NA	NA	NA	NA	NA	NA
DWR	WCR1981-000061	NA	77028	Water Supply Domestic	37.81725	-121.4446	Centroid of Section	NA	NA	01S	05E	29	NA	7/2/1981	80	NA	NA	NA
DWR	WCR0118174	NA			37.81725	-121.4446	Centroid of Section	NA	NA	01S	05E	29	NA	NA	NA	NA	NA	NA
DWR	WCR1986-007552	NA	61498	Water Supply Domestic	37.81725	-121.4446	Centroid of Section	NA	NA	01S	05E	29	NA	6/1/1986	90	NA	NA	NA
DWR	WCR1999-002585	NA	715079	Water Supply Domestic	37.81725	-121.4446	Centroid of Section	NA	NA	01S	05E	29	NA	9/15/1999	67	40	60	10
DWR	WCR0173869	NA	61498	Water Supply Domestic	37.81725	-121.4446	Centroid of Section	NA	NA	01S	05E	29	NA	NA	90	55	85	10
DWR	WCR1999-002586	NA	715080	Water Supply Domestic	37.81725	-121.4446	Centroid of Section	NA	NA	01S	05E	29	NA	9/15/1999	77	60	70	12
DWR	WCR1990-012755	NA	370466	Water Supply Domestic	37.81722	-121.4447		NA	NA	01S	05E	29	189-120-13	11/4/1990	400	NA	NA	NA

Table A-15 (cont.)

Data Source	WCR Number	Wells from GAMA	Legacy Log Number	Planned Use or Former Use	LAT (DWR)	LONG (DWR)	LAT & LONG Accuracy (DWR)	LAT (GAMA)	LONG (GAMA)	T	R	S	APN	Date Work Ended	Total Completed Depth	Top of Perforated Interval	Bottom of Perforated Interval	Static Water Level
DWR	WCR1985-001635	NA	150861	Water Supply Domestic	37.81725	-121.4446	Centroid of Section	NA	NA	01S	05E	29	NA	8/27/1985	172	NA	NA	NA
DWR	NA	01N05E34H001M	NA	Water Supply	NA	NA	NA	37.8904	-121.406	01N	05E	34	NA	NA	NA	NA	NA	NA
DWR	NA	01N05E34M001M	NA	Water Supply	NA	NA	NA	37.8868	-121.42	01N	05E	34	NA	NA	NA	NA	NA	NA
WB_ILRP	NA	AGW080021029-TRT-JRWELL	NA	Water Supply Domestic	NA	NA	NA	37.888809	-121.397747	01N	05E	35	NA	NA	NA	NA	NA	NA
WB_ILRP	NA	AGW080018185-BALMATWELL	NA	Water Supply Domestic	NA	NA	NA	37.887410	-121.389044	01N	05E	35	NA	NA	NA	NA	NA	NA
WB_ILRP	NA	AGW080021028-TRT-DDWELL	NA	Water Supply Domestic	NA	NA	NA	37.887014	-121.386371	01N	05E	35	NA	NA	NA	NA	NA	NA
DWR	NA	01S05E02E002M	NA	Water Supply	NA	NA	NA	37.876	-121.402	01S	05E	2	NA	NA	NA	NA	NA	NA
DWR	NA	01S05E12D001M	NA	Water Supply	NA	NA	NA	37.8651	-121.383	01S	05E	12	NA	NA	NA	NA	NA	NA
WB_ILRP	NA	AGW080018610-RANCHWELL1	NA	Water Supply Domestic	NA	NA	NA	37.844099	-121.422379	01S	05E	16	NA	NA	NA	NA	NA	NA
DDW	NA	CA3900713_001_001	NA	Water Supply Municipal	NA	NA	NA	37.84	-121.44	01S	05E	17	NA	NA	NA	23	53	NA
DDW	NA	CA3900583_001_001	NA	Water Supply Municipal	NA	NA	NA	37.84	-121.44	01S	05E	17	NA	NA	NA	NA	NA	NA
USGS_NWIS	NA	375000121260001	NA	Water Supply Municipal	NA	NA	NA	37.849972	-121.445778	01S	05E	17	NA	NA	83	NA	NA	NA
GAMA_USGS	NA	TRCY-07	NA	Water Supply Municipal	NA	NA	NA	37.849972	-121.445778	01S	05E	17	NA	NA	90	23	73	NA
WB_ILRP	NA	AGW080020866-PACKNGSHED	NA	Water Supply Domestic	NA	NA	NA	37.839119	-121.418216	01S	05E	22	NA	NA	NA	NA	NA	NA
DPR	NA	77958	NA	Water Supply Domestic	NA	NA	NA	37.812639	-121.424143	01S	05E	28	NA	NA	NA	NA	NA	NA
WB_CLEANUP	NA	T0607700643-MW1	NA	Monitoring	NA	NA	NA	37.821940	-121.448846	01S	05E	29	NA	NA	23.6	NA	NA	NA
WB_CLEANUP	NA	T0607700643-MW2	NA	Monitoring	NA	NA	NA	37.822129	-121.449030	01S	05E	29	NA	NA	18.1	NA	NA	NA
WB_CLEANUP	NA	T0607700643-MW3	NA	Monitoring	NA	NA	NA	37.822165	-121.448711	01S	05E	29	NA	NA	23.6	NA	NA	NA
WB_CLEANUP	NA	T0607700643-MW4	NA	Monitoring	NA	NA	NA	37.821921	-121.449087	01S	05E	29	NA	NA	23.9	NA	NA	NA
WB_CLEANUP	NA	T0607700643-MW5	NA	Monitoring	NA	NA	NA	37.822155	-121.449240	01S	05E	29	NA	NA	24.4	NA	NA	NA
WB_CLEANUP	NA	T0607700643-MW6	NA	Monitoring	NA	NA	NA	37.822314	-121.448703	01S	05E	29	NA	NA	24.75	NA	NA	NA
WB_CLEANUP	NA	T0607700643-MW7	NA	Monitoring	NA	NA	NA	37.821691	-121.449155	01S	05E	29	NA	NA	24.6	NA	NA	NA
WB_CLEANUP	NA	T0607700643-DW1	NA	Water Supply Domestic	NA	NA	NA	37.821632	-121.449186	01S	05E	29	NA	NA	NA	NA	NA	NA

Notes:
1 = all depths are based on feet below ground surface
WCR = Department of Water Resources Well Completion Report
LAT = Latitude
LONG = Longiutde T = Township
R = Range S = Section
APN = Assessor Parcel Number
NA = Data are not available or not applicable
GAMA = State Water Board's GAMA website

Table A-16. Formation Fluid Properties

Formation Fluid Property	Formation Water	Formation Gas
Density, g/cm^3	1.0082	0.00076
Viscosity, cp	1.26	0.029
TDS, ppm	~15,000	NA

Table A-17. Injectate Compositions

Component	Mass %	
	Injectate 1	Injectate 2
CO_2	99.213%	99.884%
H_2	0.051%	0.006%
N_2	0.643%	0.001%
H_2O	0.021%	0.000%
CO	0.029%	0.001%
Ar	0.031%	0.000%
O_2	0.004%	0.000%
SO_2+SO_3	0.003%	0.000%
H_2S	0.001%	0.014%
CH_4	0.004%	0.039%
NO_x	0.002%	0.000%
NH_3	0.000%	0.000%
C_2H_6	0.000%	0.053%
Ethylene	0.000%	0.002%
Total	**100.00%**	**100.00%**

Table A-18. Simplified 4-Component Composition for Injectate 1 and Injectate 2

Injectate 1	
Component	Mass %
CO_2	99.213%
N_2	0.643%
SO_2+SO_3	0.003%
H_2S	0.001%

Injectate 2	
Component	Mass %
CO_2	99.884%
CH_4	0.039%
C_2H_6	0.053%
H_2S	0.014%

Table A-19. Injectate Properties Range over Project Life at Downhole Conditions for Injectate 1 and Injectate 2

Injectate Property at Downhole Conditions	Injectate 1	Injectate 2
Viscosity, cp	0.022 – 0.054	0.022 – 0.056
Density, lb/ft^3	9.1 - 40.6	9.1 – 41.5
Compressibility factor, Z	0.81 - 0.67	0.80 – 0.66